Department of Water Resources

684 Winder Highway • Lawrenceville, GA 30045-5012
678.376.6700
www.gwinnettcounty.com

gwinnettcounty

March 23, 2015

Mr. Charles D. Williams
Program Manager, Response and Remediation Program
Georgia Department of Natural Resources, Environmental Protection Division (EPD)
2 Martin Luther King Jr. Drive, S.E., Suite 1054 East
Atlanta, Georgia 30334

RE: In response to EPD letters dated January 15, 2015 & January 16, 2015
        Comments and Technical Memoranda
        Gwinnett County Fire Station No. 19 – HSI Site Number 10844

Dear Mr. Williams:

Gwinnett County, in conjunction with our technical consultant CDM Smith, has prepared this letter and the attached technical memoranda in response to your letters dated January 15, 2015 and January 16, 2015 regarding the Fire Station 19 property. The requirements listed in the January 15th letter are noted, and Gwinnett County will comply with the identified reporting schedule. Additionally, included with this letter is an affidavit that has been filed with the clerk of the Superior Court of Gwinnett County and recorded in the clerk's deed records pursuant to O.C.G.A § 44-2-20.

Regarding Georgia Environmental Protection Division (EPD) comments on the Voluntary Investigation and Remediation Plan (VIRP) provided in the January 16th letter, we offer the following responses:

1. According to Section 4 of the VIRP, in-vitro bioaccessibility (IVBA) testing has been proposed to determine the potential human uptake of arsenic from the soil onsite. Regarding this IVBA testing, EPD recommends the collection of 20 samples rather than the proposed 10 samples, based on the recommendations included in the referenced U.S. EPA Region 8 December 2012 Final Report (ESTCP Project ER-200916). In addition, it should be noted that according to the information available at the time of this review EPD is not aware of this particular methodology having wide-spread regulatory application at Voluntary Remediation or Hazardous Site Response Act sites in GA. Therefore, EPD will defer formal approval and any further comments regarding this approach until the agency has had the opportunity to review the results of the full analysis.

    Twenty samples were submitted for IVBA analyses. Please see the enclosed memo regarding the IVBA methodology and results for Fire Station 19.

2. According to Section 4 of the VIRP, utilization of an electron microprobe (EMP) analysis has been proposed to determine the form and species of arsenic in soil, which will contribute to a background demonstration for the arsenic in soil. While EPD does not have any formal objections to this particular approach at this time, EPD cannot provide formal approval of this approach as there is not a sufficient amount of supporting documentation to confirm that the methodology associated with the EMP analysis conforms with any federal or state regulatory approved methodologies. Please note that EPD will defer further comments regarding this approach until the agency has had the opportunity to review the results of the full analysis.

   Please see the enclosed memo regarding the EMP methodology and results. These analyses concluded that the source of arsenic appears to be agricultural rather than naturally occurring. As such, we do not propose using an alternate background concentration for arsenic at this time.

3. Please provide details associated with the standard operating procedures that are employed for the proposed sample collection and analysis activities that are proposed as part of the EMP and in-vitro bioaccessibility testing.

   The sample collection procedures used for the soil EMP / IVBA samples followed standard U.S. Environmental Protection Agency (EPA) Region 4 protocols for soil sample collection using a hand auger. Details on the analyses and data interpretation for the EMP and IVBA studies are included in the respective technical memorandums enclosed.

4. Please ensure that the two groundwater monitoring locations that were installed onsite are surveyed, and utilize the neighboring properties' groundwater monitoring well locations and associated groundwater level data to construct a groundwater potentiometric map for the site.

   A potentiometric surface map is enclosed. Note that wells on the adjacent GRDC property were abandoned by GRDC shortly after CDM Smith collected the groundwater levels.

5. In support of addressing the delineation requirements included in Section 12-8-108 of the Act, please include a table that indicates the site specific delineation criteria and cleanup standards that will be used at the site as they are applied to each applicable exposure pathway (soils, sediment, groundwater, surface water, etc.).

   Revised Risk Reduction Standards (RRSs) are identified in the enclosed memorandum and summarized here:

   Arsenic in Surface Soil: *127 mg/kg, site-specific, non-residential Type 4 RRS developed using IVBA analyses*

Arsenic in Subsurface Soil: *2,940 mg/kg, site-specific, construction worker Type 5 RRS developed using IVBA analyses*

Arsenic in Sediment: *Not applicable, sediments do not exist in the delineation area*

Arsenic in Groundwater: *0.010 mg/L, Type 1 RRS*

Arsenic in Surface Water: *Not applicable, surface water does not exist in the delineation area*

6. Once the RRS have been established for the applicable exposure pathways, please include an evaluation of the overland run-off route from the site and determine the potential for any offsite impacts to surface water/sediment as the result of surface erosion of impacted soils.

   A large portion of the site is paved or covered by buildings, and rainfall runoff from these features enters storm water drains. The site is nearly flat with no defined natural drainage patterns, and rainfall onto the grassed surface primarily infiltrates. Should sufficient rainfall occur to cause runoff from the grassed surfaces, it would be primarily in the form of sheet runoff until it found its way to the paved surfaces. The overall slope is to the east toward North Berkeley Lake Road, which is bordered by curbing that leads to storm water drains.

7. EPD understands that the VIRP Application has indicated that the groundwater exposure pathway is incomplete based on the data provided, but requests that any environmental covenant that is to be placed on the site property as part of the planned corrective measures incorporate a groundwater use restriction to eliminate any future groundwater exposure potential.

   Gwinnett County understands that any environmental covenant that could be placed on the site property as part of the planned corrective measures will incorporate a groundwater use restriction for Parcel No. 6-267-028.

8. In order to complete the risk reduction standards requirements for the subject site, please ensure that a Type 4 RRS is derived for the protection of groundwater. In addition, please revised Figure 2-3 to include the potentially complete exposure scenario of the construction worker to the migration of subsurface soil to groundwater, and revised Table 3-1 to include the footnote for the site-specific exposure frequency.

   The groundwater depth on the site was measured to be over 20 feet and as a result, construction worker exposure to groundwater is not considered a complete pathway. The EMP results demonstrate that the arsenic is bound primarily to iron hydroxides (~95%), and the EMP technical memorandum explains that arsenic in this phase is not easily leached. Assuming that no dilution/attenuation occurs, CDM Smith calculates that a soil arsenic concentration of 25 mg/kg could produce an equilibrium concentration in water

> *of 0.010 mg/L arsenic using the arsenic/iron hydroxide Langmuir Adsorption Isotherms presented in Attachment E to the EMP technical memorandum. The maximum observed soil concentration is soil is 491 mg/kg and the average is 81 mg/kg. For groundwater to exceed the 0.010 mg/L RRS, the dilution/attenuation factor (DAF) would have to be less than 20, assuming the maximum soil concentration and approximately 3 assuming the average. These DAFs are lower than the most conservative DAFs that have routinely been accepted by EPA. Because arsenic has not been detected in groundwater and highly conservative calculations indicate that arsenic in groundwater should not be expected, we propose not conducting additional analyses or calculations to develop a soil to groundwater RRS at this time.*

After you have had a chance to perform a preliminary review of the enclosed documents, we would like to set up a meeting at your offices to discuss the results and the next steps for this project. Please let me know what time would be convenient for you. I can be reached at (678) 376-6953 or richard.shoeck@gwinnettcounty.com. In the meantime, please do not hesitate to contact me with any questions on these responses for the enclosed documents.

Sincerely,
GWINNETT COUNTY DEPARTMENT OF WATER RESOURCES

Richard Schoeck, P.E., PMP
Division Director of Project Controls

Enclosures

cc: Tom Duffey, CDM Smith
       J.C. Lan, GCDWR
       John Reichling, CDM Smith
       Andrew Romanek, CDM Smith
       Mike Ludwiczak, GC

Legend

⊕ Shallow Monitor Well

—1,042— Potentiometric Surface (1-Foot Contour Intervals)

Well ID	TOC	DTW	Water Elevation
MW-1	1,067.66	22.30	1,045.36
MW-2	1,068.42	26.84	1,041.58
MW-4	1,054.17	14.34	1,039.83
MW-5	1054.86*	11.05	1,043.81
MW-6	1,053.76	8.88	1,044.88

Notes:

Water levels collected 2/16/15

Elevations given in NAVD 88

TOC: Top of casing

DTW: Depth to water

GW: Groundwater

* MW-5 was abandoned before the TOC was surveyed. The well cover was surveyed, and TOC is estimated to be 6-inches below the cover.

Map labels:

MW-4 1,039.83

MW-6 1,044.88

MW-1 1,045.36

MW-2 1,041.58

MW-5 1,043.81

Contour labels: 1,042 · 1,043 · 1,044 · 1,045 · 1,044 · 1,043 · 1,042

N

Scale in Feet

0   300   600

CDM Smith

Potentiometric Surface

Fire Station 19

(HSI #10844)

Duluth, Gwinnett County, Georgia

BK53411 PG0249

FILED & RECORDED
CLERK SUPERIOR COURT
GWINNETT COUNTY, GA.

2015 MAR -4 PM 1:09

RICHARD ALEXANDER. CLERK

301604

Gwinnett County Fire Station 19
3275 North Berkeley Lake Road
Duluth, GA 30096
Gwinnett County Deed Book 05422, Page 00222

AFFIDAVIT

THIS AFFIDAVIT is made this __3RD__ day of __MARCH__, 2015 by Gwinnett County (hereinafter referred to as "Declarant").

WITNESSETH:

WHEREAS, Declarant owns the property more particularly described as Tax Map and Parcel 6-267-028 as recorded in the Gwinnett County Deed Book 05422, Page 00222 (the "Property") and;

WHEREAS, The Director of the Georgia Environmental Protection Division directed Declarant to file this Affidavit by letter dated January 15, 2015 pursuant to O.C.G.A § 44-2-20.

NOW, THEREFORE, Declarant does hereby state and avert as follows:

The Property has been listed on the state's Hazardous Site Inventory and has been designated as needing corrective action due to the presence of hazardous wastes, hazardous constituents, or hazardous substances regulated under state law. Contact the property owner or the Georgia Environmental Protection Division for further information concerning this property. This notice is provided in compliance with the Georgia Hazardous Site Response Act and Georgia Voluntary Remediation Program.

IN WITNEES WHEREOF, Declarant has signed and sealed this Affidavit, on the day, month, and year first above written.
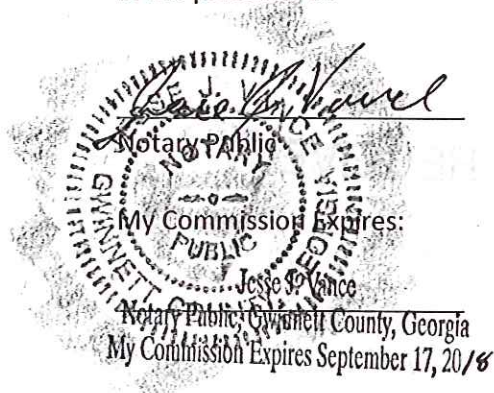
Signed, sealed and delivered
In the presence of:

Notary Public

My Commission Expires:

Jesse J. Vance
Notary Public, Gwinnett County, Georgia
My Commission Expires September 17, 20/8

0016776

DECLARANT

Gwinnett County

By: _____

Name: *RICHARD SCHOECK*

Title: *DIVISION DIRECTOR OF PROJECT CONTROLS, GWINNETT COUNTY DEPARTMENT OF WATER RESOURCES*

Technical Memorandum
Soil Electron Microprobe Analyses

Fire Station 19, HSI #10844
Duluth, Gwinnett County, Georgia

March 17, 2015

A Voluntary Investigation and Remediation Plan (VIRP) has been approved for the Fire Station 19 site. The VIRP recommended evaluation of the arsenic bioaccessibility in soil. Electron microprobe (EMP) analyses were recommended to support the bioaccessibility evaluation and to evaluate potential sources of the arsenic in soil at Fire Station 19. All sampling and the bioaccessibility/EMP analyses were completed from October 21st to November 24th of 2014. The Georgia Environmental Protection Division (EPD) approved the VIRP on January 15, 2015. This technical memorandum presents the results of the EMP analyses.

1.0 Introduction

Twenty soil samples were collected from Fire Station 19 on October 21, 2014. The samples were delivered to CDM Smith's Denver laboratory for preparation and then delivered to the University of Colorado Geological Sciences Laboratory for analyses. All twenty samples were analyzed for total arsenic and additional bioaccessibility testing. The bioaccessibility testing is reported in a separate technical memorandum. Ten of the twenty samples were selected for EMP analyses. The prepared samples selected for EMP analyses all exceeded the 100 mg/kg concentration requirement for EMP analyses and were representative of the observed arsenic range in the prepared samples (103 mg/kg – 554 mg/kg). The EMP results were used to support the bioaccessibility evaluation and to evaluate potential arsenic sources at Fire Station 19.

2.0 EMP Analyses Methods and Analyses

EMP analyses were performed on 10 soil samples. The methodology used and samples analyzed are summarized in this section.

2.1 EMP Overview

Samples were analyzed on a JEOL 8600 Superprobe located in the Department of Geological Sciences, University of Colorado, Boulder, Colorado. The analyses were conducted by Dr. John W. Drexler, Professor Emeritus. Analyses on single particulate grains and single precipitate crystals were accomplished using an EMP. Not only can analyses be made on particles as small as 1 micron (μm), but the EMP also provides a visual picture of the particulate at magnifications ranging from 40x to 300,000x. The visual mode is referred to as the "backscatter mode." The resulting "picture" is recorded and referred to as a "photomicrograph". Information about the relative atomic number of the compounds can be obtained in the backscatter mode due to the contrast in brightness between the low atomic number compounds and the compounds with high atomic numbers. For example, metal (e.g., iron, zinc, copper, etc.) compounds or metal containing particulates, which have high mean atomic numbers,

tend to be bright white in backscatter mode, while silica compounds, with lower mean atomic numbers, are gray and organic carbon is nearly black. Direct visual inspection of the particulate also provides information on the associations, morphology, and any reaction rims on the particles; all of which provide insight into the bioaccessibility, geochemical history and source of the sample.

2.2 EMP Methodology

2.2.1 Sample Preservation and Drying

Samples were received at CDM Smith's laboratory in Denver, Colorado in October 2014 where they were air dried, homogenized and sieved to collect the <250 µm fraction. Splits of the <250 µm fraction were sent to the University of Colorado Laboratory for Environmental and Geological Sciences (LEGS) in Boulder, Colorado. The samples were prepared and analyzed according to the standard operating procedure (SOP) for EMP (see Attachment A). This SOP is summarized in the following sections.

2.2.2 Sample Mount Preparation

At LEGS, a 1 gram split of each sample (the <250 µm fraction) was used to prepare epoxy grain mounts (see figure). The procedure for preparing the mounts included pouring the sample into a 1-inch diameter mold and covering with a thin layer of air-cured epoxy. The grains were then blended with the epoxy using a disposable wood stirring rod and additional epoxy was added. After curing at room temperature, the mount was removed and ground flat, forming a cross sectional cut through the grains. Polishing of the mount was performed using successively finer grades of oil-based diamond paste. The final step in the preparation of the grain mounts was to apply a thin carbon coating to the surface of the mount or "puck" in order to allow proper conduction during microprobe analysis. The pucks were then stored in the glove box until the EMP analyses could be performed.

2.2.3 Operating Conditions

Operating conditions included a 15 KeV (15,000 electron volts), accelerating voltage, 17 NanoAmp cup current, and a 1 to 2 µm beam size. Certified pure element standards were used to determine phase compositions. Wavelength dispersive spectrometer (WDS) crystals were used for the analyses: LIF for zinc, copper, and iron; TAP for arsenic, silicon, and aluminum; PET for antimony lead, cadmium, and sulfur; and LDE for oxygen.

2.2.4 Analytical Procedure

Sample pucks were scanned for arsenic-containing minerals using backscattered electron images. The scanning was performed manually by systematically traversing from left to right until the edge of the mount was reached. The puck was then moved up one field of view and scanned from right to left. This process was repeated until the whole mount was scanned or at a minimum, 100 arsenic containing grains were identified.

Typically, the magnification used for scanning samples was 40-100X and 300-600X, depending on the individual sample's grain size distribution. The higher magnification allowed the smallest identifiable (1 to 2 µm) phases to be found. Once a candidate particle was identified, the backscatter image was optimized to differentiate any different phases within the particle or its association. Identification of the metal-bearing phases was performed using both energy-dispersive and wavelength-dispersive spectrometers set for analyses of arsenic, iron, and oxygen. A macro was prepared to take into account the absorption of x-rays by elements such as iron using a ZAF correction (Sweatman and Long 1969).

2.3 Samples Analyzed

A total of 10 sieved samples were analyzed by EMP, as shown in Table 1 below. The arsenic results shown in Table 1 below are for soil particles less than 250 µm and in general, the sieved soils results have slightly higher arsenic concentrations than the total arsenic concentrations in soil (not sieved) reported in the Corrective Action Plan.

Table 1 - Samples Analyzed by EMP

Sample ID	mg/kg As (<250 µm sample)
SB-3	554
SB-14	310
SB-21	144
SB-24	314
SB-25	207
SB-27	205
SB-30	134
SB-34	103
SB-39	127
SB-52	195
SB-3	554
SB-14	310

All six sieved samples with reported values of IVBA (in vitro bioaccessibility) above the detection limit were analyzed by EMP. An additional four samples were also analyzed by EMP. These were selected based on arsenic concentration and spatial distributions.

2.4 Quantitative Analysis

All samples were analyzed for a quantitative full speciation of the arsenic bearing grains. Overall a minimum of 100 arsenic-bearing grains or particles were identified and recorded for each of the ten samples. The following information was recorded for each grain:

- The identification of the phase (determined from the elemental energy dispersive spectra, rate counts, or analytical results);

- The longest dimension of the grain in µm; and

- Association of the grain (free or liberated, included within a second phase, cemented or rimming).

The amount of arsenic within each phase was determined by analysis of a representative number of grains. For each sample, the following quantities were determined:

- The frequency of the grains of each phase in percent; and

- The relative arsenic mass within each phase in percent.

The grain frequency was determined by dividing the number of grains of the phase in question by the total number of grains counted times 100%.

However, because the percentages of metals (arsenic in this case) within each phase and the sizes of the grains are different, grain frequency can be misleading. For example, small abundant grains with low metals concentrations would be over-represented compared to large grains with high metals concentrations. The size, arsenic concentration and density of the phase were used to calculate the relative arsenic mass in each phase. The equations and parameters used to calculate the relative mass are provided in Attachment A.

3.0 Summary of EMP Results
3.1 Phases, Associations, Frequency and Relative Mass

Attachment B provides the information collected for each of the 10 samples. On the left hand side of each page is the list of all arsenic-bearing grains or particles identified. A minimum of 100 particles were identified and as previously discussed, the following information was recorded for each particle (or grain):

- Phase or form;

- Association (liberated, rimming, cemented); and

- Size (longest dimension in μm).

The arsenic bearing phases identified included:

- Iron oxyhydroxides (Fe or FeOOH);

- Manganese oxyhydroxides (Mn or MnOOH);

- Clay;

- Cesium oxyhydroxides (Ce or CeO2); and

- Others, including iron phosphates and sulfates.

Overall 1,093 arsenic containing particles were identified in the 10 samples (note: a minimum of 100 particles were identified in each sample; this is not the total number of arsenic containing particles but provides an adequate number to statistically represent the phase distribution in each sample; see

Attachment A). The following Table 2 provides a summary of the various phases present in all 10 samples.

Table 2 - Number of Particles and Frequency of Phases

Phase	Number of Particles	Frequency (%)
FeOOH	1,033	94.5
MnOOH	28	2.56
CeO2	27	2.47
Clay	3	0.27
Other	2	0.18
Total	1,093	100.0

As shown, the vast majority of arsenic bearing particles (94.5 %) were iron oxyhydroxides. Overall the iron oxyhydroxides contributed 98 percent of the arsenic mass in the samples. The size of the arsenic containing iron oxyhydroxide particles ranged from 1 to 78 µm (longest dimension) and the mean length was 12.9 µm. The information concerning number of particles in each phase, mean dimensions, range of dimensions and relative mass in each phase for each sample is provided on the right hand side of each of individual sample sheets in Attachment B. Attachment B also provides the relative mass and frequency of each of the phases in each sample in graphical form.

3.2 Photomicrographs and Energy Dispersive Spectra

Typically a minimum of five representative photomicrographs and energy dispersive spectra (EDS) were recorded for each sample. Attachment C provides examples of each of the various types of association observed for the iron oxyhydroxides.

Photomicrographs 1, 2, 3 and 4 provide images of liberated arsenic containing iron oxyhydroxides grains. Liberated or free particles were the most abundant type of phases observed (see Attachment B). As previously discussed, the lighter (or whiter) colors represent higher molecular weight phases (in this case iron). The lighter color (grey) grains are typically aluminum silicates or quartz particles. Grains of quartz are observed in most photomicrographs (e.g., Photomicrograph 4) based on their angular nature and overall uniform grey color (typically the whiteness scale is adjusted so that quartz, SiO2, is a grey color).

The EDS is provided below each photomicrograph. The major elemental composition is identified on the EDS and confirms that the major element in the grains is iron (largest peak – identified as "Fe" on all spectra and as the Fe L Alpha spectral peak at an energy of 6.40 KeV on Photomicrograph 1; and also a minor peak identified as the Fe K beta peak at an energy of 7.06 KeV). As observed on the EDS, arsenic is also present (identified as "As" on all spectra and as the As L alpha, As L beta and As K alpha spectral peaks at energies of 1.28, 1.32 and 10.54 KeV on Photomicrograph 1). Other peaks identified on the EDS include those of aluminum (Al), silicon (Si), and titanium (Ti). These elements are typical mineral forming elements and may be incorporated into iron oxyhydroxides.

A scale bar is also provided on the lower left part of the photomicrographs. As shown, the individual iron oxyhydroxides were 10 to 20 µm in diameter on Photomicrographs 1 to 4. The relatively small sizes and liberated form of these particles probably represent dissolved iron that precipitated from the aqueous phase within the soils resulting in individual solid iron oxyhydroxide particles. As

discussed later in this document, arsenic will adsorb onto or coprecipitate with the iron oxyhydroxides.

Photomicrographs 5, 6 and 7 provide images of arsenic bearing iron oxyhydroxides phases that are cemented or rimming. Photomicrograph 5 shows a particle that appears to be a precipitate or cement of iron oxyhydroxides (observe the various areas or layers of precipitates). Photomicrograph 6 shows an iron oxyhydroxide rimming other particles. Photomicrograph 7 shows a precipitated or cemented iron oxyhydroxide. Again, the various layers of precipitation can be observed. These phases of iron oxyhydroxides formed on or around existing soil particles.

Photomicrographs 8 and 9 provide images of arsenic bearing iron oxyhydroxides that have a "cellular" structure. These iron oxyhydroxides may have resulted from a biological process or been adsorbed onto organic matter with a cellular structure.

The amount of arsenic in each of the various types of iron oxyhydroxide and manganese oxyhydroxide phases was quantitatively determined on selected particles using the WDS. The arsenic concentration in the iron oxyhydroxides averaged 0.009 wt% (90 mg/kg) with a standard deviation of 0.009. A large range in concentrations was observed with some particles as high as 0.04 wt% (400 mg/kg). Manganese oxyhydroxide was the only other phase in significant amount and it averaged 0.0011 wt% arsenic with a standard deviation of 0.0008. As shown on Table 1, the overall average arsenic concentration in the 10 samples (<250 μm fraction) was 229 mg/kg (0.0229 wt%). The Table 1 analyses resulted from digestion and ICP-MS analyses of the soil samples (EPA SW-846 methods 3050 and 6020). The WDS analyses were conducted on selected individual particles and probably indicates that the larger sized arsenic containing iron oxyhydroxides grains analyzed by WDS had the larger arsenic concentrations (i.e., 400 mg/kg) resulting in an overall average concentration of 229 mg/kg by ICP-MS.

4.0 Evaluation of Potential Sources
4.1 Arsenic Geochemistry and Fate Mechanisms

Overall the photomicrographs show arsenic associated with iron oxyhydroxides. Iron hydroxides have an extremely high capacity to adsorb dissolved arsenic from the aqueous solutions. Granular ferric oxides (GFOs) are the most widely used media to remove arsenic from drinking water. As shown in Pierce and Moore (1981 – see Attachment D), the arsenic adsorption capacity is pH dependent and also depends upon the arsenic species present in aqueous phase (arsenite, +3 species, or arsenate, +5 species). At a neutral pH, 34,000 mg of arsenate (as arsenic) can theoretically be adsorbed per kg of iron hydroxide (see Pierce and Moore 1981). As stated, the amount of adsorption also depends upon the species of arsenic present in the aqueous phase. The species present depends upon the oxidation-reduction (redox) conditions and pH of the aqueous phase. A discussion of the geochemistry, species and fate mechanism of arsenic is provided in Attachment E. As discussed and shown on the Eh-pH diagram in Attachment E, arsenic occurs in two oxidation states in natural waters, +3 (arsenite) and +5 (arsenate). As(+5) exists under more oxidizing conditions and is present predominantly as a negatively charged ion (anion) above a pH of about 2. As(+5) is predominantly monovalent (charge of -1) over the pH range of 2 to 7 ($H_2AsO_4^-$), divalent from pH 7 to 11.5 ($HAsO_4^{2-}$) and trivalent at pH values above 11.5 (AsO_4^{3-}). As(+3) exists under more reducing conditions and is present predominantly as a neutral species ($H_3AsO_3^0$) below a pH of about 9.

$H_2AsO_3^-$ and $HAsO_3^{-2}$ do not become important until the pH exceeds 9 su, which is higher than observed in the vast majority of natural waters.

Overall, the arsenic containing iron oxyhydroxide phases observed were the result of arsenic (either arsenite or arsenate) in aqueous phase and subsequent incorporation into the iron oxyhydroxide solid phase by either of two mechanisms:

- Adsorption of dissolved arsenic onto existing solid iron oxyhydroxide phases in the soil; and

- Co-precipitation or adsorption of the arsenic with the precipitation of dissolved aqueous phase iron (forming solid iron oxyhydroxides).

Observation of the photomicrographs shows that the second mechanism may be the most prevalent mechanism. However, either mechanism must have a soluble source of the arsenic. The source of soluble arsenic is discussed in the next section. Water (e.g., rainfall and infiltration into the soil) must also be available to solubilize and transport the arsenic.

It should be noted that no relic of mineral bound arsenic such as observed in arsenic-containing pyrite was observed.

4.3 Potential Sources of Arsenic

As discussed in the previous section, the resulting forms of arsenic containing particles resulted from dissolved arsenic in aqueous solution. A soluble source of arsenic is necessary to provide the dissolve aqueous phase arsenic. A variety of solid and aqueous phase arsenic compound could have provided the aqueous phase arsenic. Arsenous and arsenic acid exist as liquids and have been used in the past to manufacture solid arsenic compounds. However, these acids are typically not used in wide spread application directly. Various solid phase arsenic compounds have been used extensively in the past as pesticides and herbicides. These compounds may include lead arsenate, calcium or sodium arsenate (or arsenite), copper-arsenic compounds and organic arsenic containing compounds. Typically the solid compounds were dissolved in water for direct spray application to the plants. Calcium arsenate was once a common herbicide and insecticide used mainly for protection of cotton crops. In 1942 alone, over 38,000,000 kg of calcium arsenate was produced in the United States (Kirk-Othmer Encyclopedia of Chemical Technology 1995). In particular, calcium arsenate was used on cotton in Georgia. The following information is from A Century of Georgia Agriculture, 1850 – 1950 (Willard Range 1954):

- "Boll weevil damage, moreover, remained rather slight for several years, causing only a 3 per cent loss by 1916 and only a 10 per cent loss by 1918. Apathy toward the impending disaster was encouraged by the announcement of The United States Department of Agriculture that effective weevil control measures (dusting with calcium arsenate) had been discovered."

- "Beginning with the crop of 1919, however, boll weevil damage became serious; and during 1921-23 it became disastrous when Georgia's yield fell 30 per cent to 45 per cent below normal each year. In some counties the yield dropped from around 200 pounds to 80 pounds per acre. The state's total crop dropped from an average of about 1,500,000 to 2,000,000 bales per year to a low in 1923 of less than 600,000 bales. Greene County, which in 1919 had produced more than 20,000 bales, produced only 333 bales in 1923. For the years 1920-1924 Georgia's cotton yield per acre averaged only 133 pounds, the lowest five-year average

recorded since the 1870's and one of the lowest in the state's history. With this turn of events, Georgia's general apathy toward the "winged demon" turned into panic. The State Department of Entomology annually loaded "Peddler Cars" with calcium arsenate, sidetracked a car at virtually every important railroad station, and begged farmers to buy the poison. In 1923, 150 cars of poison were sold. Newspapers also broadcast control measures and bankers appealed to their debtors to accept the proffered advice."

Review of past aerial photographs and historic topographic maps in the area of Fire Station 19 show the presence of row crops (probably cotton).

The typical calcium arsenate used for pesticide control was typically 80 – 85 % $Ca_3(AsO_4)_2$. The remaining amounts were typically calcium carbonate or hydroxide or waters of hydration. Literature values (Robinson 1918) report a solubility of this compound in water between 130 and 140 mg/L. Thermodynamic calculations show that the solubility is highly pH dependent. At a pH of 7, the calculated theoretical solubility is 2,800 mg/L as arsenic (see Attachment F). Overall, calcium arsenate represents a highly soluble compound that will result in elevated aqueous concentrations of arsenic when exposed to or dissolved in water.

5.0 Conclusions

As discussed above, calcium arsenate was used historically in Georgia as an insecticide on cotton to control boll weevils. Calcium arsenate is highly soluble in water and was probably applied to the cotton (or other crops) as a liquid solution. Some solid phase calcium arsenate probably resulted in the soils at shallow depth due to evaporation of the liquid solutions. This solid phase calcium arsenate could subsequently be dissolved by infiltration (rainfall) and transported deeper into the soils. The dissolved arsenic is attenuated in the soil by precipitation of iron oxyhydroxides (iron existing in the soils could also be dissolved by infiltration) or adsorption onto existing iron oxyhydroxide minerals in the soil. This dissolution and precipitation/adsorption mechanism for arsenic in the soils is illustrated by the soil sample collected at Fire Station 19 (see Corrective Action Plan). Most soil samples collected from 0.5 – 2 ft bgs had elevated arsenic concentrations. At selected locations, the sample collected at a depth of 4 feet had higher concentrations than the sample from the shallower depth (e.g., SB-7: 14.5 mg/kg from 0.5 -2 ft and 491 mg/kg at 4 ft; SB-13: 37.4 mg/kg from 0.5 to 2 ft and 274 mg/kg at 4 ft; SB-38: 98.3 mg/kg from 0.5 to 2 ft and 371 mg/kg at 4 ft). These examples probably indicate that arsenic applied to the surface soils has been transported to deeper soil layers. However as also discussed, the existing iron minerals in the soils or newly precipitated iron oxyhydroxides are an important attenuation mechanism. As a result of such attenuation and/or lack of saturated vadose zone flow, no arsenic is present in the groundwater at the site (arsenic concentrations were below detection in monitoring wells MW-1 screened from 35-40 ft and MW-2 screened from 30-35 ft).

6.0 References

Pierce, M.L. and Moore, C. B. 1982. Adsorption of Arsenite and Arsenate on Amorphous Iron Hydroxide. Water Res. Vol 16. pp 1247 – 1253

Kirk-Othmer Encyclopedia of Chemical Technology. 1995. 4th ed. New York, NY. John Wiley and Sons. p 528.

Range, Willard. 1954. A Century of Georgia Agriculture 1850 – 1950. University of Georgia Press. Athens, Georgia.

Robinson, R.H. 1918. The Calcium Arsenates. Oregon Agricultural College Experiment Station. Station Bulletin 131.

Sweatman, T.R. and J.V.P. Long. 1969. Quantitative electron-probe microanalysis. Journal of Petrology. v. 10, p. 332-379.

Attachment A

EMPA-SOP

1.0 OBJECTIVES

The objectives of this Standard Operating Procedure (SOP) are to specify the proper methodologies and protocols to be used during metal speciation of various solid samples including; tailings, slags, sediments, dross, bag house dusts, wipes, paint, soils, and dusts for metals. The metal speciation data generated from this SOP may be used to assess the solid samples as each phase relates to risk. Parameters to be characterized during the speciation analyses include particle size, associations, stoichiometry, frequency of occurrence of metal-bearing forms and relative mass of metal-bearing forms. This electron microprobe (EMPA) technique, instrument operation protocols and sample preparation to be used during implementation of the Metals Speciation SOP are discussed in the following sections.

2.0 BACKGROUND

To date, numerous metal-bearing forms of soils have been identified from various environments within western mining districts (Emmons et al., 1927; Drexler, 1991 per. comm.; Drexler, 1992; Davis et al., 1993; Ruby et al., 1994; CDM, 1994; WESTON, 1995). This listing does not preclude the identification of other metal-bearing forms, but only serves as an initial point of reference. Many of these forms are minerals with varying metal concentrations (e.g., lead phosphate, iron-lead oxide, and slag). Since limited thermodynamic information is available for many of these phases and equilibrium conditions are rarely found in soil environments, the identity of the mineral class (e.g., lead phosphate) will be sufficient and exact stoichiometry is not necessary.

It may be important to know the particle-size distribution of metal-bearing forms in order to assess potential risk. It is believed that particles less than 250 microns (µm) are most available for human ingestion and/or inhalation (Bornschein, et al., 1987). For this study, the largest dimension of any one metal-bearing form will be measured and the frequency of occurrence weighted by that dimension. Although not routinely performed, particle area can be determined, it has been shown (CDM, 1994) that data collected on particle area produces similar results. These measurements add a considerable amount of time to the procedure, introduce new sources of potential error and limit the total number of particles or samples that can be observed in a study.

Mineral association may have profound effects on the ability for solubilization. For example, if a lead-bearing form in one sample is predominantly found within quartz grains while in another sample it is free in the sample matrix, the two samples are likely to pose significantly different risk levels to human health. Therefore, associations of concern include the following:

1. free or liberated
2. inclusions within a second phase
3. cementing rimming

3.0 SAMPLE SELECTION

Samples should be selected and handled according to the procedure described in the Project Plan. Unless help in determination of sample selection and frequency is requested by the client it is their responsibility to provide a "representative" number of samples to the laboratory for analyses.

4.0 SCHEDULE

A schedule for completion of projects performed under this Metals Speciation SOP will be provided in writing or verbally to the contractor along with monthly reporting requirements if large projects are performed. These schedules are based on an aggressive analytical program designed to ensure that the metals speciation analyses are completed in a timely period. Monthly reports are expected to reflect schedule status.

5.0 INSTRUMENTATION

Speciation analyses will be conducted at the Laboratory for Environmental and Geological Studies (LEGS) at the University of Colorado, Boulder or other comparable facilities. Primary equipment used for this work will include:

Electron Microprobe (JEOL 8600) equipped with four wavelength spectrometers, energy dispersive spectrometer (EDS), BEI detector and the Geller, dQuant data processing system. Geller dPict hardware may be used for image storage and processing. An LEDC spectrometer crystal for carbon and LDE-1 crystal for oxygen analyses are essential.

6.0 PRECISION AND ACCURACY

The precision of the EMPA speciation will be evaluated based on sample duplicates analyzed at a frequency of 10% as selected by the laboratory, however the client may also submit "blind" duplicates for analyses. The precision of the data generated by the "EMPA point count" will be evaluated by calculating RPD values for all major (>20% frequency) phases, comparing the original result with the duplicate result. If the duplicate analyses are from samples that have produced at least 100 total particles it is expected that all (100%) of the dominant species (representing 60% of frequency) be found in both, and that their individual frequency of occurrence not vary by more than 30% , relative. In the evaluation of the method precision it is most important to consider the variation in results among all samples studied for a particular media, since the overall particle count is very large Data generated by the "EMPA point count" will be further evaluated statistically based on the methods of Mosimann (1965) at the 95% confidence level on the frequency data following Equation 1.

$$E_{0.95} = 2P(100\text{-}P)/N$$

Where: $E_{0.95}$ = Probable error at the 95% confidence level

P = Percentage of N of an individual metal-bearing phase based on percent length frequency

N = Total number of metal-bearing grains counted

Accuracy of quantitative metal analyses on non-stoichimetric metal phases is based on established EMPA procedures, and data reduction, Heinrich, 1981 and is generally 1-2% relative. All quantitative analyses will be performed using a series of certified mineral standards. In general, site-specific concentrations for these variable, metal-bearing forms will be determined by performing "peak counts" on the appropriate wavelength spectrometer. Average concentrations will then be used for further calculations. Data on specific gravity will be collected from referenced databases or estimated based on similar compounds.

7.0 PERSONNEL RESPONSIBILITY

The analysts will carefully read this SOP prior to any sample examination.

It is the responsibility of the laboratory supervisor and designates to ensure that these procedures are followed, to examine quality assurance (QA) samples and replicate standards, and to check EDS and WDS calibrations. The laboratory supervisor will collect results, ensure they are in proper format, and deliver them to the contractor.

Monthly reports summarizing all progress, with a list of samples speciated to date with data analyses sheets (DAS), will be submitted each month.

It is also the responsibility of the laboratory supervisor to notify the contractor representative of any problems encountered in the sample analysis process.

8.0 SAMPLE PREPARATION

Grain mounts (1.5 inches in diameter) of each sample will be prepared using air-cured epoxy. Previous work (CDM, 1994, Weston, 1995) found that neither using mono-layer mounts nor repetitive exposure of deeper layers within the epoxy puck produced speciation results outside those errors observed from single sample duplicates. Once a sample is well stirred within the epoxy minimal settling was observed. This grain mounting technique is appropriate for most speciation projects, however polished thin-sections, paint chips, dust wipes, or filters may be prepared in a similar manner. The grain mounting is performed as follows:

1. Log the samples for which polished mounts will be prepared.
2. Inspect all disposable plastic cups, making sure each is clean and dry.
3. Label each "mold" with its corresponding sample number.
4. All samples will be split to produce a homogeneous 1-4 gram sample.
5. Mix epoxy resin and hardener according to manufacturer's directions.

6. Pour 1 gram of sample into mold. Double check to make sure sample numbers on mold and the original sample container match. Pour epoxy into mold to just cover sample grains.
7. Use a new wood stirring stick with each sample, carefully blend epoxy and grains so as to coat all grains with epoxy.
8. Set molds to cure at ROOM TEMPERATURE in a clean restricted area. Add labels with sample numbers and cover with more epoxy resin. Leave to cure completely at room temperature.
9. One at a time remove each sample from its mold and grind flat the back side of the mount.
10. Use 600 grit wet abrasive paper stretched across a grinding wheel to remove the bottom layer and expose as many mineral grains as possible. Follow with 1000 grit paper.
11. Polish with 15 um oil-based diamond paste on a polishing paper fixed to a lap. Use of paper instead of cloth minimizes relief.
12. Next use 6um diamond polish on a similar lap.
13. Finally polish the sample with 1um oil-based diamond paste on polishing paper, followed by 0.05 um alumina in water suspension. The quality should be checked after each step. Typical polishing times are 30 minutes for 15 um, 20 minutes for 6 um, 15 minutes for 1 um, and 10 minutes for 0.05 um.

    NOTE: use low speed on the polishing laps to avoid "plucking" of sample grains.

14. Samples should be completely cleaned in an ultrasonic cleaner with isopropyl alcohol or similar solvent to remove oil and fingerprints.
15. To ensure that no particles of any metal are being cross-contaminated during sample preparation procedures, a blank (epoxy only) mold will be made every 20th sample (5% of samples) following all of the above procedures. This mold will then be speciated along with the other samples.
16. Each sample must be carbon coated. Once coated, the samples should be stored in a clean, dry environment with the carbon surface protected from scratches or handling.

9.0 GEOCHEMICAL SPECIATION USING ELECTRON MICROPROBE

All investigative samples will also be characterized using EMPA analysis to determine the chemical speciation, particle size distribution and frequency for several target metals.

10.1 Concentration Prescreening

All samples will be initially examined using the electron microprobe to determine if the number of particles are too great to obtain a representative count. The particle counting will be considered representative if the entire sample (puck) has been traversed about the same time in which the counting criteria are achieved.

If this examination reveals that one metal is highly abundant (> 10,000 mg/kg in concentration), clean quartz sand ($SiO2$) will be mixed with the sample material. The sand should be certified to be free of target analytes. The quartz sand should be added to an aliquot of the investigative sample, then mixed by turning the sample for a minimum of one hour, or until the sample is fully

homogenized. The initial mass of the investigative sample aliquot, and the mass of the quartz addition must be recorded on the Data Analysis Sheet (DAS).

10.2 Point Counting

Counts are made by traversing each sample from left-to-right and top-to-bottom as illustrated in Figure 10-1. The amount of vertical movement for each traverse would depend on magnification and CRT (cathode-ray tube) size. This movement should be minimized so that NO portion of the sample is missed when the end of a traverse is reached. Two magnification settings generally are used. One ranging from 40-100X and a second from 300-500X. The last setting will allow one to find the smallest identifiable (1-2 micron) phases.

Figure 10-1
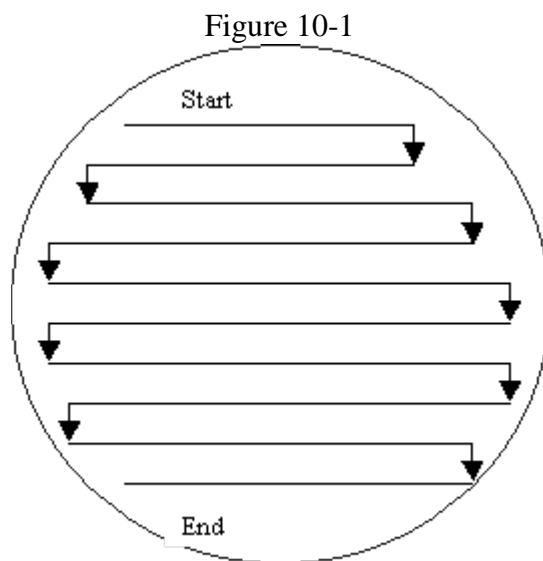
The portion of the sample examined in the second pass, under the higher magnification, will depend on the time available, the number of metal-bearing particles, and the complexity of metal mineralogy. A maximum of 8 hours will be spent on each analysis or a total particle count of 100.

The point counting procedure in petrography is a well established technique as outlined by Chayes, 1949. For our procedure we have simply substituted the electron microprobe for a simple petrographic microscope as a means of visually observing a particle and identifying its composition using the attached x-ray analyzers. The operator error (identification of phase and sizing) is generally negligible. However the particle counting error can be significant depending on the total number of particles counted and the individual component (species) percent. Based on studies in El-Hinnawi, 1966, it was shown that the relative error of a point count based on 100 total particles versus one of 300 total particles is only 10% and 6% , respectively (for a species representing 30% of the count). It is our belief that this small decrease in error is not justified when cost and time of analysis are considered, and that it is much more beneficial to increase your total sample population and address representativeness.

10.3 Data Reduction

Analysts will record data as they are acquired from each sample using the LEGS software (10-3), which places all data in a spreadsheet file format. Columns have been established for numbering the metal-bearing phase particles, their identity, size of longest dimension in microns, along with their association (L = liberated, C= cementing, R = rimming, I = included) (10-2). The analyst may also summarize his/her observations in the formatted data summary files.

The frequency of occurrence and relative metal mass of each metal-bearing form as it is distributed in each sample will be depicted graphically as a frequency bar-graph (10-5). The particle size distribution of metal-bearing forms will be depicted in a histogram. Size-histograms of each metal-bearing form can be constructed from data in the file.

Data from EMPA will be summarized using two methods. The first method is the determination of FREQUENCY OF OCCURRENCE. This is calculated by summing the longest dimension of all the metal-bearing phases observed and then dividing each phase by the total.

Equation 2 will serve as an example of the calculation.

$$F_M \text{ in phase-1} = \frac{\Sigma(PLD)_{\text{phase 1}}}{\Sigma(PLD)_{\text{phase-1}} + \Sigma(PLD)_{\text{phase-2}} + \Sigma(PLD)_{\text{phase-n}}}$$

Where:

F_M = Frequency of occurrence of metal in a single phase.

PLD = An individual particle's longest dimension.

$\%F_M$ in phase-1 = F_M in phase-1 * 100

These data thus illustrate which metal-bearing phase(s) are the most commonly observed in the sample or relative volume percent.

The second calculation used in this report is the determination of RELATIVE METAL MASS. These data are calculated by substituting the PLD term in the equation above with the value of MM. This term is calculated as defined below.

$$M_M = FM * SG * ppm_M$$

Where:

M_M = Mass of metal in a phase

SG = Specific Gravity of a phase

ppm_M = Concentration in ppm of metal in a phase

The advantage in reviewing the RELATIVE METAL MASS determination is that it gives one information as to which metal-bearing phase(s) in a sample are likely to control the total bulk concentration for a metal of interest. For example, PHASE-1 may comprise 98% relative volume of the sample; however, it has a low specific gravity and contains only 1,000 parts per million

(ppm) arsenic. PHASE-2 comprised 2% of the sample, has a high specific gravity, and contains 850,000 ppm of arsenic. In this example it is PHASE-2 that is the dominant source of arsenic to the sample.

Finally, a concentration for each phase is calculated. This quantifies the concentration of each metal-bearing phase. This term is calculated as defined below (Eq. 4).

$$ppm_M = M_M * \text{Bulk metal concentration in ppm}$$

10.4 Analytical Procedure

A brief visual examination of each sample will be made, prior to EMPA examination. This examination may help the operator by noting the occurrence of slag and/or organic matter. Standard operating conditions for quantitative and qualitative analyses of most metal-bearing forms are given in Figure 10-4. However, it is the responsibility of the operator to select the appropriate analytical line (crystal/KeV range) to eliminate peak overlaps and ensure proper identification/quantification of each analyte. Quality control will be maintained by analyzing duplicates at regular intervals (Section 6).

The backscattered electron threshold will be adjusted so that all particles in a sample are seen. This procedure will minimize the possibility that low metal-bearing minerals may be overlooked during the scanning of the polished grain mount. The scanning will be done manually in a manner similar to that depicted in Figure 10-1. Typically, the magnification used for scanning all samples except for airborne samples will be 40-100X and 300-600X. The last setting will allow the smallest identifiable (1-2 um) phases to be found. Once a candidate particle is identified, then the backscatter image will be optimized to discriminate any different phases that may be making up the particle or defining its association. Identification of the metal-bearing phases will be done using both EDS and WDS on an EMPA, with spectrometers typically peaked at sulfur, oxygen, carbon and the metal(s) of concern (M). The size of each metal-bearing phase will be determined by measuring in microns the longest dimension.

As stated previously, a maximum of 8 hours will be spent in scanning and analyzing each mount. For most speciation projects the goal is to count between 100-300 particles. In the event that these goals are achieved in less than 8 hours, particle counting may be stopped so the analyst may move to another sample in order to increase the sample population.

Quantitative Analyses

Quantitative analyses are required to establish the average metal content of the metal-bearing minerals, which have variable metal contents as: Iron-(M) sulfate, Iron-(M) oxide, Manganese-(M) oxide, organic, and slag. These determinations are important, especially in the case of slag, which is expected to have considerable variation in their dissolved metal content.

Results will be analyzed statistically to establish mean values. They may also be depicted as histograms to show the range of metal concentrations measured as well as the presence of one or more populations in terms of metal content. In the later case, non-parametric statistics may have

to be used or the median value has to be established.

Associations

The association of the metal-bearing forms will be established from the backscattered electron images. Particular attention will be paid in establishing whether the grains are totally enclosed, encapsulated or liberated. The rinds of metal-bearing grains will be identified. Representative photomicrographs of backscatter electron images establishing the association of the principal metal-bearing forms will be obtained for illustration purposes.

10.5 Instrument Calibration and Standardization

The WDS will have spectrometers calibrated for the metal of concern, carbon, oxygen and sulfur on the appropriate crystals using mineral standards. The EDS will have multi-channel analyzer (MCA) calibrated for known peak energy centroids. Calibration will be performed so as to have both low (1.0-3.0 KeV) and high (6.0-9.0 KeV) energy peaks fall within 0.05 KeV of its known centroid.

The magnification marker on the instrument will be checked once a week. This will be performed by following manufacturer instructions or by measurement of commercially available grids or leucite spheres. Size measurements must be within 4 microns of certified values.

Initial calibration verification standards (ICVs) must be analyzed at the beginning of each analytical batch or once every 48 hours, whichever is more frequent. A set of mineral or glass standards will be run quantitatively for the metal of concern, sulfur, oxygen and carbon. If elemental quantities of the ICVs do not fall within +/- 5% of certified values for each element, the instrument must be recalibrated prior to analysis of investigative samples.

The metal-bearing forms in these samples will be identified using a combination of EDS, WDS and BEI. Once a particle is isolated with the backscatter detector, a 5-second EDS spectra is collected and peaks identified. The count rates for the metal(s) of concern, sulfur, carbon and oxygen can be either visually observed on the wavelength spectrometers or K-ratios calculated.

10.6 Documentation

Photomicrographs along with EDS x-ray spectra should be taken for each sample, at a rate of 5% (1 photograph per 20 particles counted), or a minimum of 10 per sample and submitted with the results. Particles selected for photography must be recorded on the EMPA graph, as well as in the Electron Micrograph Logbook. Any additional photographs should be labeled as "opportunistic".

A 128x128 (minimum) binary image in ".tif" format may be stored. Recorded on each photomicrograph will be a scale bar, magnification, sample identification , date and phase identification. Abbreviations for the identified phases can be used. A final list must be submitted with the laboratory report.

10.0 PERSONAL HEALTH AND SAFETY

Each individual operating the electron microprobe instruments will have read the "Radiation Safety Handbook" prepared by the University and follow all State guidelines for operation of X-ray equipment.

Latex gloves and particulate masks will be worn during preparation of sample cups. All material that comes in contact with the samples or used to clean work surface areas will be placed in poly-bags for disposal.

11.0 FINAL REPORT

A final laboratory report will be provided to the Contractor. The report will include all EMPA data including summary tables and figures. Individual sample data will be provided on disk.

Speciation results will include: 1) a series of tables summarizing frequency of occurrence for each metal phase identified along with a confidence limit; 2) summary histograms of metal phases identified for each waste type; 3) a summary histogram of particle size distribution in each waste type; and 4) a summary of metal phase associations. Representative .tif images and EDS x-ray spectra will also be included in the final report.

12.0 REFERENCES

Bornschein, R.L., P.A. Succop, K.M. Kraft, and C.S. Clark. 1987. Exterior surface lead dust, interior lead house dust and childhood lead exposure in an urban environment. In D.D. Hemphil, Ed., Trace Substances in Environmental Health XX Proceedings of the University of Missouri's 20th Annual Conference. June 1986, pp 322-332. University of Missouri, Columbia, MO.

CDM (Camp Dresser and McKee). 1994. Metal Speciation Data Report, Leadville, CO. CERCLA Site. September, 1994.

Chayes, F., 1949, A simple point counter for thin section analysis. Am. Mineralogist, V. 34, p. 1.

Drexler, J.W. 1992. Speciation Report on the Smuggler Mine, Aspen CO., Prepared for EPA.

Davis, A., J.W. Drexler, M.V. Ruby, and A. Nicholson. 1993. The micromineralogy of mine wastes in relation to lead bioavailability, Butte, Montana. Environ. Sci. Technol. (In Press).

El-Hinnawi, E.E., 1966, Methods in chemical and mineral microscopy, Elsevier Publishing Co., New York, 222p.

Emmons, S.F., J.D. Irving, and G.F. Loughlin. 1927. Geology and Ore Deposits of the Leadville Mining District, Colorado. USGS Professional Paper 148.

Heinrich, K.F.J., 1981, Electron beam x-ray microanalysis. Van Nostrand-Reinhold Co., Dallas, 578p.

Mosimann, J.E. 1965. Statistical methods for the Pollen Analyst. In: B. Kummel and D. Raup (EDS.). Handbook of Paleontological Techniques. Freeman and Co., San Francisco, pp. 636-673.

Ruby, M.V., A. Davis, J.H. Kempton, J.W. Drexler, and P.D. Bergstrom. 1992. Lead bioavailability: Dissolution kinetics under simulated gastric conditions. Environ. Sci. Technol. 26(6): pp 1242-1248.

WESTON (Roy F. Weston, Inc.). 1995. Metal Speciation Interpretive Report, Leadville, CO. CERCLA Site. March, 1995.

Figure 10-2

NOTES	IDENTITY	SIZE Length-longest dimension (µm)	Liberated	Inclusions	ICemented	Rim

Figure 10-3

Figure 10-4

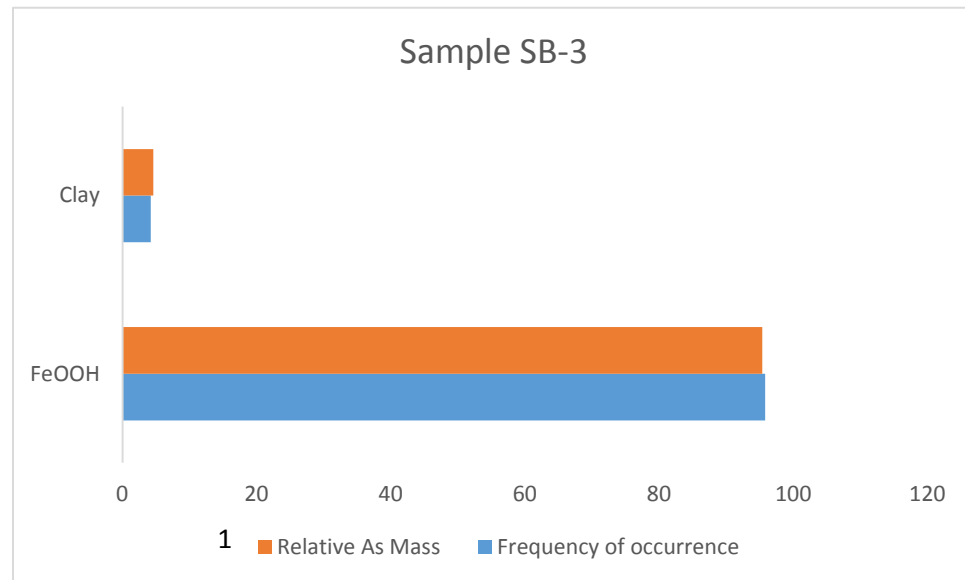|	WDS	EDS
Accelerating Voltage	15 KV	15-20 KV
Beam Size	1-2 microns	1-2 microns
Cup Current	10-30 NanoAmps	10-30 NanoAmps
Ev/Channel	N/A	10 or 20
Stage Tilt	N/A	Fixed
Working Distance	N/A	Fixed
MCA Time Constant	N/A	7.5-12 microseconds
X-Ray Lines	S K-alpha PET O K-alpha LDE1 C K-alpha LDEC Zn K-alpha PET As L-alpha TAP Cu K-alpha LIF Cd L-alpha PET Pb M-alpha PET Pb L-alpha LIF In L-alpha PET Tl L-alpha LIF Hg L-alpha LIF Se L-alpha LIF Sb L-alpha PET	S K-alpha 2.31 KeV O K-alpha 0.52 KeV C K-alpha 0.28 KeV Pb M-alpha 2.34 KeV Pb L-alpha 10.5 KeV Zn K-alpha 8.63 KeV Cu K-alpha 8.04 KeV As K-alpha 10.5 KeV As L-alpha 1.28 KeV Cd L-alpha 3.13 KeV In L-alpha 3.28 KeV Tl M-alpha 2.27 KeV Tl L-alpha 10.26 KeV Hg L-alpha 9.98 KeV Hg M-alpha 2.19 KeV Se L-alpha 1.37 KeV Sb L-alpha 3.60 KeV

Figure 10-5
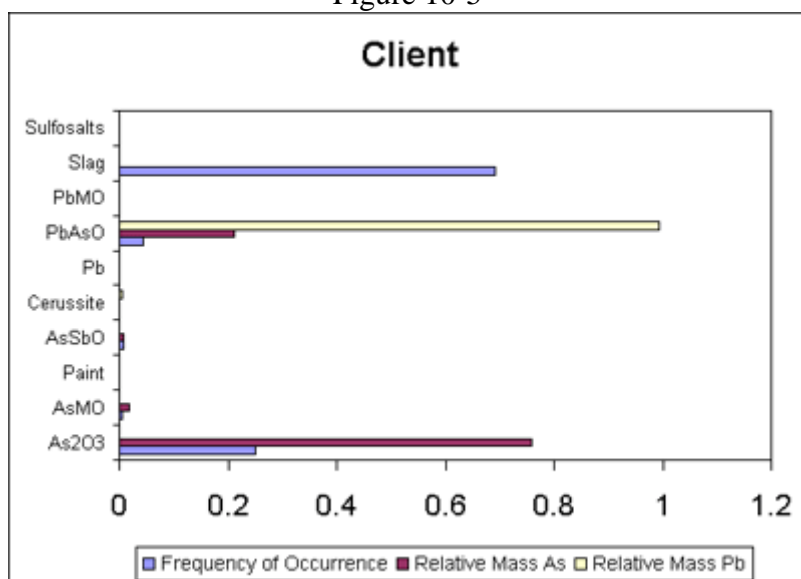
Attachment B

SB-3

Form	Association	Size (micron)
Fe	Liberated	3
Clay	Liberated	15
Fe	Liberated	5
Fe	Liberated	22
Fe	Liberated	14
Fe	Liberated	9
Fe	Liberated	12
Fe	Rimming	5
Fe	Liberated	6
Fe	Liberated	3
Fe	Rimming	6
Fe	Liberated	11
Clay	Liberated	21
Fe	Cemented	13
Fe	Liberated	10
Fe	Liberated	7
Fe	Rimming	6
Fe	Liberated	14
Fe	Liberated	12
Fe	Liberated	5
Fe	Liberated	10
Fe	Liberated	17
Fe	Liberated	19
Fe	Liberated	18

Form	Number	Mean	Std-Dev	Range low	Range high
total	102	13.24	7.48	3	34
FeOOH	99	13.06	7.5	3	34
Clay	3	19	3.46	15	21

Form %	(linear) freq %	Rm As %	Error-95%
FeOOH	95.78	95.38	3.9
Clay	4.22	4.62	3.9

Sample SB-3

1 ■ Relative As Mass ■ Frequency of occurrence

Fe	Liberated	9
Fe	Liberated	20
Fe	Liberated	27
Fe	Liberated	10
Fe	Liberated	14
Fe	Liberated	10
Fe	Rimming	16
Fe	Liberated	11
Fe	Liberated	6
Fe	Liberated	9
Fe	Rimming	31
Fe	Liberated	5
Fe	Cemented	14
Fe	Liberated	4
Fe	Liberated	3
Fe	Rimming	28
Fe	Liberated	15
Fe	Liberated	8
Fe	Liberated	21
Fe	Liberated	24
Fe	Liberated	18
Fe	Rimming	9
Fe	Liberated	16
Fe	Liberated	9
Fe	Liberated	29
Fe	Liberated	14
Fe	Rimming	21
Fe	Liberated	13
Fe	Liberated	12
Fe	Liberated	14
Fe	Liberated	7

Fe	Liberated	7
Fe	Liberated	11
Fe	Liberated	28
Fe	Liberated	34
Fe	Liberated	10
Fe	Liberated	13
Fe	Liberated	17
Fe	Rimming	6
Fe	Rimming	3
Fe	Liberated	7
Fe	Liberated	9
Fe	Liberated	5
Fe	Liberated	16
Fe	Liberated	15
Fe	Rimming	9
Fe	Liberated	7
Fe	Liberated	14
Fe	Liberated	8
Fe	Liberated	12
Fe	Liberated	8
Fe	Liberated	21
Fe	Liberated	23
Fe	Liberated	13
Fe	Liberated	5
Fe	Rimming	4
Clay	Liberated	21
Fe	Rimming	13
Fe	Liberated	11
Fe	Liberated	12
Fe	Cemented	6
Fe	Liberated	14

Fe	Liberated	6
Fe	Liberated	11
Fe	Liberated	10
Fe	Liberated	34
Fe	Rimming	18
Fe	Liberated	10
Fe	Rimming	13
Fe	Rimming	34
Fe	Liberated	13
Fe	Liberated	12
Fe	Liberated	26
Fe	Liberated	7
Fe	Liberated	4
Fe	Liberated	15
Fe	Liberated	26
Fe	Rimming	19

SB-14

Form	Association	Size (microns)
Fe	Rimming	28
Fe	Rimming	4
Fe	Liberated	5
Fe	Liberated	10
Fe	Liberated	8
Fe	Liberated	16
Fe	Liberated	5
Fe	Rimming	7
Fe	Liberated	20
Fe	Liberated	21
Fe	Liberated	9
Fe	Liberated	5
Fe	Liberated	4
Fe	Rimming	24
Fe	Liberated	4
Fe	Rimming	13
Fe	Liberated	44
Fe	Liberated	15
Fe	Liberated	32
Fe	Liberated	16
Fe	Liberated	4
Fe	Liberated	8
Fe	Liberated	30
Fe	Liberated	5

Form	Number	Mean	Std-Dev	Range low	Range high
total	114	14.8	12.58	2	78
FeOOH	106	15.46	12.77	2	78
MnOOH	3	9.33	2.52	7	12
CeO2	5	4	1.87	2	7

Form %	(linear) freq %	Rm As %	Error-95%
FeOOH	97.15	98.9	3.05
MnOOH	1.66	0.6	2.35
CeO2	1.19	0.5	1.99

Sample SB-14

Legend: ■ Relative As Mass ■ Frequency of Occurrence
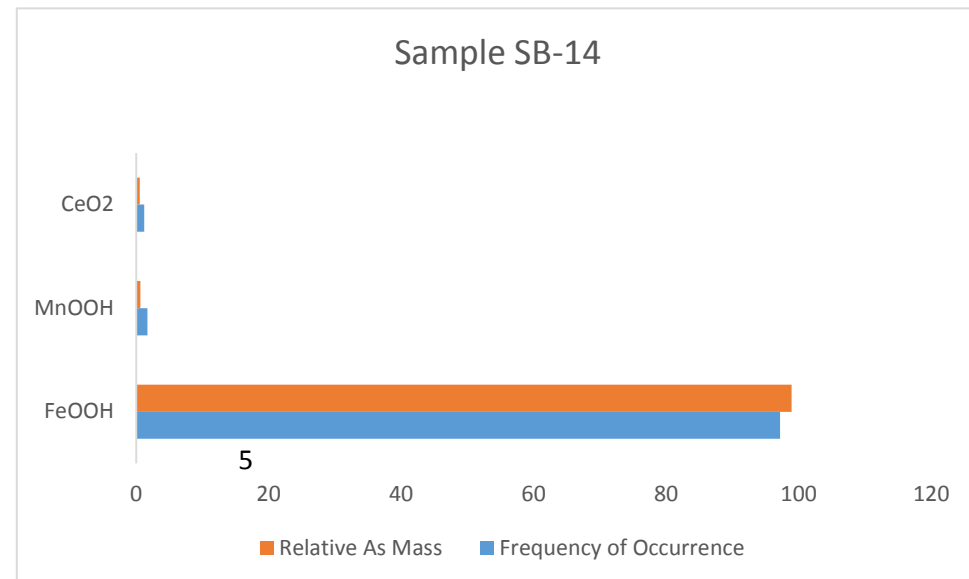
Fe	Rimming	3
Fe	Rimming	2
Fe	Liberated	14
Fe	Liberated	7
Fe	Liberated	10
Fe	Rimming	4
Fe	Liberated	11
Fe	Liberated	9
Fe	Liberated	6
Fe	Rimming	25
Fe	Rimming	6
Fe	Rimming	6
Fe	Rimming	6
Fe	Rimming	6
Fe	Rimming	6
Fe	Liberated	25
Fe	Rimming	10
Fe	Liberated	6
Fe	Liberated	5
Fe	Liberated	22
Fe	Liberated	6
Fe	Liberated	17
Fe	Liberated	6
Fe	Liberated	5
Fe	Liberated	19
Fe	Liberated	17
Fe	Liberated	18
Mn	Liberated	7
Fe	Liberated	5
Fe	Liberated	24
Fe	Rimming	32

Fe	Liberated	43
Fe	Liberated	45
Fe	Rimming	8
Fe	Liberated	18
Fe	Liberated	14
Fe	Liberated	4
Fe	Liberated	25
Fe	Liberated	23
Fe	Rimming	9
Fe	Liberated	4
Fe	Liberated	7
Fe	Liberated	30
Fe	Rimming	16
Fe	Liberated	4
Fe	Liberated	14
Fe	Liberated	5
Fe	Liberated	2
Fe	Liberated	4
Fe	Liberated	8
Fe	Liberated	11
Fe	Liberated	14
Fe	Liberated	23
Fe	Liberated	28
Fe	Liberated	10
Fe	Liberated	7
Fe	Rimming	55
Fe	Liberated	12
Fe	Rimming	14
Fe	Liberated	27
Fe	Liberated	6
Fe	Liberated	36

Fe	Liberated	33
Fe	Liberated	11
Fe	Liberated	8
Fe	Liberated	10
Fe	Liberated	45
Fe	Liberated	35
Fe	Liberated	6
Fe	Liberated	24
Fe	Liberated	15
Fe	Liberated	5
Fe	Liberated	11
Mn	Liberated	9
Fe	Liberated	31
Fe	Liberated	12
Fe	Liberated	26
Fe	Liberated	16
Fe	Liberated	13
Fe	Liberated	10
Fe	Liberated	22
Mn	Liberated	12
Fe	Liberated	15
Fe	Liberated	12
Fe	Liberated	78
Ce	Liberated	2
Ce	Liberated	3
Ce	Liberated	7
Ce	Liberated	4
Ce	Liberated	4

SB-21

Form	Association	Size (microns)
Fe	Liberated	4
Fe	Liberated	7
Fe	Liberated	10
Fe	Cemented	27
Fe	Liberated	5
Fe	Liberated	4
Fe	Liberated	4
Fe	Liberated	8
Fe	Rimming	3
Fe	Liberated	2
Fe	Liberated	7
Fe	Liberated	36
Mn	Liberated	16
Fe	Liberated	11
Fe	Liberated	4
Fe	Liberated	3
Fe	Liberated	12
Fe	Cemented	26
Fe	Rimming	48
Fe	Rimming	14
Fe	Liberated	5
Fe	Liberated	9
Fe	Liberated	8
Mn	Liberated	64

Form	Number	Mean	Std-Dev	Range low	Range high
total	115	14.44	13.41	1	73
FeOOH	106	14.51	12.9	2	73
MnOOH	6	19	22.37	5	64
CeO2	3	3	2	1	5

Form	(linear) freq %	Rm As %	Error-95%
FeOOH	92.59	98.84	4.79
MnOOH	6.86	0.92	4.62
CeO2	0.54	0.24	1.34

Sample SB-21

9

Relative As Mass   Frequency of Occurrence
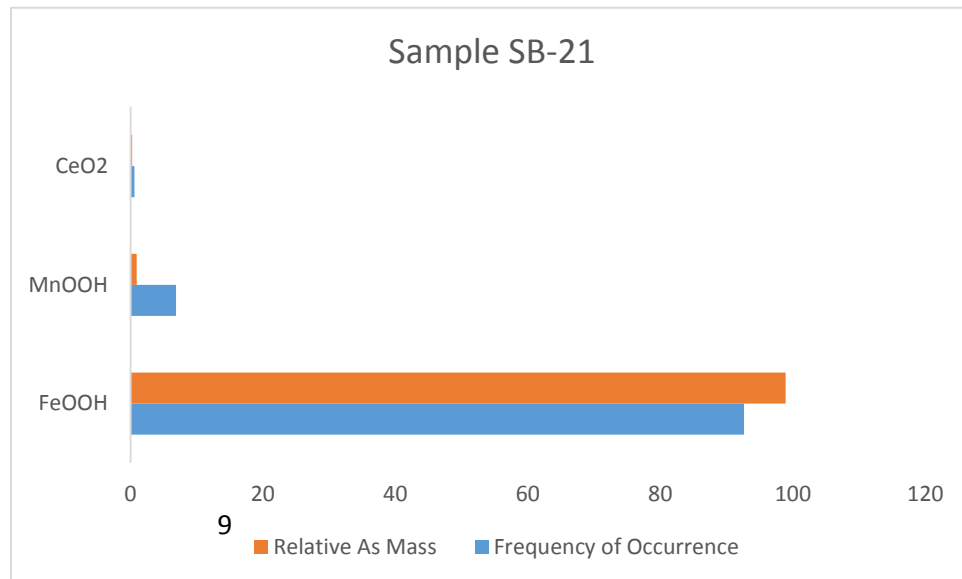
Fe	Liberated	12
Fe	Liberated	15
Fe	Cemented	9
Fe	Liberated	13
Fe	Liberated	8
Mn	Rimming	11
Fe	Cemented	32
Fe	Liberated	12
Fe	Rimming	7
Fe	Cemented	4
Fe	Rimming	24
Fe	Liberated	13
Fe	Liberated	4
Fe	Liberated	3
Fe	Liberated	16
Fe	Liberated	21
Fe	Rimming	9
Fe	Liberated	8
Fe	Liberated	13
Fe	Liberated	9
Fe	Rimming	5
Fe	Liberated	4
Fe	Liberated	10
Fe	Liberated	73
Fe	Liberated	14
Fe	Liberated	7
Fe	Liberated	6
Fe	Liberated	8
Fe	Liberated	14
Fe	Liberated	40
Mn	Liberated	5

Fe	Rimming	8
Fe	Liberated	19
Fe	Liberated	25
Fe	Liberated	6
Mn	Liberated	11
Fe	Cemented	8
Mn	Liberated	7
Fe	Liberated	13
Fe	Rimming	8
Fe	Liberated	22
Fe	Liberated	35
Fe	Liberated	5
Fe	Rimming	5
Fe	Liberated	6
Fe	Liberated	14
Fe	Liberated	24
Fe	Rimming	16
Fe	Liberated	17
Fe	Liberated	7
Fe	Liberated	4
Fe	Liberated	6
Fe	Liberated	9
Fe	Liberated	9
Fe	Liberated	13
Fe	Liberated	9
Fe	Rimming	3
Fe	Liberated	8
Fe	Liberated	7
Fe	Liberated	6
Fe	Liberated	46
Fe	Liberated	34

Fe	Liberated	20
Fe	Liberated	33
Fe	Liberated	10
Fe	Liberated	11
Fe	Liberated	5
Fe	Liberated	2
Fe	Liberated	4
Fe	Liberated	21
Fe	Liberated	10
Fe	Liberated	7
Fe	Liberated	18
Fe	Liberated	11
Fe	Rimming	19
Fe	Liberated	9
Fe	Liberated	5
Fe	Liberated	27
Fe	Liberated	14
Fe	Liberated	6
Fe	Liberated	7
Fe	Liberated	35
Fe	Liberated	28
Fe	Liberated	17
Fe	Liberated	13
Fe	Cemented	44
Fe	Liberated	38
Fe	Cemented	62
Ce	Liberated	1
Ce	Liberated	3
Ce	Liberated	5

SB-24

Form	Association	Size (microns)
Mn	Liberated	9
Fe	Liberated	4
Fe	Liberated	11
Mn	Liberated	9
Fe	Liberated	2
Fe	Liberated	4
Fe	Liberated	11
Fe	Liberated	11
Fe	Liberated	8
Fe	Liberated	8
Fe	Liberated	5
Fe	Liberated	14
Fe	Rimming	4
Fe	Rimming	3
Fe	Cemented	6
Fe	Rimming	4
Fe	Liberated	8
Fe	Liberated	10
Fe	Liberated	9
Fe	Liberated	14
Fe	Liberated	10
Fe	Liberated	12
Fe	Liberated	17

Form	Number	Mean	Std-Dev	Range low	Range high
total	106	11.52	7.73	1	46
MnOOH	7	10.57	5.38	4	19
FeOOH	95	11.88	7.91	1	46
CeO2	4	4.5	1	4	6

Form %	(linear) freq %	Rm As %	Error- 95%
MnOOH	6.06	1.59	4.54
FeOOH	92.47	97.74	5.02
CeO2	1.47	0.67	2.29

Sample SB-24
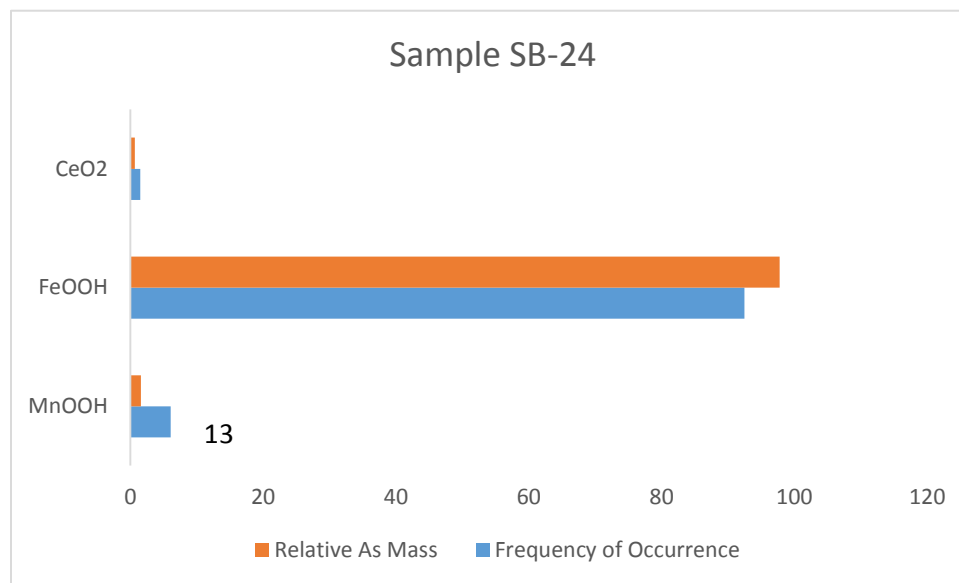
Fe	Liberated	14
Fe	Liberated	9
Fe	Liberated	40
Fe	Liberated	13
Fe	Liberated	9
Fe	Cemented	23
Fe	Liberated	7
Fe	Liberated	9
Fe	Liberated	24
Fe	Liberated	5
Fe	Liberated	7
Fe	Liberated	12
Fe	Liberated	10
Fe	Cemented	6
Fe	Liberated	14
Fe	Liberated	8
Fe	Liberated	23
Fe	Liberated	26
Fe	Liberated	9
Fe	Liberated	7
Fe	Liberated	3
Fe	Liberated	11
Fe	Rimming	15
Mn	Liberated	5
Fe	Liberated	5
Fe	Cemented	22
Fe	Liberated	5
Fe	Liberated	6
Fe	Liberated	12
Fe	Liberated	5
Fe	Liberated	9

Fe	Liberated	29
Fe	Rimming	5
Fe	Liberated	7
Fe	Liberated	8
Fe	Liberated	4
Mn	Liberated	14
Fe	Rimming	16
Fe	Liberated	7
Fe	Liberated	20
Fe	Liberated	12
Fe	Rimming	6
Fe	Liberated	5
Fe	Liberated	1
Fe	Liberated	18
Fe	Liberated	8
Fe	Liberated	12
Fe	Liberated	13
Fe	Liberated	12
Fe	Liberated	10
Fe	Liberated	8
Fe	Liberated	14
Fe	Liberated	32
Fe	Liberated	23
Fe	Rimming	12
Fe	Cemented	13
Fe	Rimming	26
Mn	Liberated	19
Fe	Liberated	12
Fe	Liberated	14
Fe	Liberated	12
Fe	Liberated	3

Fe	Liberated	12
Fe	Rimming	15
Fe	Cemented	26
Fe	Liberated	10
Fe	Liberated	4
Fe	Liberated	9
Fe	Liberated	9
Fe	Liberated	4
Fe	Liberated	12
Fe	Liberated	11
Fe	Liberated	13
Mn	Cemented	4
Mn	Rimming	14
Fe	Liberated	20
Fe	Liberated	12
Fe	Liberated	21
Fe	Cemented	46
Ce	Liberated	6
Ce	Liberated	4
Ce	Liberated	4
Ce	Liberated	4

SB-25

Form	Association	Size (microns)
Fe	Liberated	13
Fe	Rimming	12
Fe	Rimming	19
Fe	Rimming	24
Fe	Rimming	14
Fe	Liberated	5
Fe	Liberated	3
Fe	Liberated	12
Fe	Rimming	11
Fe	Liberated	8
Fe	Liberated	7
Fe	Liberated	8
Fe	Liberated	6
Fe	Liberated	5
Fe	Liberated	8
Mn	Liberated	9
Fe	Liberated	15
Fe	Rimming	4
Fe	Liberated	7
Fe	Liberated	5
Fe	Cemented	9
Fe	Liberated	11
Fe	Liberated	9
Fe	Liberated	8

Form	Number	Mean	Std-Dev	Range low	Range high
total	107	11.79	8.77	1	42
FeOOH	102	11.77	8.37	1	42
MnOOH	2	8	0	7	9
FeSO4	1	41	0	41	41
CeO2	2	2	0	1	3

Form	(linear) freq %	Rm As %
%	%	%
FeOOH	95.17	93.42
MnOOH	1.27	0.46
FeSO4	3.25	6.01
CeO2	0.32	0.12

Sample SB-25
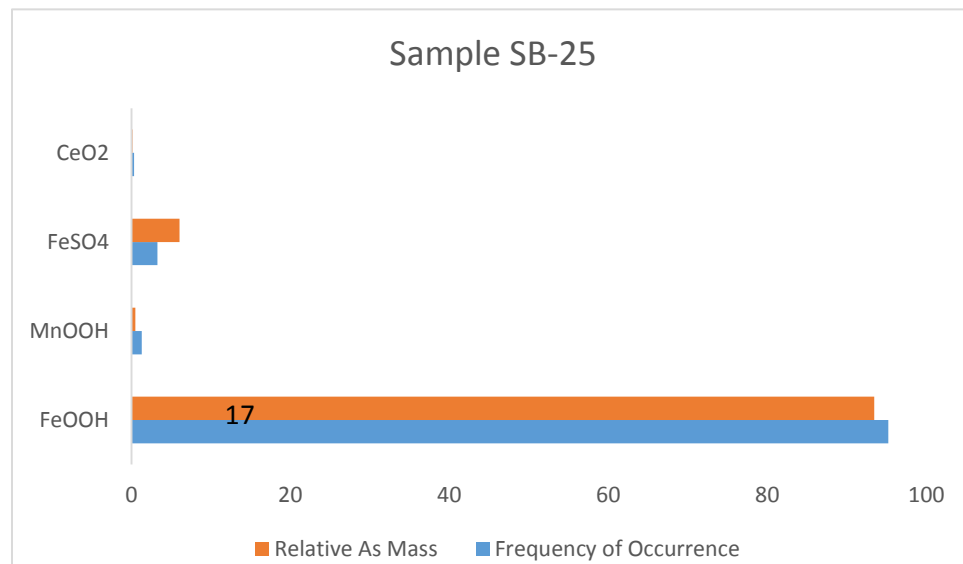
Fe	Liberated	6
Fe	Rimming	5
Fe	Liberated	11
Fe	Liberated	5
Fe	Liberated	20
Fe	Liberated	10
Fe	Liberated	15
Fe	Liberated	8
Fe	Liberated	35
Fe	Liberated	7
Fe	Liberated	2
Fe	Liberated	6
Fe	Liberated	28
Fe	Liberated	22
Fe	Liberated	5
Fe	Liberated	3
Fe	Liberated	25
Fe	Liberated	4
Fe	Liberated	5
Fe	Liberated	12
Sulf	Liberated	41
Fe	Liberated	18
Fe	Rimming	17
Fe	Liberated	23
Fe	Rimming	9
Fe	Liberated	12
Fe	Cemented	42
Fe	Liberated	14
Fe	Liberated	6
Fe	Liberated	3
Fe	Liberated	3

Fe	Liberated	16
Fe	Liberated	5
Fe	Liberated	9
Fe	Liberated	4
Fe	Liberated	4
Fe	Liberated	4
Fe	Liberated	4
Fe	Liberated	5
Fe	Liberated	41
Fe	Rimming	12
Fe	Liberated	13
Fe	Cemented	3
Fe	Liberated	4
Fe	Liberated	15
Fe	Liberated	30
Fe	Liberated	9
Fe	Liberated	8
Fe	Liberated	4
Fe	Rimming	13
Fe	Liberated	11
Fe	Liberated	9
Fe	Liberated	21
Fe	Rimming	25
Fe	Rimming	14
Fe	Liberated	9
Mn	Liberated	7
Fe	Liberated	10
Fe	Liberated	11
Fe	Liberated	22
Fe	Liberated	7
Fe	Liberated	24

Fe	Liberated	12
Fe	Liberated	10
Fe	Liberated	34
Fe	Liberated	14
Fe	Cemented	15
Fe	Liberated	11
Fe	Liberated	14
Fe	Liberated	24
Fe	Liberated	7
Fe	Rimming	13
Fe	Liberated	7
Fe	Liberated	5
Fe	Liberated	6
Fe	Liberated	17
Fe	Liberated	10
Fe	Liberated	12
Fe	Liberated	1
Fe	Liberated	1
Fe	Liberated	18
Ce	Liberated	1
Ce	Liberated	3

SB-27

Form	Association	Size (microns)
Fe	Liberated	41
Fe	Liberated	4
Fe	Liberated	14
Fe	Cemented	22
Fe	Rimming	11
Fe	Liberated	8
Fe	Liberated	4
Fe	Rimming	18
Fe	Liberated	6
Fe	Liberated	6
Fe	Rimming	6
Fe	Liberated	23
Fe	Liberated	12
Fe	Liberated	4
Fe	Liberated	25
Fe	Liberated	9
Fe	Rimming	7
Fe	Liberated	9
Fe	Cemented	18
Fe	Liberated	7
Fe	Liberated	5
Fe	Cemented	23
Fe	Liberated	5
Fe	Liberated	21

Form	Number	Mean	Std-Dev	Range low	Range high
total	110	14.26	10.98	2	55
FeOOH	103	14.7	11.16	2	55
MnOOH	4	11	2.94	7	14
CeO2	3	3.67	1.15	3	5

form	(linear) freq	Rm As	Error-
%	%	%	95%
FeOOH	96.49	99.02	3.44
MnOOH	2.8	0.66	3.09
CeO2	0.7	0.32	1.56

Sample SB-27

21
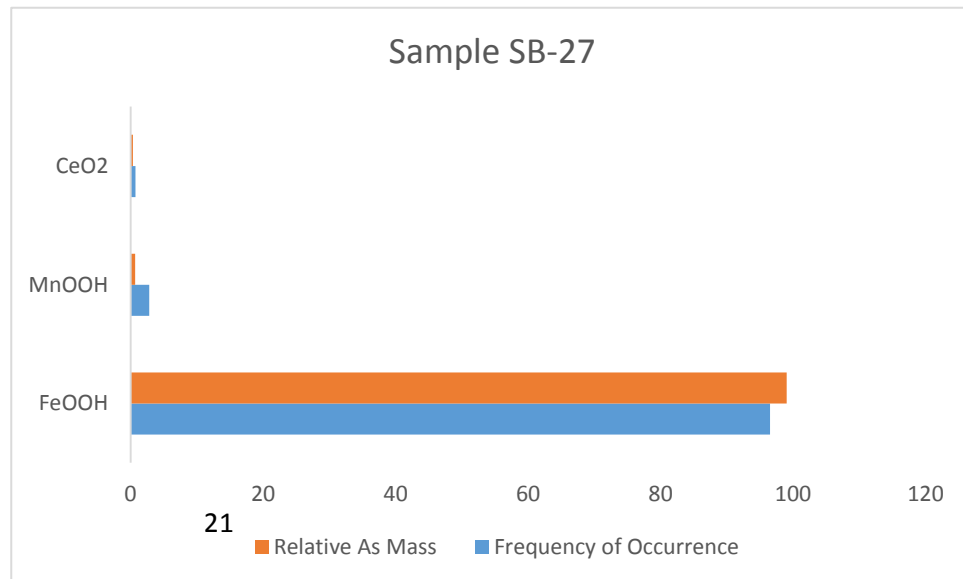
Fe	Liberated	14
Fe	Liberated	6
Mn	Liberated	7
Fe	Liberated	7
Fe	Liberated	12
Fe	Liberated	9
Fe	Liberated	11
Fe	Cemented	45
Fe	Liberated	7
Fe	Liberated	18
Fe	Liberated	8
Fe	Liberated	10
Fe	Cemented	9
Fe	Rimming	13
Fe	Liberated	11
Fe	Liberated	13
Fe	Liberated	35
Fe	Cemented	12
Mn	Rimming	14
Fe	Liberated	41
Fe	Cemented	11
Fe	Rimming	12
Fe	Liberated	5
Fe	Rimming	5
Fe	Liberated	36
Fe	Rimming	5
Fe	Liberated	50
Fe	Rimming	28
Fe	Liberated	9
Fe	Liberated	29
Fe	Liberated	18

Fe	Rimming	7
Fe	Cemented	14
Fe	Liberated	16
Fe	Rimming	9
Fe	Liberated	5
Fe	Cemented	4
Fe	Liberated	55
Fe	Liberated	15
Fe	Liberated	7
Fe	Liberated	8
Fe	Liberated	7
Fe	Rimming	9
Fe	Liberated	7
Fe	Liberated	9
Fe	Liberated	13
Fe	Liberated	11
Fe	Liberated	13
Fe	Liberated	4
Fe	Liberated	2
Fe	Liberated	5
Fe	Cemented	22
Fe	Liberated	15
Fe	Liberated	10
Fe	Liberated	40
Fe	Liberated	24
Fe	Cemented	13
Fe	Liberated	6
Fe	Liberated	23
Fe	Cemented	11
Fe	Liberated	14
Fe	Liberated	29

Fe	Rimming	23
Fe	Liberated	9
Fe	Liberated	30
Fe	Cemented	12
Fe	Liberated	10
Fe	Rimming	9
Fe	Rimming	49
Fe	Liberated	16
Fe	Liberated	8
Fe	Liberated	9
Fe	Liberated	12
Fe	Liberated	17
Fe	Cemented	12
Fe	Liberated	8
Fe	Liberated	8
Fe	Liberated	10
Fe	Liberated	9
Fe	Liberated	10
Fe	Liberated	29
Mn	Rimming	11
Mn	Rimming	12
Ce	Liberated	3
Ce	Liberated	3
Ce	Liberated	5

SB-30

Form	Association	Size(microns)
Fe	Liberated	13
Fe	Liberated	5
Fe	Liberated	6
Fe	Liberated	2
Fe	Cemented	5
Fe	Liberated	11
Fe	Liberated	6
Fe	Liberated	6
Fe	Liberated	4
Fe	Liberated	26
Fe	Cemented	41
Fe	Liberated	5
Fe	Rimming	12
Fe	Rimming	9
Fe	Liberated	20
Fe	Liberated	16
Fe	Liberated	7
Fe	Liberated	57
Fe	Liberated	8
Fe	Liberated	22
Fe	Liberated	8
Fe	Liberated	7
Fe	Liberated	9
Fe	Liberated	11

Form	Number	Mean	Std-Dev	Range low	Range high
total	100	12.66	10.98	1	65
FeOOH	98	12.56	11.01	1	65
MnOOH	2	17.5	0	9	26

Form %	(linear) freq %	Rm As %	Error- 95%
FeOOH	97.24	99.44	3.21
MnOOH	2.76	0.56	3.21
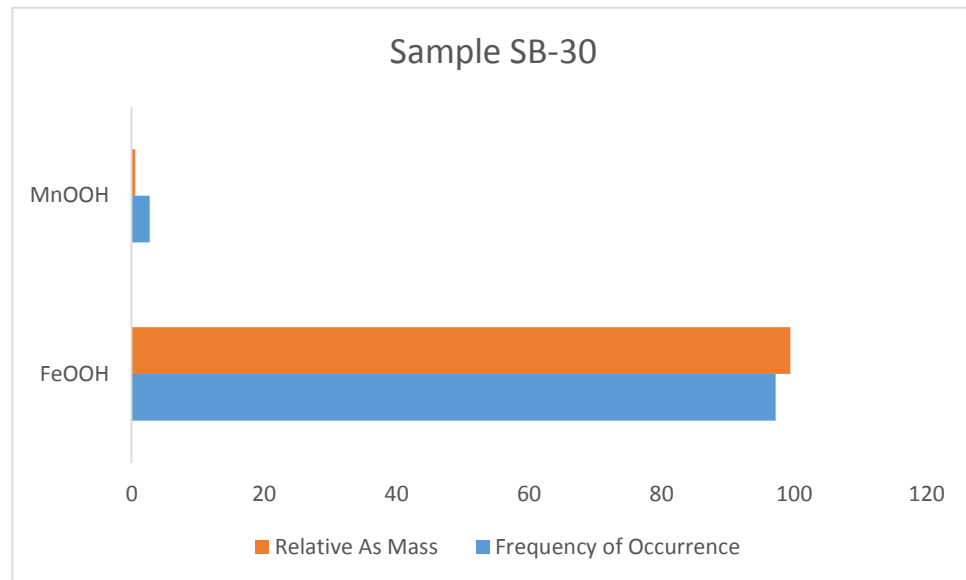
Sample SB-30

Relative As Mass   Frequency of Occurrence

25

Fe	Liberated	10
Fe	Liberated	10
Fe	Liberated	8
Fe	Liberated	5
Fe	Liberated	9
Fe	Liberated	7
Fe	Liberated	6
Fe	Liberated	13
Fe	Liberated	5
Fe	Liberated	7
Fe	Rimming	10
Fe	Liberated	12
Fe	Liberated	4
Fe	Liberated	22
Fe	Liberated	7
Fe	Liberated	20
Fe	Rimming	9
Fe	Liberated	5
Fe	Liberated	5
Fe	Liberated	7
Fe	Cemented	21
Fe	Liberated	30
Fe	Liberated	9
Fe	Liberated	8
Fe	Liberated	23
Fe	Liberated	12
Fe	Rimming	7
Fe	Liberated	14
Fe	Liberated	44
Fe	Liberated	9
Fe	Liberated	65

Fe	Liberated	19
Fe	Liberated	4
Fe	Liberated	4
Fe	Rimming	15
Fe	Liberated	6
Fe	Liberated	5
Fe	Cemented	2
Fe	Liberated	5
Fe	Liberated	10
Fe	Liberated	6
Fe	Liberated	9
Fe	Cemented	1
Fe	Cemented	11
Fe	Liberated	11
Fe	Liberated	9
Fe	Liberated	15
Fe	Liberated	23
Fe	Liberated	6
Fe	Liberated	7
Fe	Liberated	11
Fe	Liberated	28
Fe	Liberated	22
Fe	Liberated	14
Fe	Liberated	8
Fe	Liberated	8
Fe	Liberated	7
Mn	Cemented	26
Fe	Liberated	5
Fe	Liberated	1
Fe	Cemented	9
Fe	Liberated	11

Mn	Liberated	9
Fe	Rimming	11
Fe	Liberated	8
Fe	Liberated	20
Fe	Liberated	35
Fe	Liberated	8
Fe	Liberated	9
Fe	Liberated	5
Fe	Liberated	7
Fe	Liberated	8
Fe	Liberated	6
Fe	Liberated	27
Fe	Liberated	21
Fe	Liberated	35

SB-34

Form	Association	Size (microns)
Fe	Cemented	21
Fe	Liberated	3
Fe	Liberated	12
Fe	Liberated	25
Fe	Liberated	11
Fe	Liberated	9
Fe	Liberated	14
Fe	Liberated	9
Fe	Liberated	12
Fe	Liberated	16
Fe	Liberated	6
Fe	Liberated	4
Fe	Liberated	5
Fe	Liberated	8
Fe	Liberated	7
Fe	Liberated	9
Fe	Liberated	12
Fe	Liberated	7
Fe	Liberated	13
Fe	Liberated	6
Fe	Cemented	40
Fe	Liberated	12
Fe	Liberated	16
Fe	Liberated	20

Form	Number	Mean	Std-Dev	Range low	Range high
total	105	13.14	9.85	1	46
FeOOH	100	13.51	9.9	2	46
MnOOH	3	8.67	4.73	5	14
CeO2	2	1.5	0	1	2

Form %	(linear) freq %	Rm As %	Error- 95%
FeOOH	97.9	99.13	2.74
MnOOH	1.88	0.77	2.6
CeO2	0.22	0.1	0.89

Sample SB-34

29

Relative As Mass   Frequency of Occurrence
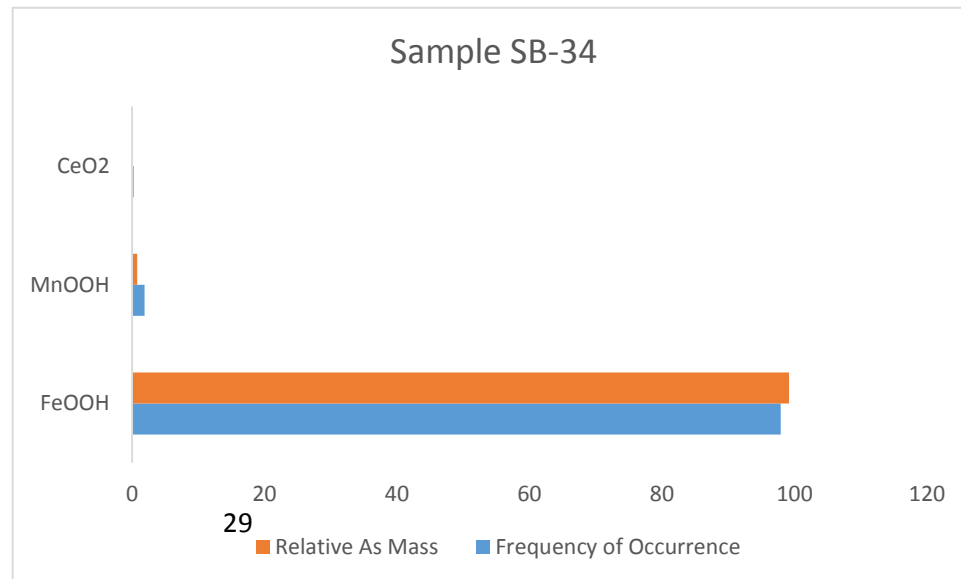
Fe	Liberated	5
Fe	Liberated	2
Fe	Liberated	14
Fe	Liberated	5
Fe	Liberated	5
Fe	Liberated	14
Fe	Liberated	6
Fe	Liberated	10
Fe	Liberated	13
Fe	Liberated	13
Fe	Liberated	6
Fe	Liberated	7
Fe	Liberated	15
Fe	Liberated	8
Fe	Liberated	10
Fe	Liberated	9
Fe	Liberated	11
Fe	Liberated	14
Fe	Liberated	12
Fe	Liberated	15
Fe	Liberated	6
Fe	Liberated	15
Fe	Rimming	22
Fe	Liberated	14
Fe	Liberated	45
Fe	Liberated	13
Fe	Liberated	10
Fe	Liberated	9
Fe	Liberated	5
Fe	Liberated	25
Fe	Liberated	21

Fe	Cemented	46
Fe	Liberated	10
Fe	Liberated	12
Fe	Liberated	15
Fe	Liberated	8
Mn	Liberated	7
Mn	Liberated	5
Fe	Liberated	7
Fe	Liberated	5
Fe	Liberated	5
Fe	Liberated	14
Fe	Liberated	6
Fe	Liberated	20
Fe	Liberated	8
Fe	Liberated	6
Fe	Liberated	10
Fe	Liberated	6
Fe	Liberated	17
Fe	Liberated	4
Fe	Liberated	6
Fe	Liberated	13
Fe	Liberated	28
Fe	Liberated	8
Fe	Liberated	32
Fe	Liberated	40
Fe	Liberated	10
Fe	Liberated	10
Fe	Liberated	12
Fe	Liberated	5
Fe	Liberated	3
Fe	Liberated	3

Fe	Liberated	3
Fe	Liberated	6
Fe	Rimming	7
Fe	Liberated	38
Mn	Liberated	14
Fe	Liberated	9
Fe	Liberated	39
Fe	Liberated	9
Fe	Liberated	18
Fe	Rimming	11
Fe	Liberated	40
Fe	Liberated	18
Fe	Liberated	32
Fe	Liberated	22
Fe	Liberated	9
Fe	Liberated	25
Fe	Liberated	20
Ce	Liberated	2
Ce	Liberated	1

SB-39

Form	Association	Size (microns)
Fe	Liberated	13
Fe	Liberated	8
Fe	Liberated	13
Fe	Liberated	7
Fe	Cemented	26
Fe	Cemented	23
Fe	Liberated	6
Fe	Liberated	28
Fe	Liberated	14
Fe	Liberated	4
Fe	Liberated	5
Fe	Liberated	7
Fe	Liberated	7
Fe	Liberated	12
Fe	Liberated	7
Fe	Rimming	10
Fe	Liberated	14
Fe	Liberated	4
Fe	Liberated	7
Fe	Liberated	11
Fe	Liberated	4
Fe	Liberated	5
Fe	Rimming	10
Mn	Rimming	22

Form	Number	Mean	Std-Dev	Range low	Range high
total	107	9.36	6.31	1	28
FeOOH	102	9.51	6.19	1	28
MnOOH	1	22	0	22	22
CeO2	4	2.5	1	2	4

Form %	(linear) freq %	Rm As %	Error-95%
FeOOH	96.81	99.21	3.33
MnOOH	2.2	0.34	2.78
CeO2	1	0.46	1.88

Sample SB-39

33

Relative As Mass   Frequency of Occurrence
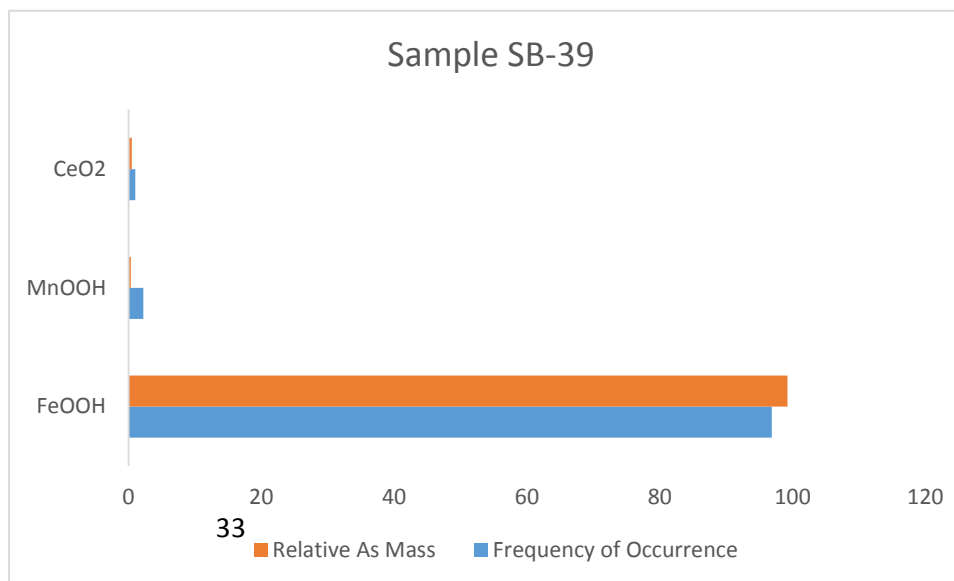
Fe	Liberated	9
Fe	Liberated	7
Fe	Liberated	7
Fe	Rimming	10
Fe	Liberated	9
Fe	Cemented	15
Fe	Cemented	8
Fe	Liberated	5
Fe	Liberated	5
Fe	Liberated	9
Fe	Cemented	16
Fe	Liberated	6
Fe	Liberated	20
Fe	Liberated	8
Fe	Liberated	10
Fe	Liberated	7
Fe	Cemented	11
Fe	Liberated	12
Fe	Rimming	6
Fe	Rimming	3
Fe	Liberated	20
Fe	Liberated	10
Fe	Liberated	13
Fe	Liberated	9
Fe	Liberated	13
Fe	Rimming	6
Fe	Liberated	6
Fe	Liberated	6
Fe	Liberated	7
Fe	Rimming	11
Fe	Liberated	24

Fe	Liberated	6
Fe	Liberated	8
Fe	Liberated	11
Fe	Cemented	1
Fe	Cemented	1
Fe	Cemented	1
Fe	Cemented	1
Fe	Cemented	1
Fe	Cemented	1
Fe	Cemented	1
Fe	Cemented	1
Fe	Cemented	1
Fe	Cemented	1
Fe	Cemented	1
Fe	Liberated	5
Fe	Cemented	14
Fe	Liberated	12
Fe	Rimming	11
Fe	Liberated	20
Fe	Liberated	22
Fe	Liberated	6
Fe	Liberated	11
Fe	Rimming	10
Fe	Liberated	9
Fe	Liberated	8
Fe	Liberated	7
Fe	Liberated	3
Fe	Liberated	12
Fe	Liberated	7
Fe	Liberated	27
Fe	Rimming	22

Fe	Liberated	9
Fe	Cemented	12
Fe	Liberated	5
Fe	Liberated	10
Fe	Liberated	11
Fe	Liberated	9
Fe	Rimming	17
Fe	Liberated	1
Fe	Liberated	9
Fe	Liberated	7
Fe	Liberated	9
Fe	Liberated	11
Fe	Liberated	9
Fe	Liberated	6
Fe	Liberated	25
Fe	Liberated	13
Fe	Liberated	12
Ce	Liberated	2
Ce	Liberated	2
Ce	Liberated	2
Ce	Liberated	4

SB-52

Form	Association	Size (microns)
Fe	Rimming	17
Fe	Liberated	14
Fe	Liberated	5
Fe	Rimming	9
Fe	Liberated	13
Fe	Liberated	10
Fe	Liberated	5
Fe	Rimming	37
Fe	Liberated	7
Fe	Rimming	9
Fe	Liberated	4
Fe	Rimming	4
Fe	Liberated	23
Fe	Liberated	5
Fe	Liberated	5
Fe	Liberated	9
Fe	Liberated	25
Fe	Liberated	6
Fe	Liberated	10
Fe	Liberated	4
Fe	Liberated	8
Fe	Cemented	2
Fe	Cemented	2
Fe	Cemented	2

Form	Number	Mean	Std-Dev	Range low	Range high
total	127	12.18	10.64	1	52
FeOOH	122	12.47	10.69	2	52
Phosphate	1	17	0	17	17
CeO2	4	2.25	2.5	1	6

Form %	(linear) freq %	Rm As %	Error-95%
FeOOH	98.32	99.22	2.24
Phosphate	1.1	0.54	1.81
CeO2	0.58	0.25	1.32

Sample SB-52

37

Relative As Mass   Frequency of Occurrence
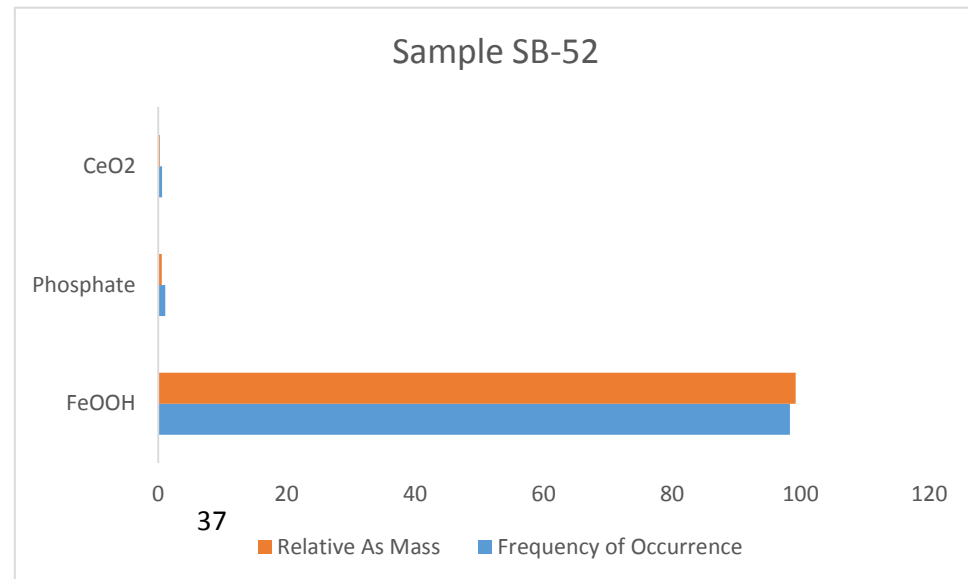
Fe	Cemented	2
Fe	Liberated	13
Fe	Liberated	4
Fe	Liberated	45
Fe	Liberated	12
Fe	Liberated	8
Fe	Liberated	11
Phos	Liberated	17
Fe	Rimming	14
Fe	Cemented	2
Fe	Cemented	2
Fe	Cemented	2
Fe	Cemented	2
Fe	Liberated	7
Fe	Liberated	9
Fe	Cemented	13
Fe	Cemented	11
Fe	Liberated	5
Fe	Liberated	21
Fe	Liberated	19
Fe	Rimming	7
Fe	Rimming	4
Fe	Liberated	4
Fe	Liberated	22
Fe	Liberated	7
Fe	Liberated	4
Fe	Rimming	5
Fe	Rimming	5
Fe	Rimming	5
Fe	Rimming	5
Fe	Rimming	5

Fe	Liberated	6
Fe	Cemented	8
Fe	Liberated	8
Fe	Liberated	12
Fe	Liberated	6
Fe	Liberated	21
Fe	Liberated	9
Fe	Rimming	7
Fe	Liberated	4
Fe	Liberated	13
Fe	Liberated	26
Fe	Liberated	6
Fe	Liberated	5
Fe	Liberated	33
Fe	Liberated	14
Fe	Rimming	9
Fe	Liberated	9
Fe	Liberated	7
Fe	Cemented	4
Fe	Rimming	12
Fe	Rimming	12
Fe	Rimming	6
Fe	Rimming	6
Fe	Rimming	6
Fe	Rimming	6
Fe	Liberated	35
Fe	Liberated	52
Fe	Cemented	12
Fe	Liberated	25
Fe	Liberated	45
Fe	Cemented	16

Fe	Liberated	17
Fe	Liberated	7
Fe	Liberated	4
Fe	Cemented	35
Fe	Liberated	10
Fe	Rimming	21
Fe	Cemented	22
Fe	Liberated	25
Fe	Rimming	4
Fe	Rimming	4
Fe	Rimming	4
Fe	Liberated	7
Fe	Liberated	3
Fe	Liberated	2
Fe	Liberated	6
Fe	Rimming	26
Fe	Liberated	6
Fe	Liberated	11
Fe	Liberated	20
Fe	Liberated	9
Fe	Liberated	14
Fe	Liberated	5
Fe	Liberated	22
Fe	Cemented	16
Fe	Rimming	23
Fe	Liberated	9
Fe	Liberated	10
Fe	Liberated	6
Fe	Liberated	6
Fe	Liberated	7
Fe	Liberated	11

Fe	Liberated	30
Fe	Liberated	27
Fe	Liberated	34
Fe	Liberated	36
Fe	Liberated	42
Fe	Liberated	30
Ce	Liberated	1
Ce	Liberated	1
Ce	Liberated	1
Ce	Liberated	6
Ce	Liberated	1

Attachment C
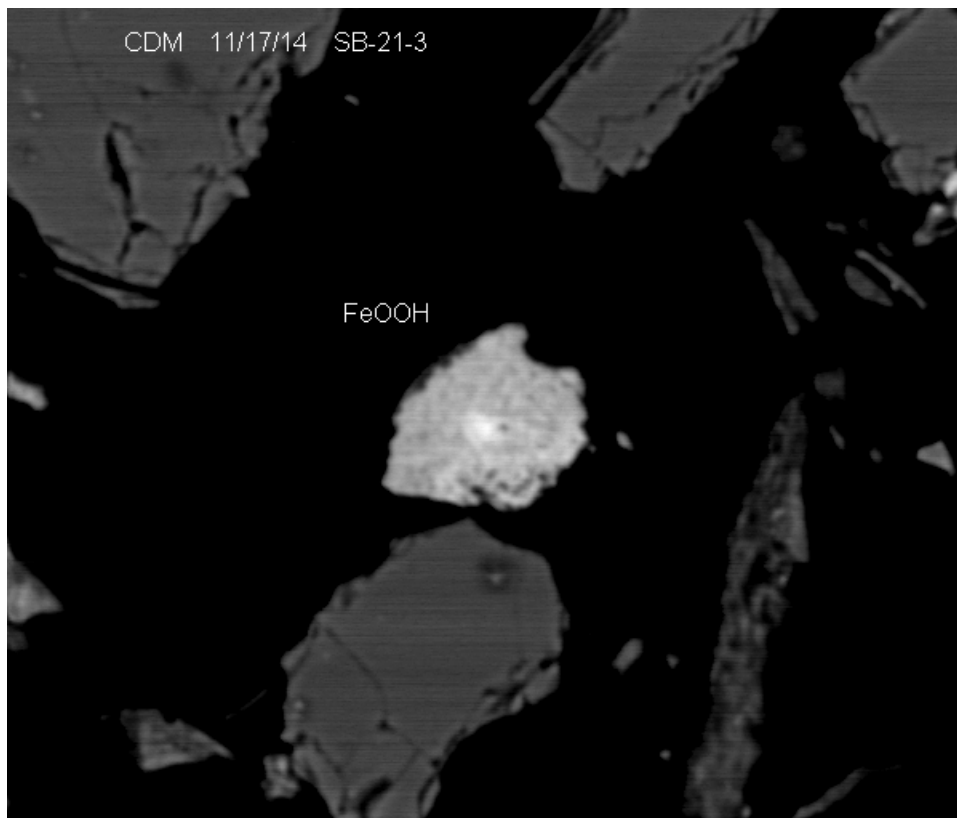
Photomicrograph 1: SB21-3
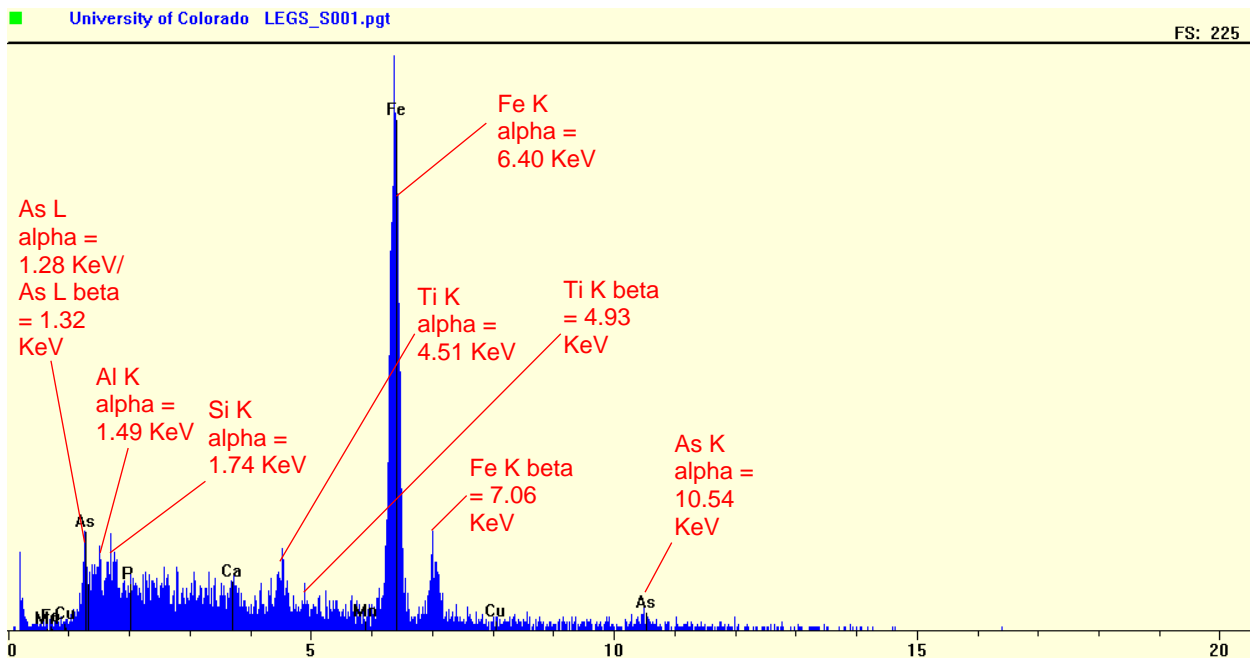
Photomicrograph 2: SB24-4
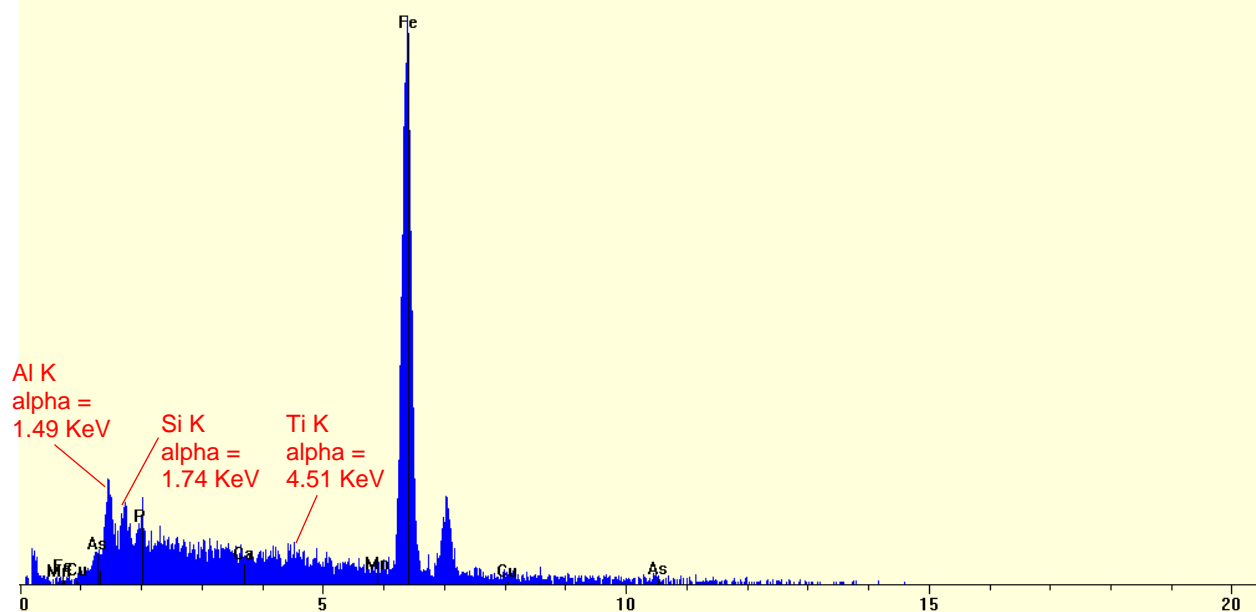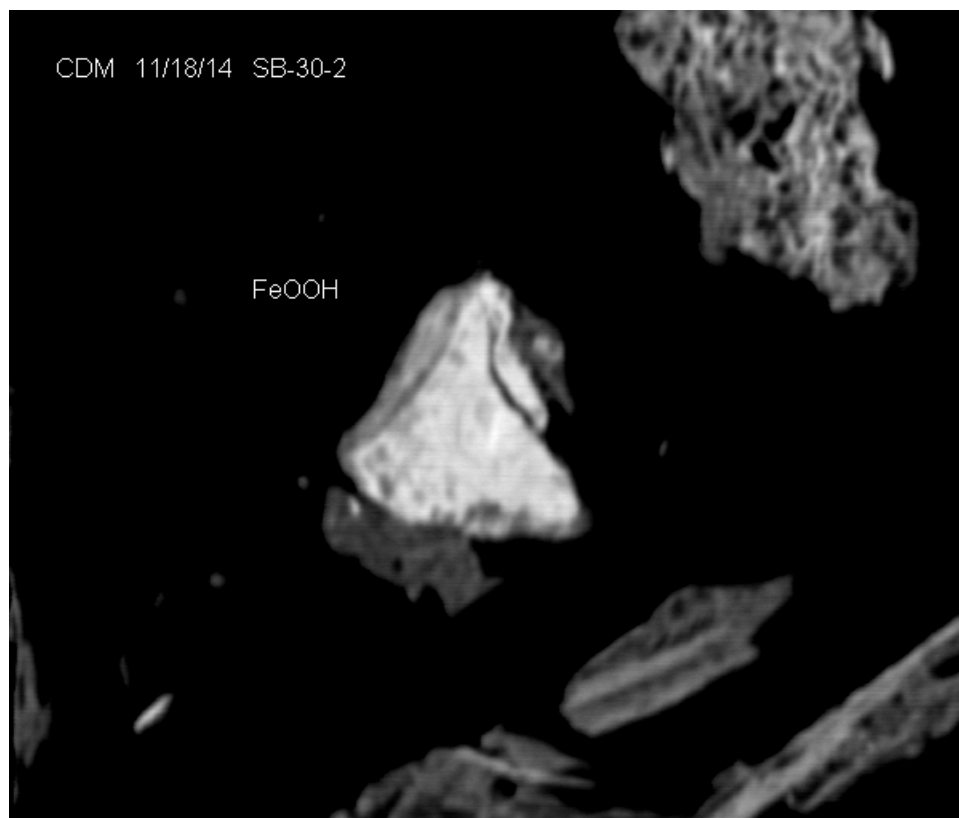
Photomicrograph 3: SB30-2
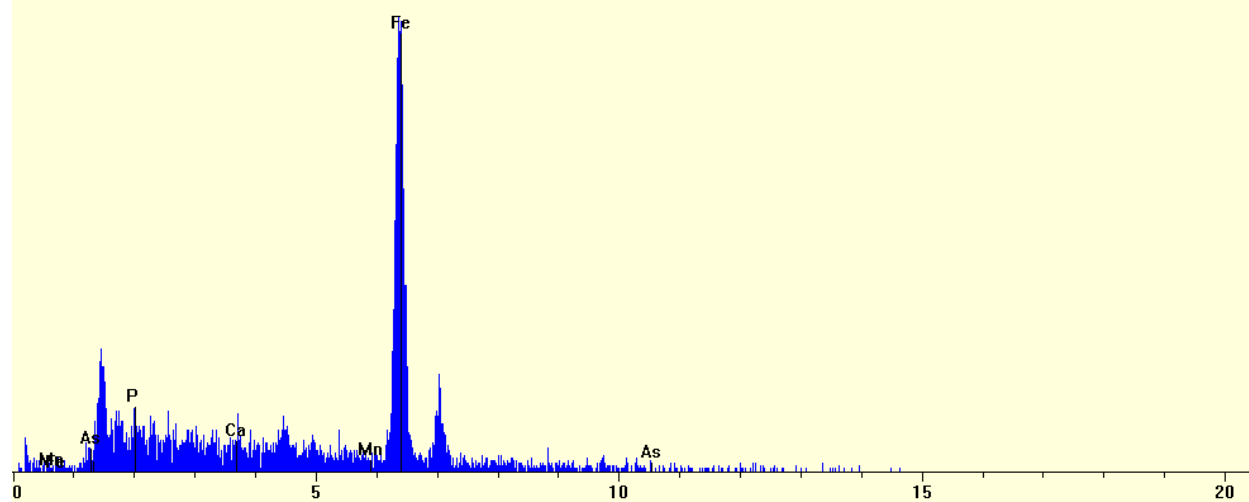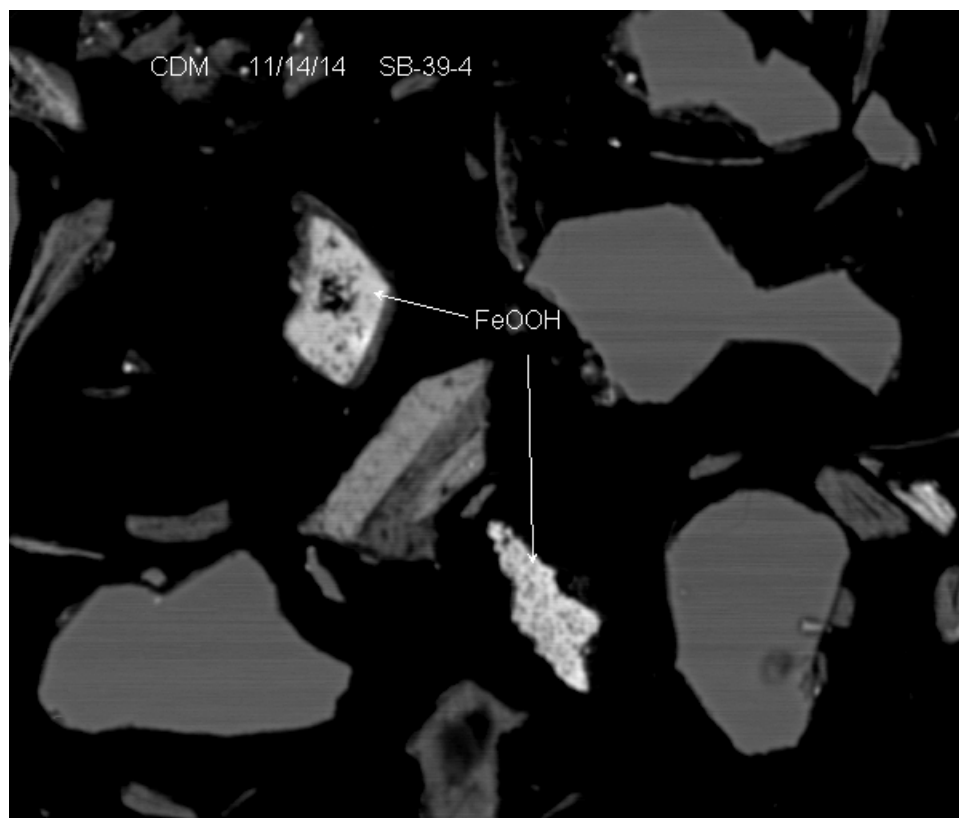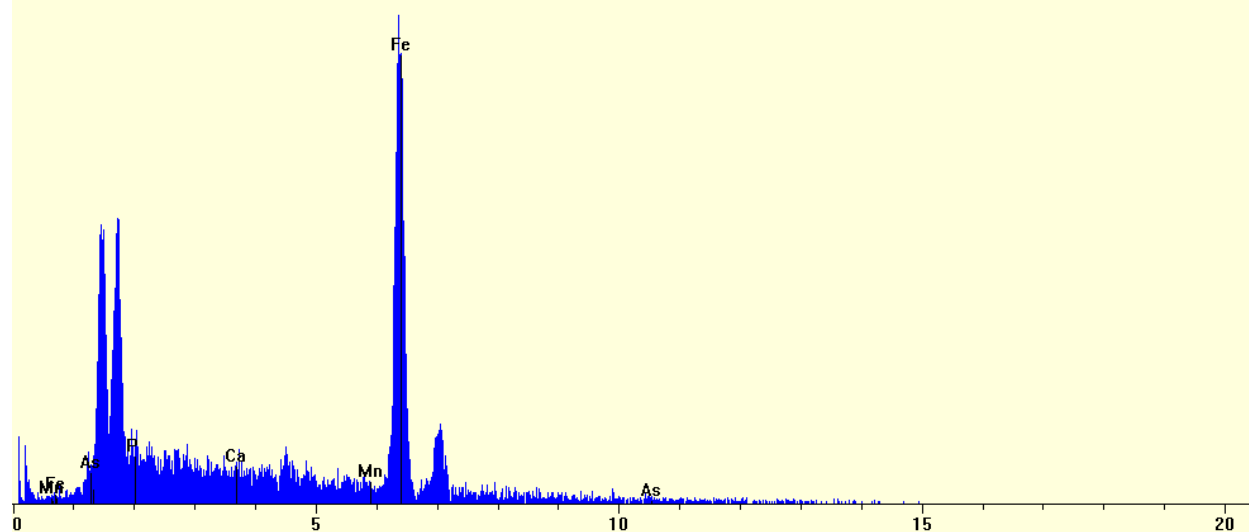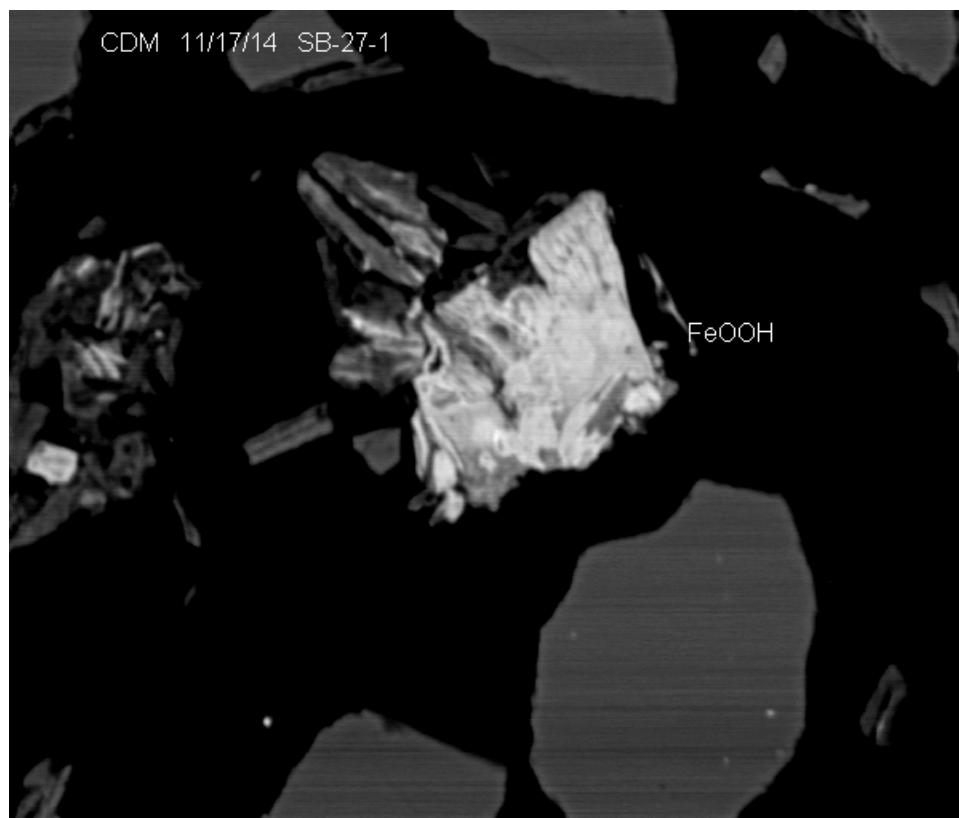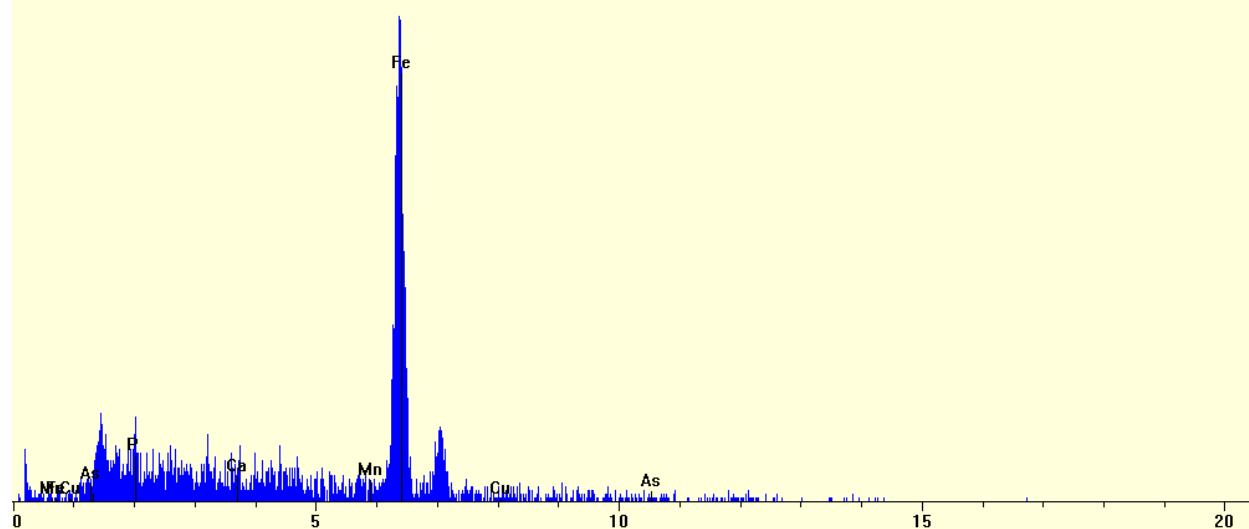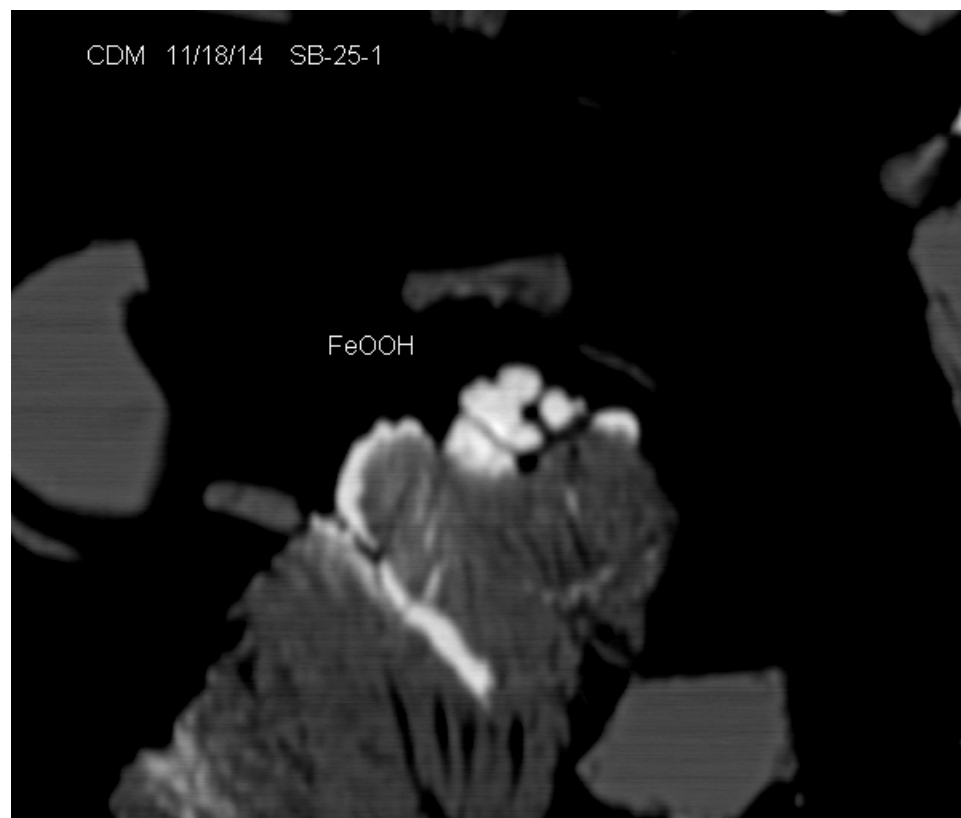
Photomicrograph 4: SB39-4

Photomicrograph 5: SB27-1

Photomicrograph 6: SB25-1
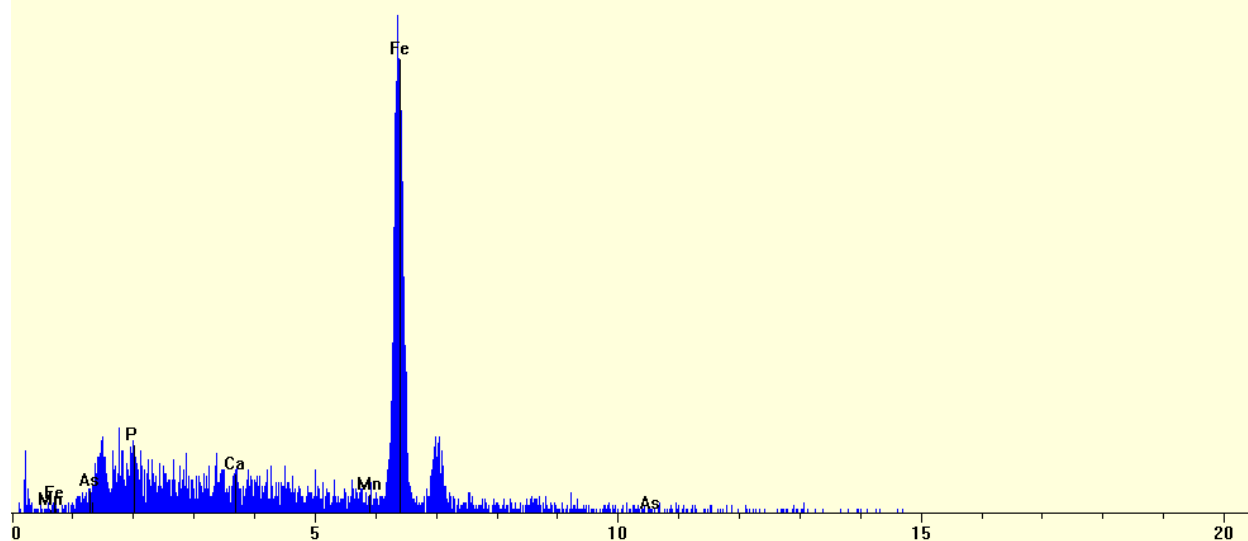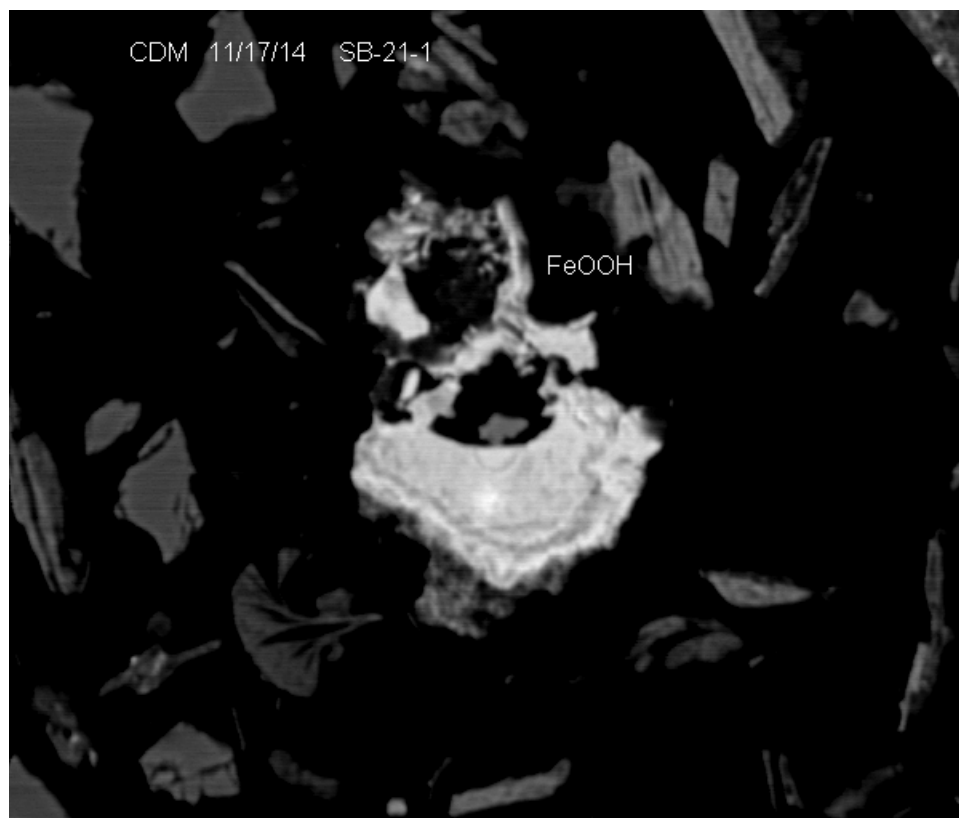
Photomicrograph 7: SB21-1
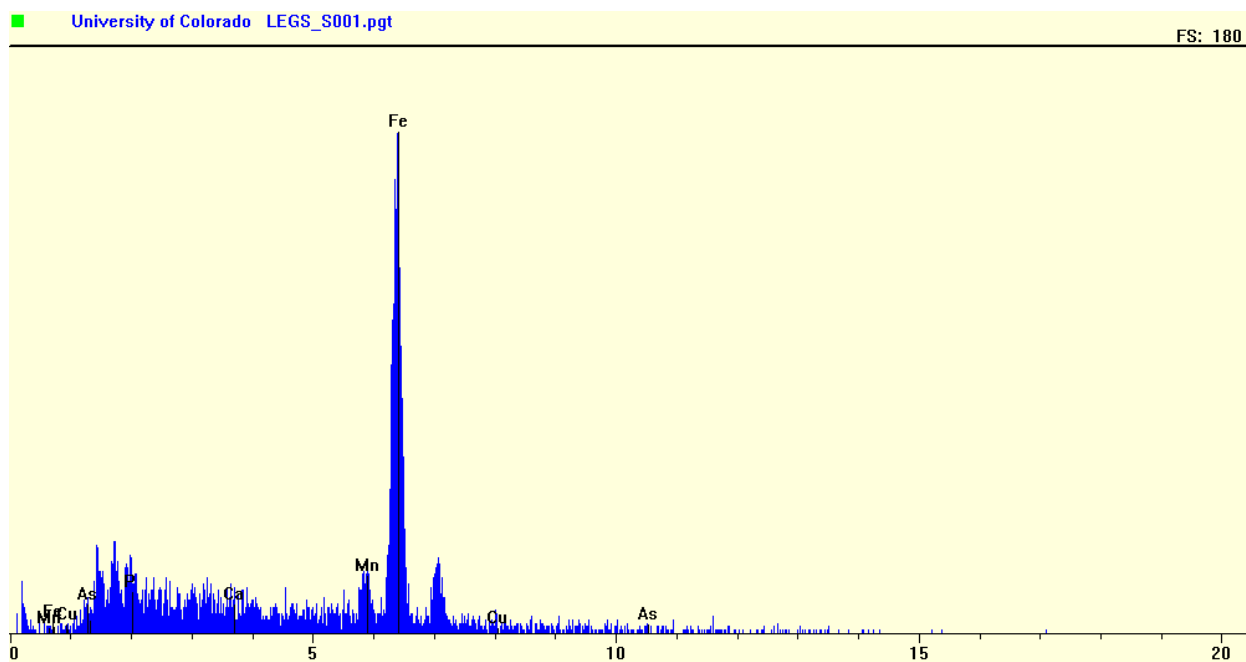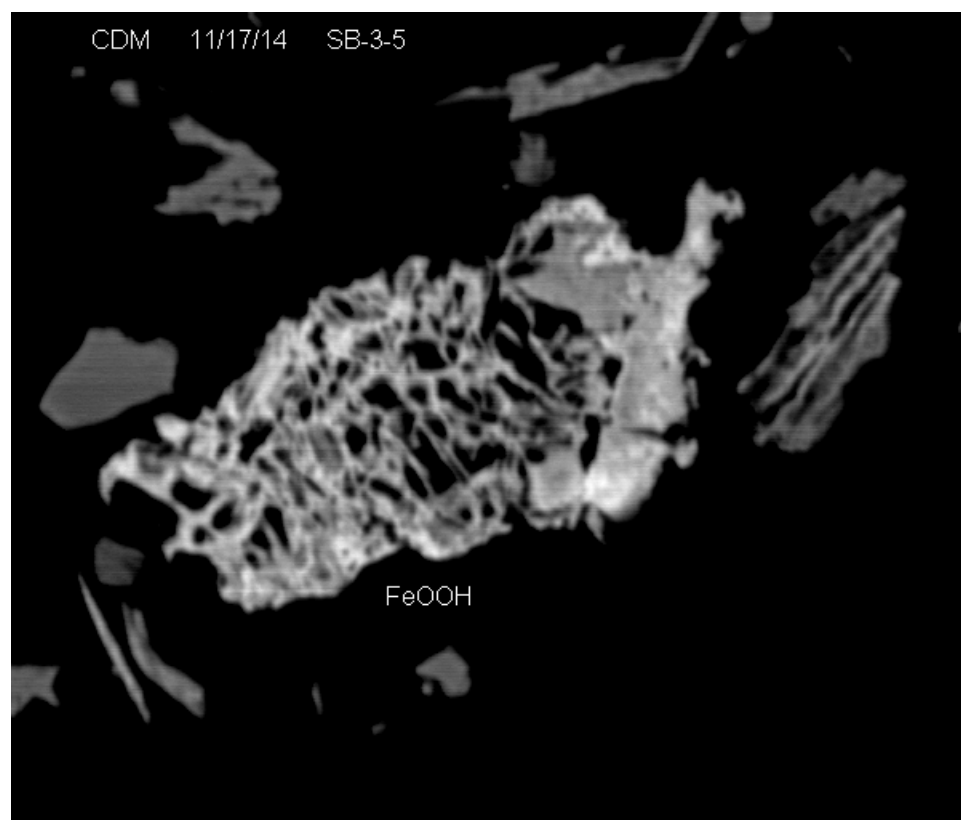
Photomicrograph 8: SB3-5
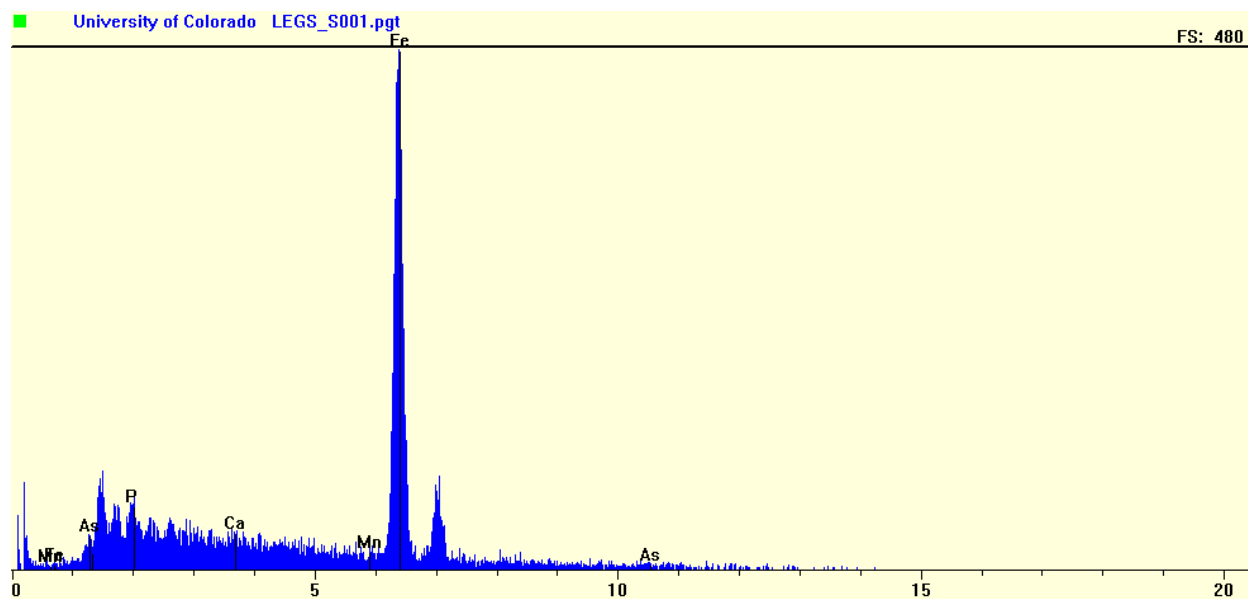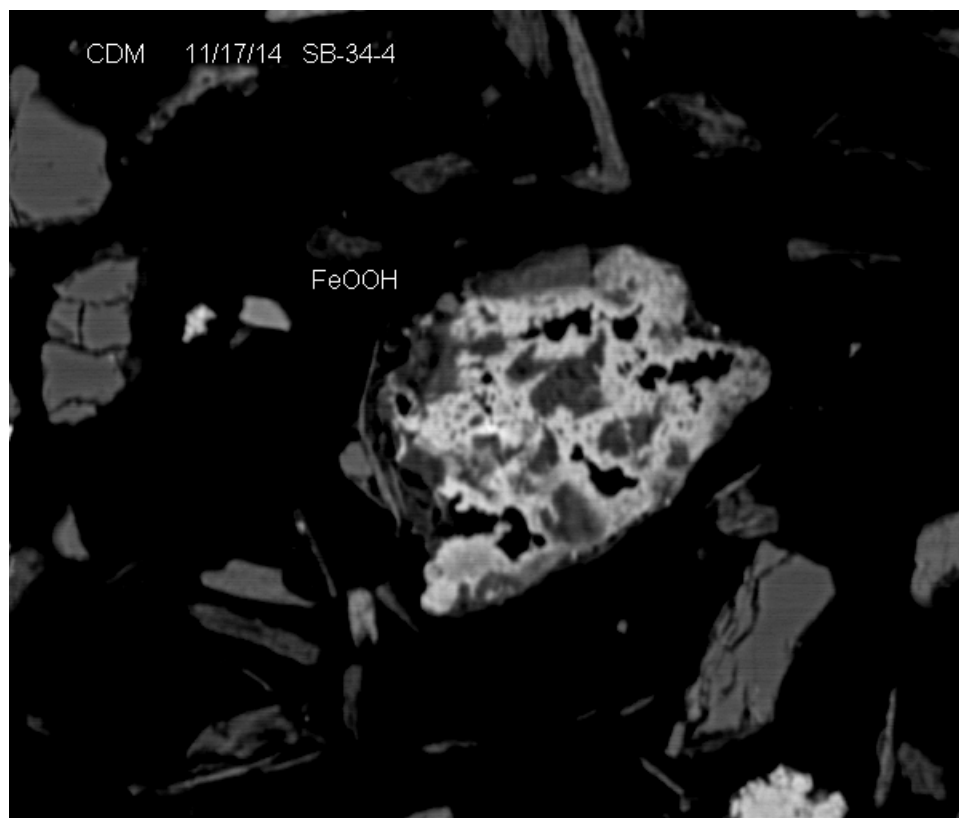
Photomicrograph 9: SB34-4
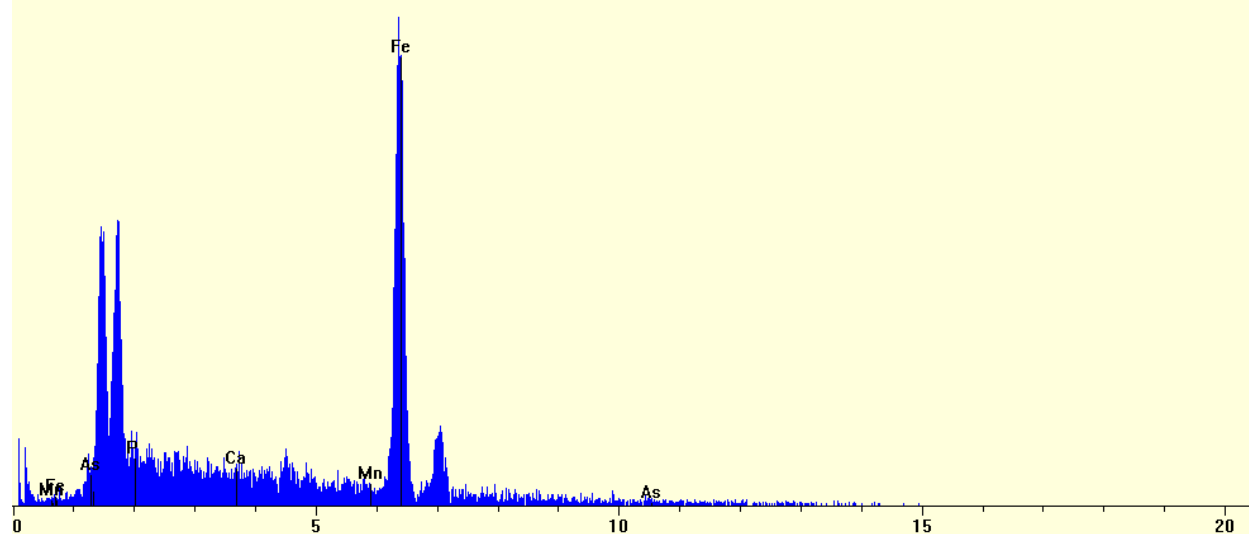
Attachment D

Results for the base case
Vater Res. **12**, 47–53.
le evaluation of control
ge process. Contributions
ute, Danish Academy of

. (1979) Real-time control
nvir. Engng Div. Am. Soc.

(1979) Methods for pre-
sludge. Wat. Pollut. Con-

a A. (1980) Fuzzy control
water treatment process.

The relationship between
the activated sludge pro-

iley J. E. (1980) Optimal
iudge processes—II Con-
trol for structured sludge

ADSORPTION OF ARSENITE AND ARSENATE ON AMORPHOUS IRON HYDROXIDE

Matthew L. Pierce* and Carleton B. Moore

Department of Chemistry, Arizona State University, Tempe, AZ 85287, U.S.A

Abstract—Adsorption isotherms in solutions with ionic strengths of 0.01 at 25°C were measured over the arsenite and arsenate concentration range 10^{-7}–10^{-3} M and the pH range 4–10. At low concentrations, these isotherms obeyed equations of the Langmuir type. At higher concentrations the adsorption isotherms were linear, indicating the existence of more than one type of surface site on the amorphous iron hydroxide adsorbent. Removal of arsenite and arsenate by amorphous iron hydroxide throughout the concentration range were determined as a function of pH. By careful selection of the relative concentration of arsenic and amorphous iron hydroxide and pH, removals on the order of 92% can be achieved.

INTRODUCTION

Arsenic, a toxic and possible carcinogenic element, is entering the oceans and surface waters in increasing amounts through the use of arsenical pesticides, mining and processing sulfide ores, and burning of fossil fuels. One of the main factors controlling arsenic in natural aquatic systems is adsorption on the sediments. It is important to acquire the capability of modeling adsorption by amorphous iron hydroxide [am-$Fe(OH)_3$] because of its universal presence in clays, soils, and sediments, both as partial coatings on other minerals and as discrete oxide particles, as well as its significant adsorptive properties (Jenne, 1968). This study investigates the interaction of arsenite and arsenate, the primary forms of arsenic in aqueous systems, with amorphous iron hydroxide.

Certain bacteria have been found not only to have oxidizing and reducing powers but also to be able to methylate organic and inorganic arsenic compounds. Biological methylation is not thermodynamically favorable in water and thus contributes little to the overall arsenic cycle in most aquatic systems (Braman & Foreback, 1973; Chau & Wong, 1978).

At the high *Eh* values encountered in oxygenated waters arsenic acid species (H_3AsO_4, $H_2AsO_4^-$, $HAsO_4^{2-}$, and AsO_4^{3-}) are stable. At *Eh* values characteristic of mildly reducing conditions, arsenous acid species (H_3AsO_3, $H_2AsO_3^-$, and $HAsO_3^{2-}$) become stable (Ferguson & Gavis, 1972). Removal of arsenic depends not only on the concentration of arsenic in solution, amount of sorptive oxides, and pH, but also on the oxidation state.

Typical adsorption studies have been carried out at relatively high concentrations (10^{-4}–10^{-2} M) compared to that found in natural waters (10^{-7}–10^{-5} M)

or even most waste waters and geothermal waters (10^{-5}–10^{-4} M) and very little at high concentrations ($>10^{-5}$ M).

Ferguson & Anderson (1974) studied adsorption characteristics of arsenite and arsenate on iron hydroxide and aluminum hydroxide at the 10^{-5}–10^{-3} M initial arsenic concentration in the pH range 6.0–7.5. They found Langmuir isotherm was obeyed. They later studied arsenate adsorption on amorphous aluminum hydroxide (Anderson *et al.*, 1976). Langmuir isotherms were followed at the 10^{-3}–10^{-5} M initial arsenic concentration and initial pH values of 3.5–10.5. Gupta & Chen (1978) found adherence to the Langmuir equation when arsenite or arsenate adsorbed on alumina and bauxite. The pH range was 6.5–8.5 and the initial arsenic concentration was 5–130 μM in both cases. Holm *et al.* (1979) found that adsorption of arsenite on river sediments was linearly dependent on concentration where as arsenate adsorption followed a Langmuir isotherm. The initial level of arsenic was 10^{-5}–10^{-4} M, and the pH at which the single isotherm was generated was not mentioned.

Some anions and cations have a specific affinity for surface metal atoms and adsorb out of all proportion to their concentration in solution. Adsorption under the combined influence of ionic and non-ionic bonding is called specific adsorption and can occur even when the surface is uncharged. Specific adsorption of anions should lower the pH of the isoelectric point (pH_{iep}). The amount of shift in the pH_{iep} depends on the particular ion and its concentration, as well as the particular solid surface. The isoelectric point is the pH at which the solid surface charge from all sources is zero.

Thus the present study was undertaken to establish quantitatively the isotherms of arsenite and arsenate adsorption on am-$Fe(OH)_3$ at concentrations which range over four orders of magnitude and a wide range of pH.

---

*Present address: DOW Chemical Texas Division, Environmental Services, Freeport, TX 77541, U.S.A.

1247

This work should not only be of interest to environmental scientists but also to engineers concerned with water and wastewater treatment as well as soil scientists concerned with nutrient retention.

EXPERIMENTAL

Amorphous iron hydroxide was prepared by the addition of 25 ml of 1 M NaOH to 1.665 g of analytical grade $Fe_2(SO_4)_3$ dissolved in 200 ml of doubly distilled water. The suspension was filtered, washed several times with doubly distilled water, and diluted up to 200 ml, so that the final suspension concentration was 4.45 g l^{-1} Fe(OH)$_3$. The flask was then immersed for 5 min in an ultrasonic bath. The suspension was soluble in acid ammonium oxalate (pH 3) and 1 M HCl, indicating that there had been little or no crystallization. This was confirmed by X-ray diffraction. A batch of fresh suspension was prepared for each experiment. Reproducible characteristics were obtained using this method.

The adsorption studies were run at a constant am-Fe(OH)$_3$ concentration of 0.00445 g l^{-1} and ionic strength of 0.01 adjusted with 1 M NaNO$_3$. Ten initial arsenite and arsenate concentrations in the form of NaAsO$_2$ and Na$_2$HAsO$_4 \cdot 7H_2O$ were 0.667, 1.33, 3.34, 6.67, 13.3, 33.4, 66.7, 133, 334, 667 μm l^{-1} As. Eight 200-ml volumetric flasks were used in each of the 10 studies, whereupon the contents containing NaNO$_3$, iron hydroxide, arsenite or arsenate, and water were transferred to Erlenmeyer flasks. The initial pH value of each of the 8 solutions was adjusted to give the desired final equilibrium pH between 4 and 10. The initial pH values were adjusted using either 1 M HNO$_3$ or 1 M NaOH to give the same final pH ($\pm$0.1 pH unit) for each of the 10 different initial arsenite or arsenate concentrations. The suspensions were mixed continuously by magnetic stirrers in stoppered 250-ml Erlenmeyer flasks for 24 h.

At the end of the reaction period, the final pH was measured, 10 ml of the mixture was centrifuged, and the supernatant analyzed for arsenic. Arsenic was determined using a Perkin–Elmer 403 atomic absorption spectrophotometer equipped with a deuterium arc background corrector, HGA 2100 graphite furnace, and electrodeless discharge lamp. Standards were diluted from a 1000-ppm arsenic stock solution, which was prepared from primary standard arsenic trioxide. A blank experiment was run without the iron hydroxide to see if arsenite or arsenate adsorbed onto the walls of the flask or magnetic stirbar.

Kinetic studies were also performed at the 0.667 and 13.3 μm l^{-1} As initial concentration of arsenite and arsenate in order to see when equilibrium was achieved. The same procedure was used in the adsorption experiment except 3-ml aliquots were removed at 0.05, 0.5, 1, 2, 4, 8, 16, 24 h and analyzed for arsenic. Three experiments were run with arsenite involving a final pH of 4.0, 6.1, and 9.8. Three experiments were also run with arsenate involving a final pH of 4.0, 8.0, and 9.9.

RESULTS AND DISCUSSION

Conversion of arsenite to arsenate takes weeks (in basic solution) before measurable air oxidation occurs. Thus errors due to the presence of arsenate did not become a factor in this investigation. Also, Gulens et al. (1979) stated that a redox reaction between Fe(III) and As(III) has not been observed, as well as heterogeneous oxidation, despite its thermodynamic favorability.

The blank experiments showed no detectable (<10^{-8} M As) arsenite or arsenate adsorbed on the walls of the flask or magnetic stirbar.

The rate of adsorption of arsenite on amorphous iron hydroxide was fast with 90% completion after 2 h of stirring at each of the three final pH values (4.0, 6.1, and 9.8). The rates at the 13.3 μm l^{-1} As initial concentration were noticeably faster than at the 0.667 μm l^{-1} As.

The rate of adsorption of arsenate was much faster than that of arsenite with 90% completion after only 1 h of stirring at each of the three final pH values (4.0, 8.0, and 9.9). The rates at the 13.3 μm l^{-1} As initial arsenate concentration were somewhat faster than at the 0.667 μm l^{-1} As.

After 4 h, 99% of the maximum adsorption had taken place with both arsenite and arsenate. Thus 24 h was adequate time for equilibration to occur. Adsorption solely due to electrostatic processes is usually very rapid on the order of seconds. The adsorption of arsenic is on the order of hours which indicates a specific adsorption or formation of a chemical bond between the arsenic species and the adsorbent.

Figure 1 shows the adsorption of arsenite per unit mass of am-Fe(OH)$_3$ plotted against final pH for the first five different initial concentrations from 0.667 to 13.3 μm l^{-1} As. The amount of arsenite taken up by the adsorbent reaches a maximum value at constant pH and this maximum value varies with pH. Adsorption increases to a maximum around pH 7, and then decreases as pH is increased with the first five of
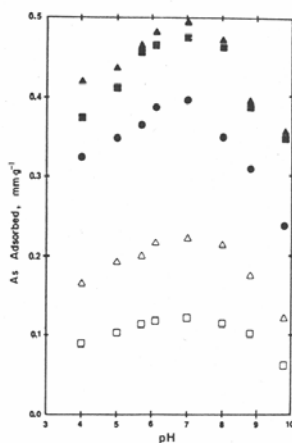
Fig. 1. Arsenite adsorption per unit mass adsorbent (Γ_A) as a function of the final pH for five different amounts of added arsenite, concentrations in μm l^{-1} As: 0.667 ($\square$); 1.33 ($\triangle$); 3.34 ($\bullet$); 6.67 ($\blacksquare$); 13.3 ($\blacktriangle$). Concentration of am-Fe(OH)$_3$, 0.00445 g l^{-1}; ionic strength, 0.01; equilibration time, 24 h.

the arsenite concentrations maxima in Fig. 1 tend to arsenite concentration is greater dependence on pH levels. At pH 7, the amount at the 0.667 μm l^{-1} As init 1.33 μm l^{-1} As, 53% at 6.67 μm l^{-1} As, and 17% at

Arsenous acid (H$_3$AsO$_3$) first pK at 9.2. The anion. coordinating to the surface bent and adsorption of the the energy of adsorption i sociate the acid. The pro remove the OH$^-$ from the surface and provide a site f cumstances anion adsorpti charge and even on negativ ease with which a proton ca sociated acid in solution wi solution. The adsorption explained by the fact that energy released upon ads required to dissociate the a

Isotherms, plotted at co amount of arsenite adsorb dition of surface saturation centration. In the concentr μm l^{-1} As, this was best rep equation, $\Gamma_A = \Gamma_{A,max} C_{equil}$ the adsorption per unit ma maximum adsorption per u is the equilibrium concent ution, and K_L is the Langs ment of this equation yields $(1/\Gamma_{A,max}) C_{equil}$. Since the obeyed, a plot of C_{equil}/Γ_A line with a slope of $1/\Gamma$
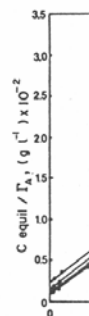

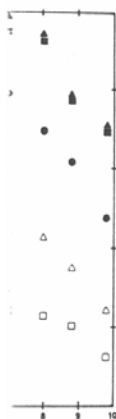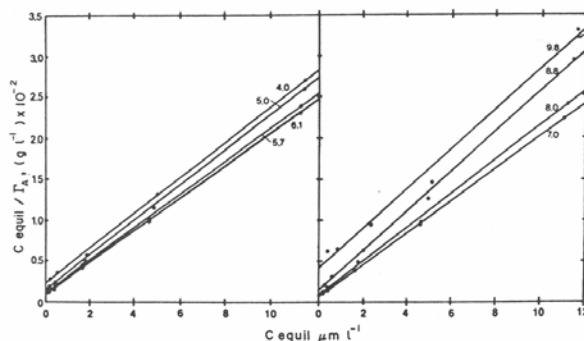Fig. 2. Equilibrium a mass adsorbent (Γ_A indicated on the gra

owed no detectable
enate adsorbed on the
tirbar.

rsenite on amorphous
% completion after 2 h
nal pH values (4.0, 6.1,
μm l⁻¹ As initial con-
faster than at the

enate was much faster
completion after only
te final pH values (4.0,
13.3 μm l⁻¹ As initial
mewhat faster than at

mum adsorption had
e and arsenate. Thus
quilibration to occur,
ctrostatic processes is
rder of seconds. The
order of hours which
n or formation of a
rsenic species and the

on of arsenite per unit
gainst final pH for the
trations from 0.667 to
f arsenite taken up by
ium value at constant
ries with pH. Adsorp-
round pH 7, and then
with the first five of

the arsenite concentrations studied. The adsorption maxima in Fig. 1 tend to be sharper as the initial arsenite concentration is increased, indicating a greater dependence on pH at higher concentration levels. At pH 7, the amount of arsenic removed is 81% at the 0.667 μm l⁻¹ As initial concentration, 74% at 1.33 μm l⁻¹ As, 53% at 3.34 μm l⁻¹ As, 32% at 6.67 μm l⁻¹ As, and 17% at 13.3 μm l⁻¹ As.

Arsenous acid (H_3AsO_3) is a weak acid with the first pK at 9.2. The anion, $H_2AsO_3^-$, is capable of coordinating to the surface metal atom of the adsorbent and adsorption of the anion will occur provided the energy of adsorption is sufficiently large to dissociate the acid. The proton produced is used to remove the OH^- from the coordinating layer of the surface and provide a site for the anion. In these circumstances anion adsorption in excess of the positive charge and even on negative surface is possible. The ease with which a proton can be removed from undissociated acid in solution will vary with the pH of the solution. The adsorption maxima at pH 7 can be explained by the fact that the difference between the energy released upon adsorption and the energy required to dissociate the acid is at a maximum.

Isotherms, plotted at constant pH, show that the amount of arsenite adsorbed increases until a condition of surface saturation is reached at some concentration. In the concentration range of 0.667–13.3 μm l⁻¹ As, this was best represented by the Langmuir equation, $\Gamma_A = \Gamma_{A.\max}C_{equil}/(K_L + C_{equil})$ where Γ_A is the adsorption per unit mass adsorbent, $\Gamma_{A.\max}$ is the maximum adsorption per unit mass adsorbent, C_{equil} is the equilibrium concentration of arsenite in solution, and K_L is the Langmuir constant. Rearrangement of this equation yields: $C_{equil}/\Gamma_A = K_L/\Gamma_{A.\max} + (1/\Gamma_{A.\max})C_{equil}$. Since the Langmuir equation is obeyed, a plot of C_{equil}/Γ_A vs C_{equil} gives a straight line with a slope of $1/\Gamma_{A.\max}$ and an intercept of

Table 1. Parameters in the Langmuir adsorption equation for arsenite

pH	$\Gamma_{A.\max}$ (μm g⁻¹)	K_L (μm l⁻¹)	Corr. coeff.*
4.0	457	1.03	0.999
5.0	463	0.657	1.000
5.7	490	0.544	0.999
6.1	503	0.457	1.000
7.0	513	0.431	1.000
8.0	488	0.493	0.999
8.8	417	0.646	0.999
9.8	417	1.82	0.989

*Correlation to a least-squares approximation of the best straight line through the points in Fig. 2.

$K_L/\Gamma_{A.\max}$. This is shown in Fig. 2 for each of the eight equilibrium pH values employed. Table 1 lists the calculated Langmuir parameters, as well as correlation coefficients to a straight line at each pH. These isotherms indicate that the coverage is monolayer. By plotting the Langmuir constants against pH, one can determine the constants at any pH. Knowing the pH and the equilibrium arsenite concentration, the amount of adsorption on the adsorbent can be calculated using the Langmuir equation.

The isoelectric points of am-Fe(OH)₃ and the first five different amounts of added arsenite were published earlier (Pierce & Moore, 1980). As predicted, the isoelectric point (pH$_{iep}$) depends on the amount of arsenic adsorbed and decreases from 8.0 with no added arsenite to 7.3 with 13.3 μm l⁻¹ As initial arsenite concentration. This shift in the pH$_{iep}$ also indicates a specific adsorption process rather than a purely electrostatic adsorption process.

The adsorption of arsenite per unit mass am-Fe(OH)₃ plotted against final pH for the last five different initial concentrations from 33.4 to

mass adsorbent (Γ_A) as
e different amounts of
μm l⁻¹ As: 0.667 (□);
(▲). Concentration of
trength, 0.01; equilibra-
h.

Fig. 2. Equilibrium arsenite concentration (C_{equil}) divided by the amount of arsenite adsorbed per unit mass adsorbent (Γ_A) as a function of the equilibrium arsenite concentration at various pH values indicated on the graph. Initial concentrations of arsenite, 0.667–13.3 μm l⁻¹ As; am-Fe(OH)₃ concentration, 0.00445 g l⁻¹; equilibration time, 24 h.
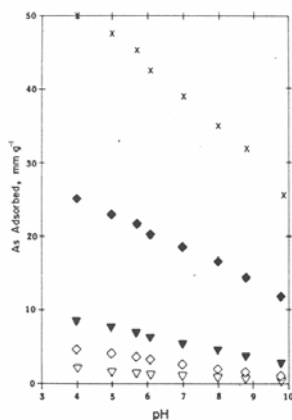
Fig. 3. Arsenite adsorption per unit mass adsorbent (Γ_A) vs final pH for five different amounts of added arsenite, concentrations in $\mu m\,l^{-1}$ As: 33.4 ($\triangledown$); 66.7 ($\diamondsuit$); 133 ($\blacktriangledown$); 334 ($\blacklozenge$); 667 ($\times$). Concentration of am-Fe(OH)$_3$, 0.00445 g l^{-1}; ionic strength, 0.01; equilibration time, 24 h.

667 $\mu m\,l^{-1}$ As is shown in Fig. 3. The amount of arsenite taken up by the adsorbent continually decreases with increasing pH with the higher concentrations showing a greater dependence on pH. This dependence on pH is clearly different from that at the lower concentrations of arsenite. This can be explained by the fact that the surface has primarily a net negative charge due to adsorption of anions. Thus adsorption of anions on a negatively charged surface should decrease as the pH is increased. At a pH of 4, removals on the order of 35% were found for all five of the initial concentrations. The eight final pH values were the same as in the earlier arsenite adsorption studies at the lower concentration range.

Figure 4 shows that the Langmuir equation is not obeyed in the arsenite initial concentration range of 33.4–667 $\mu m\,l^{-1}$ As. Rather a linear isotherm is followed whereupon the amount of arsenite adsorbed (Γ_A) vs the equilibrium concentration of arsenite in solution (C_{equil}) is a linear relationship. That is $\Gamma_A = kC_{equil}$.

The slopes of the Γ_A vs C_{equil} plots at each pH and correlation coefficients to a straight line can be found in Table 3. Knowing the pH and equilibrium concentrations of arsenite, the adsorption can be calculated as long as the equilibrium concentration is greater than 14 $\mu m\,l^{-1}$ As. Below 14 $\mu m\,l^{-1}$ As, the Langmuir equation and constants would have to be used.

This adsorption dependence on two different isotherms may be explained partially by assuming that oxide surfaces have different types of surface sites, with different affinities for adsorbate ions. The surface density of the strong binding sites would be much less

than the weaker binding sites. So adsorption proceeds until all the strong binding sites are occupied, which would follow a Langmuir isotherm. Then the anions would start to adsorb on the weaker binding sites. The linear isotherm at the high concentrations indicates that either the number of weaker adsorption sites remains constant even though the amount of anions adsorbed increases, or that the number of weaker sites is very large compared with the amount adsorbed. If the former is the case, it suggests that the adsorbate can penetrate into the oxide surface which is theoretically possible with an amorphous solid. That is, an open permeable structure exists for am-Fe(OH)$_3$.

This multisite adsorption due to heterogeneity of the surface is consistent with that proposed by Benjamin & Leckie (1981) and Davis et al. (1978).

Figure 5 shows the adsorption of arsenate per unit mass of am-Fe(OH)$_3$ plotted against final pH for the first five different initial concentrations from 0.667 to 13.3 $\mu m\,l^{-1}$ As. At the lower concentrations and at lower pH arsenate adsorption is independent of pH. But as pH increases there is a "point" where adsorption begins to decrease. This "point" shifts to lower pH values as the initial arsenate concentration is increased. At pH 4, the amount of arsenate removed is 81% at the 0.667 $\mu m\,l^{-1}$ As initial concentration, 92% at 1.33 $\mu m\,l^{-1}$ As, 78% at 3.34 $\mu m\,l^{-1}$ As, 80% at 6.67 $\mu m\,l^{-1}$ As; and 47% at 13.3 $\mu m\,l^{-1}$ As.

Arsenic acid (H$_3$AsO$_4$) has pK values of 3.6, 7.3, and 12.5, thus H$_2$AsO$_4^-$ and HAsO$_4^{2-}$ are the predominant anions in the pH range studied which would have a greater effect on the surface charge than the singly-charged anion of arsenous acid. This accounts for the "point" in the adsorption vs pH plots where the adsorption begins to decrease and the shift in that "point" to lower pH values. The pH$_{iep}$ decreases much more rapidly as compared with arsenite
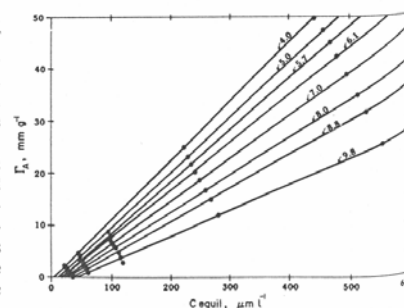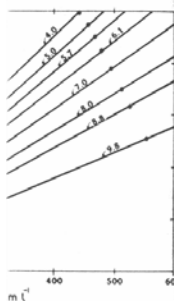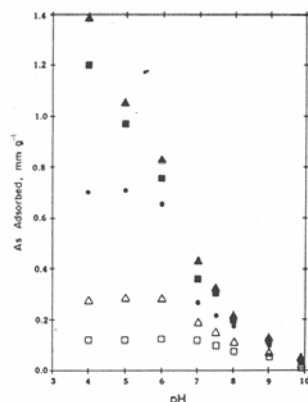

Fig. 4. The amount of arsenite adsorbed per unit mass adsorbent (Γ_A) as a function of the equilibrium arsenite concentration (C_{equil}) at various final pH values indicated on the graph. Initial concentrations of arsenite, 33.4–667 $\mu m\,l^{-1}$ As; am-Fe(OH)$_3$ concentration, 0.00445 g l^{-1}; equilibration time, 24 h.

Fig. 5. Arsenate adsorption pe a function of the final pH f added arsenate, concentratio 1.33 ($\triangle$); 3.34 ($\bullet$); 6.67 ($\blacksquare$); am-Fe(OH)$_3$, 0.0045 g l^{-1}; io tion tim

from 8.0 with no adde 13.3 $\mu m\,l^{-1}$ As initial arsen 1981).

Arsenate also showed an muir adsorption isotherm i 0.667–13.3 $\mu m\,l^{-1}$ As. Plc shown in Figure 6 yield str eight equilibrium values of lated Langmuir parameter ficients to a straight line. As of adsorption can be calcu equation and knowing t arsenate concentration.

The adsorption of arsen hydroxide plotted against initial concentrations from shown in Fig. 7. The amou

Table 2. Parameters in tion equation

pH	$\Gamma_{A,max}$ ($\mu m\,g^{-1}$)	K (μm
4.0	1530	0.6
5.0	1100	0.3
6.0	850	0.3
7.0	454	0.8
7.5	344	0.8
8.0	226	0.7
9.0	136	0.8
9.9	482	1.5

*Correlation to a k mation of the best st: points in Fig. 6.

o adsorption proceeds
:s are occupied, which
erm. Then the anions
weaker binding sites.
h concentrations indi-
of weaker adsorption
hough the amount of
that the number of
ared with the amount
case, it suggests that
nto the oxide surface
: with an amorphous
ble structure exists for

ie to heterogeneity of
hat proposed by Ben-
is *et al.* (1978).
n of arsenate per unit
gainst final pH for the
trations from 0.667 to
concentrations and at
is independent of pH.
"point" where adsorp-
"point" shifts to lower
te concentration is in-
of arsenate removed is
tial concentration, 92%
34 μm l^{-1} As, 80% at
.3 μm l^{-1} As.
pK values of 3.6, 7.3,
HAsO$_4^{2-}$ are the pre-
range studied which
the surface charge than
arsenous acid. This
adsorption vs pH plots
decrease and the shift
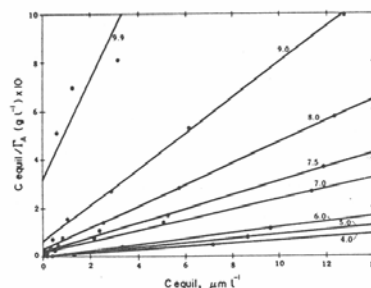values. The pH$_{iep}$ de-
compared with arsenite

Fig. 5. Arsenate adsorption per unit mass adsorbent (Γ_A) as a function of the final pH for five different amounts of added arsenate, concentrations in μm l^{-1} As: 0.667 ($\square$); 1.33 ($\triangle$); 3.34 ($\bullet$); 6.67 ($\blacksquare$); 13.3 ($\blacktriangle$). Concentration of am-Fe(OH)$_3$, 0.0045 g l^{-1}; ionic strength, 0.01; equilibration time, 24 h.

from 8.0 with no added arsenate to 4.7 with 13.3 μm l^{-1} As initial arsenate concentration (Pierce, 1981).

Arsenate also showed an adherence to the Langmuir adsorption isotherm in the concentration range 0.667–13.3 μm l^{-1} As. Plots of C_{equil}/Γ_A vs C_{equil} shown in Figure 6 yield straight lines for each of the eight equilibrium values of pH. Table 2 lists the calculated Langmuir parameter as well as correlation coefficients to a straight line. As with arsenite, the amount of adsorption can be calculated using the Langmuir equation and knowing the pH and equilibrium arsenate concentration.

The adsorption of arsenate per unit mass of iron hydroxide plotted against final pH for five different initial concentrations from 33.4 to 667 μm l^{-1} As is shown in Fig. 7. The amount of arsenate taken up by

Fig. 6. Equilibrium arsenate concentration (C_{equil}) divided by the amount of arsenite adsorbed per unit mass adsorbent (Γ_A) as a function of the equilibrium arsenate concentration at the various pH values indicated. Initial concentrations of arsenate; 0.667–13.3 μm l^{-1} As; am-Fe(OH)$_3$ concentration, 0.0045 g l^{-1}; equilibration time, 24 h.

.65 mg/l

the adsorbent continually decreases with increasing pH with the higher concentrations showing a greater dependence on pH. At a pH of 4, removals on the order of 35% were found for all five of the initial concentrations similar to arsenite. The eight equilibrium pH values were the same as in the earlier arsenate adsorption studies at the lower concentration range of 0.667–13.3 μm l^{-1} As.

Figure 8 shows that the Langmuir equation is not followed in the arsenate initial concentration range of 33.4–667 μm l^{-1} As. A linear isotherm is followed whereupon the amount of arsenate adsorbed (Γ_A) vs
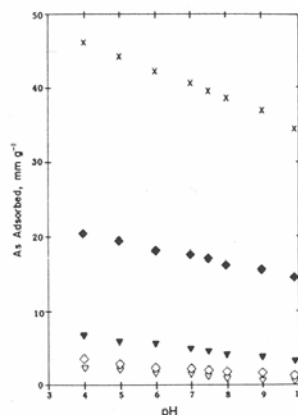

Table 2. Parameters in the Langmuir adsorption equation for arsenate

$\Gamma_{A,max}$ (mg/kg)	pH	$\Gamma_{A,max}$ (μm g^{-1})	K_L (μm l^{-1})	K_L (mg/l)	Corr. coeff.*
114,630	4.0	1530	0.683	0.051	0.974
	5.0	1100	0.396		0.993
63,682	6.0	850	0.309	0.023	0.998
34,014	7.0	454	0.872	0.065	0.989
25,773	7.5	344	0.839	0.063	0.995
	8.0	226	0.719		0.999
10,189	9.0	136	0.868	0.065	0.998
	9.9	482	1.51		0.986

*Correlation to a least-squares approximation of the best straight line through the points in Fig. 6.

W.R. 16/7—L

dsorbed per unit mass
he equilibrium arsenite
nal pH values indicated
ns of arsenate, 33.4–667
tion, 0.00445 g l^{-1}; equi-
24 h.

Fig. 7. Arsenate adsorption per unit mass adsorbent (Γ_A) as a function of the final pH for five different amounts of added arsenate, concentrations in μm l^{-1} As: 33.4 ($\triangledown$); 66.7 ($\diamond$); 133 ($\blacktriangledown$); 334 ($\blacklozenge$); 667 ($\times$). Concentration of am-Fe(OH)$_3$, 0.00445 g l^{-1}; ionic strength, 0.01; equilibration time, 24 h.
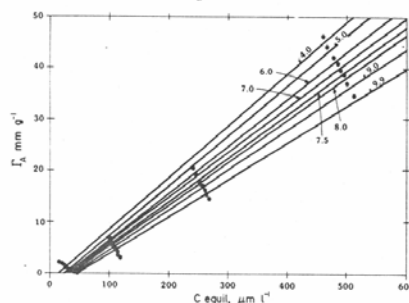
MATTHEW L. PIERCE and CARLETON B. MOORE

Fig. 8. The amount of arsenate adsorbed per unit mass adsorbent (Γ_A) as a function of the equilibrium arsenate concentration (C_{equil}) at various final pH values indicated on the graph. Initial concentrations of arsenate, 33.4–667 μm l^{-1} As; am-Fe(OH)$_3$ concentration, 0.00445 g l^{-1}; equilibration time, 24 h.

the equilibrium concentration of arsenate in solution (C_{equil}) is a linear relationship. The slopes of the Γ_A vs C_{equil} plots at each pH and correlation coefficients to a straight line can be found in Table 3. Above an equilibrium concentration of 14 μm l^{-1} the amount of adsorption taking place can be calculated knowing the pH and the equilibrium concentration and using the linear isotherm equation. In Fig. 8, the set of points at 66.7 μm l^{-1} As initial concentration are not shown due to some overlap with the points at 33.4 μm l^{-1} As.

CONCLUSIONS

The adsorptive capacity of am-Fe(OH)$_3$ is extremely high for arsenic. Adsorption continued to take place even at the highest concentrations of arsenic studied. Up to 667 μm l^{-1} (50 ppm) As initial concentration of arsenite or arsenate, removals on the order of 35% (at pH 4) were found, which amounted to an adsorption of 50 mm g^{-1} at pH 4. This adsorption is in the linear isotherm region where doubling the initial concentration would approximately double the amount adsorbed. The extremely high adsorptive capacity of amorphous iron hydroxide for arsenic can

be explained by visualizing a loose, highly hydrated structure which is permeable to hydrated ions. The ions are free to diffuse throughout the structure and are not restricted to external surface sites such as the case with more crystalline solids.

Anderson et al. (1976) studied the adsorption of arsenate on amorphous aluminum hydroxide only up to 1.5 mm g^{-1} of arsenic adsorbed. They found adherence to a Langmuir isotherm at all equilibrium pH's studied. The extents of adsorption as well as the general dependence of adsorption on pH are similar to that found in this study of arsenate up to approx. 1.5 mm g^{-1} of arsenic adsorbed. In the adsorption vs pH plot, the "points" at which the adsorption begins to decrease are not the same as in this study because of the difference in the isoelectric points of am-Fe(OH)$_3$ and am-Al(OH)$_3$.

Competition from adsorption of other ions is important when considering natural aquatic systems or wastewater treatment. Phosphate is known to be very adsorptive on iron and aluminum oxide surfaces and indeed is very close to that or arsenate (Pierce, 1981). Addition of phosphate or sulfate after arsenate or arsenite had been adsorbed, has very little affect on the adsorption of arsenic. A significant effect on the

Table 3. Parameters in the linear adsorption equation for arsenite and arsenate

	Arsenite			Arsenate	
pH	$k(1000 \, \text{l g}^{-1})$	Corr. coeff.*	pH	$k (1000 \, \text{l g}^{-1})$	Corr. coeff.†
4.0	0.116	0.998	4.0	0.101	0.988
5.0	0.107	0.998	5.0	0.097	0.989
5.7	0.101	0.998	6.0	0.092	0.989
6.1	0.093	0.998	7.0	0.087	0.989
7.0	0.084	0.997	7.5	0.085	0.990
8.0	0.073	0.996	8.0	0.083	0.989
8.8	0.065	0.985	9.0	0.079	0.989
9.8	0.050	0.995	9.9	0.073	0.989

*Correlation to a least-squares approximation of the best straight line through the points in Fig. 4.
†Correlation to a least-squares approximation of the best straight line through the points in Fig. 8.

adsorption of arsenic at low concentrations is evident after phosphate or sulfate had already been adsorbed.

In the rates of adsorption experiments, more than 50% of the arsenic was adsorbed before a sample could be taken. Thus, even in fast flowing rivers, a significant amount of arsenic would be adsorbed, as soon as the arsenic species came in contact with the surface of the oxide.

Adsorption of arsenic onto am-Fe(OH)₃ generally is inconsistent with a homogeneous surface site model except at very low adsorption density. Up to 0.5 mm g^{-1} As (+3) adsorbed ($13.3 \mu\text{m l}^{-1}$ As initial concentration) at pH 7 and 1.5 mm g^{-1} As (+5) adsorbed ($13.3 \mu\text{m l}^{-1}$ as initial concentration) at pH 4, the data can be fit using a Langmuir isotherm. At greater adsorption densities, the data can be fit using a linear isotherm. The range of surface coverages where the isotherm type changes is well below that at which one would expect site limitation to be important. In none of the experiments studied is there an indication that adsorption density is approaching a maximum, limiting value.

A heterogeneous site model for the surface of am-Fe(OH)₃ is conceptually consistent with all the observations. Many adsorption studies of oxide surfaces presently available include the assumption that all surface sites are equivalent. Thus it is important to perform model experiments over wide ranges of concentration of adsorbate and adsorbent in order to predict the removal of ions in natural systems accurately.

Based on the experimental results of this work, the following conditions are necessary for maximum arsenic removal. Amorphous hydroxides with a high isoelectric point such as am-Fe(OH)₃ or am-Al(OH)₃ are extremely efficient adsorbers. The oxidation state of the arsenic species is another important factor with the +5 oxidation state adsorbing to a greater extent than the +3 oxidation state at concentrations normally found in natural water. One of the most critical parameters is the solution pH. At concentrations normally found in natural waters, a pH of 7 is optimum for arsenite and a pH of 4 is optimum for arsenate.

This study not only identifies the ideal conditions necessary for maximum removal of arsenic in aqueous systems but also helps to explain the differences in the adsorption dependence on pH.

REFERENCES

Anderson M. A., Ferguson J. F. & Gavis J. (1976) Arsenate adsorption on amorphous aluminum hydroxide. *J. Colloid Interface Sci.* **54**, 391–399.

Benjamin M. M. & Leckie J. O. (1981) Multiple-site adsorption of Cd, Cu, Zn and Pb on amorphous iron oxyhydroxide. *J. Colloid Interface Sci.* **79**, 209–221.

Braman R. S. and Foreback C. C. (1973) Methylated forms of arsenic in the environment. *Science* **182**, 1247–1249.

Chau Y. K. & Wong P. T. S. (1978) Occurrence of biological methylation of elements in the environment. *Am. Chem. Soc. Symp. Ser.* **92**, 39–53.

Davis J. A., James R. O. & Leckie J. O. (1978) Surface ionization and complexation at the oxide/water interface. *J. Colloid Interface Sci.* **63**, 480–499.

Ferguson J. F. & Anderson M. A. (1974) Chemical form of arsenic in water supplies and their removal. In *Chemistry of Water Supply, Treatment, and Distribution* (Edited by Rubin, A. J.), pp. 137–158. Ann Arbor Science, Ann Arbor, MI.

Ferguson J. F. & Gavis J. (1972) A review of the arsenic cycle in natural waters. *Wat Res.* **6**, 1259–1274.

Gulens J., Champ D. R. & Jackson R. E. (1979) Influence of redox environments on the mobility of arsenic in ground water. *Am. Chem. Soc. Symp. Ser.* **83**, 81–95.

Gupta S. K. & Chen K. Y. (1978) Arsenic removal by adsorption. *J. Wat. Pollut. Control Fed.* **50**, 493–506.

Holm T. R., Anderson M. A., Iverson D. G. & Stanforth R. S. (1979) Heterogeneous of arsenic in aquatic systems. *Am. Chem. Soc. Symp. Ser.* **93**, 711–736.

Jenne E. A. (1968) Controls on Mn, Fe, Co, Ni, Cu, and Zn concentrations in soils and water: the significant role of hydrous Mn and Fe oxides. *Am. Chem. Soc. Adv. Chem. Ser.* **73**, 337–387.

Pierce M. L. (1981) Chemical modeling of arsenic in aqueous systems. Ph.D. Dissertation, Arizona State University.

Pierce M. L. & Moore C. B. (1980) Adsorption of arsenite on amorphous iron hydroxide from dilute aqueous solution. *Envir. Sci. Technol.* **14**, 214–216.

Arsenic Geochemistry

1.0 Arsenic Aqueous Speciation

Arsenic occurs in two oxidation states in natural waters, +3 (arsenite) and +5 (arsenate). As(+5) exists predominantly as a negatively charged ion (anion) above a pH of about 2. As(+5) is predominantly monovalent (charge of -1) over the pH range of 2 to 7 (H_2AsO_4), divalent from pH 7 to 11.5 ($HAsO_4^{2-}$) and trivalent at pH values above 11.5 (AsO_4^{3-}), as shown in Figure 1.
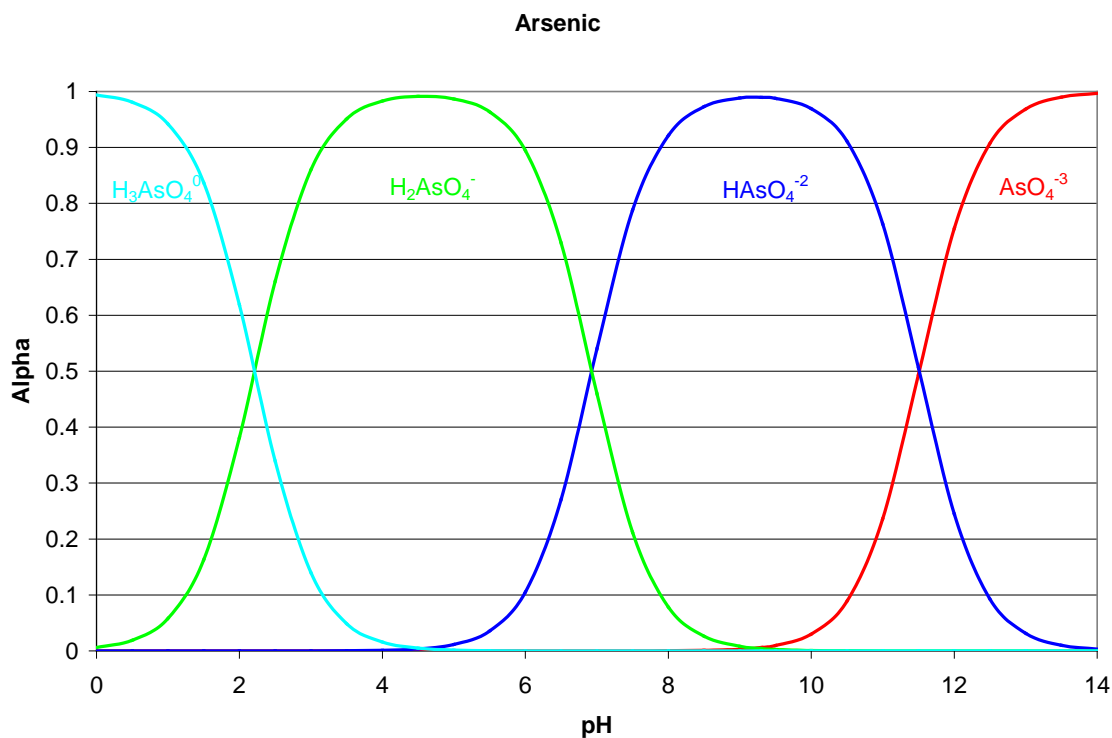
Arsenic

Figure 1 – Arsenate speciation as a function of pH (alpha is the fraction of the total dissolved arsenate consisting of the given species).

The aqueous arsenate and arsenite species distribution with Eh and pH are shown in Figure 2.
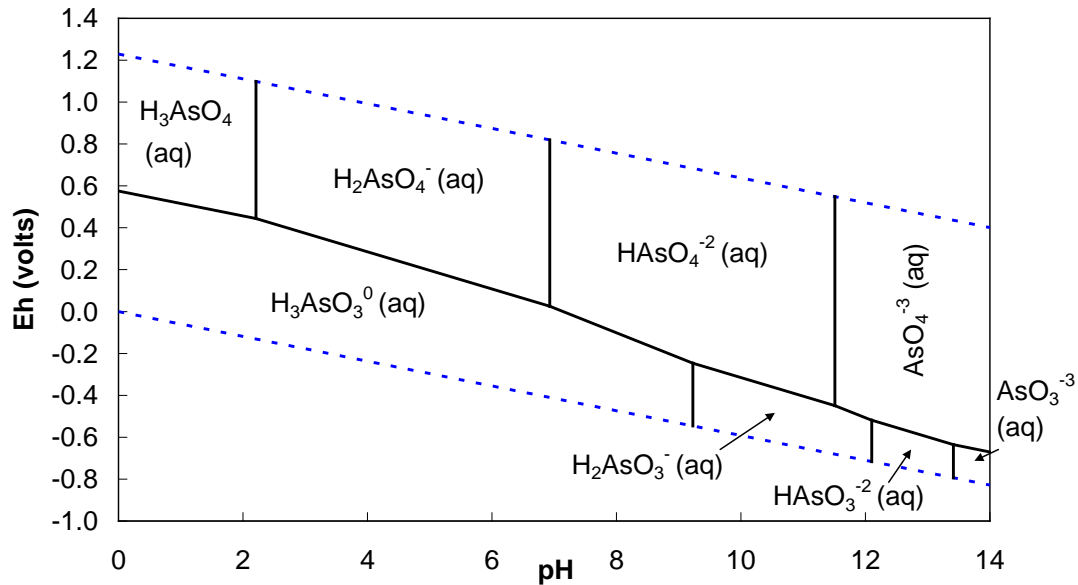
Figure 2 – Eh-pH diagram for the system As-O-H at 25⁰ C and 1 atm.

As(+3) is predominantly a neutral species ($H_3AsO_3^0$) below a pH of about 9. $H_2AsO_3^-$ and $HAsO_3^{-2}$ do not become important until the pH exceeds 9 su, which is higher than observed in the vast majority of natural waters.

2.0 Arsenic Pure Solid Phase Minerals

Pure phase arsenic minerals such as orpiment (As_2S_3), realgar (AsS), and arsenopyrite ($FeAsS$) occur mainly in ore deposits formed from hydrothermal fluids within the Earth's crust. A few pure phase arsenic minerals occur under low temperature and low pressure conditions at the Earth's surface, such as scorodite ($FeAsO_4 \cdot 2H_2O$ at low pH), and arsenic sulfides (under reducing conditions). However, the vast majority of pure phase arsenic minerals are too soluble to be present in soils that are in contact with water.

3.0 Arsenic Solid-Solution Phases

Arsenic forms solid-solution phases with ferric hydroxide and iron hydroxysulfates such as jarosite ($HFe_3(OH)_6(SO_4)_2$) and schwertmannite ($Fe_8O_8(OH)_6SO_4$) and with amorphous silica. Arsenate, like silicate, has a tetrahedral form (a central atom coordinated with four oxygen atoms) which may facilitate the incorporation of arsenate into amorphous silica.

Amorphous phases such as ferric hydroxide or schwertmanite tend to substitute hydroxide or sulfate for arsenate. A reaction to form an iron-arsenic solid-solution is as follows:

$$Fe^{+3} + xAsO_4^{-3} + (3-3x)\ OH^- \rightarrow [FeAsO_4\ 2H_2O]_x[Fe(OH)_3]_{1-x}$$
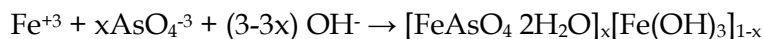
The amount of substitution of arsenic into ferric hydroxide is determined by the pH of the solution (more arsenic substitution occurs at lower pH values) and the concentration of arsenic in solution (higher arsenic concentrations result in more substitution).

2

4.0 Arsenic Adsorption

Arsenic adsorbs to solid surfaces due partly to interactions between the negatively charged ions and a positively charged surface. Therefore, arsenic adsorption tends to be favored for solid materials which are positively charged. The surface charge of the material depends on the type of solid, the pH of the water, and the concentration of other anions in solution.

At low pH values, the water and mineral surfaces have higher concentrations of hydronium ion (H_3O^+) which imparts a positive charge to the surface. As the pH increases, the hydronium ion concentration decreases relative to the hydroxide ion (OH^-) concentration in both the water and the solid materials within the water. At a specific threshold pH value called the pH of the zero-point-of-charge (pH_{ZPC}), the surface charge transitions from positive to neutral to negative. Once the surface charge becomes negative, adsorption of the negatively charged arsenate ions become less prevalent. The pH_{ZPC} is different for different materials, as shown in Table 1.

Table 1 pH of the Zero-Point-of-Charge (pH_{ZPC}) for Various Minerals[1]

Material	Formula	pH_{ZPC}
Magnetite	Fe_3O_4	6.5
Goethite	$FeOOH$	7.8
Hematite	Fe_2O_3	6.7
Amorphous Ferric hydroxide	$Fe(OH)_3$	8.5
Aluminum Hydroxide	γ-$AlOOH$	8.2
Aluminum Hydroxide	$Ā$-$Al(OH)_3$	5.0
Amorphous Silica	SiO_2	2.0
Manganese Dioxide	δ-MnO_2	2.8
Montmorillonite Clay	$Na_{0.2}Ca_{0.1}Al_2Si_4O_{10}(OH)_2 \cdot 10\,H_2O$	2.5
Kaolinite Clay	$Al_2Si_2O_5(OH)_4$	4.6

1. Data from Stumm and Morgan (1981)

The materials with a higher pH_{ZPC} are able to maintain a positive charge at a higher pH than for materials with a lower pH_{ZPC}. Of the materials listed in Table 1, amorphous ferric hydroxide is the best anion adsorbent at higher pH values (below 8.5).

Under typical Eh/pH conditions, As(+3) is a neutral ion and does not adsorb well to negatively or positively charged surfaces. Therefore, As(+3) is roughly 4-10 times more mobile than As(+5) (Duel and Swoboda, 1972). In addition, As(+3) is about 60 times more toxic to humans than arsenate (Hounslow, 1980).

Arsenic has a strong affinity for iron phases and minerals. Strong correlations between arsenic and iron have been found in soils (Woolson et al., 1971; Duel and Swoboda 1972); in ores (Shnyukov, 1963); within ferrihydrite impurities in phosphate pebbles (Stow, 1969); and in sediments impacted by arsenic-containing groundwaters (Whiting, 1992).

The solid material properties not only control the degree to which arsenic is adsorbed at a given pH, but also the amount of arsenic that can be adsorbed before the surface of the solid becomes saturated. The process is described mathematically by the Langmuir Isotherm, which is as follows:

$$C\ (solid) = Kl*Am*C(soln)/(1+Kl*C(soln)) \tag{2}$$

Where,

C(solid)   =   concentration of arsenic adsorbed to the solid phase (mg/kg)
C(soln)   =   concentration of arsenic dissolved in the solution phase (mg/L)
Am   =   maximum adsorption capacity of the solid (mg/kg)
Kl   =   Langmuir adsorption constant

Examples of Langmuir Adsorption Isotherms for three different solid materials are illustrated in Figure 3.
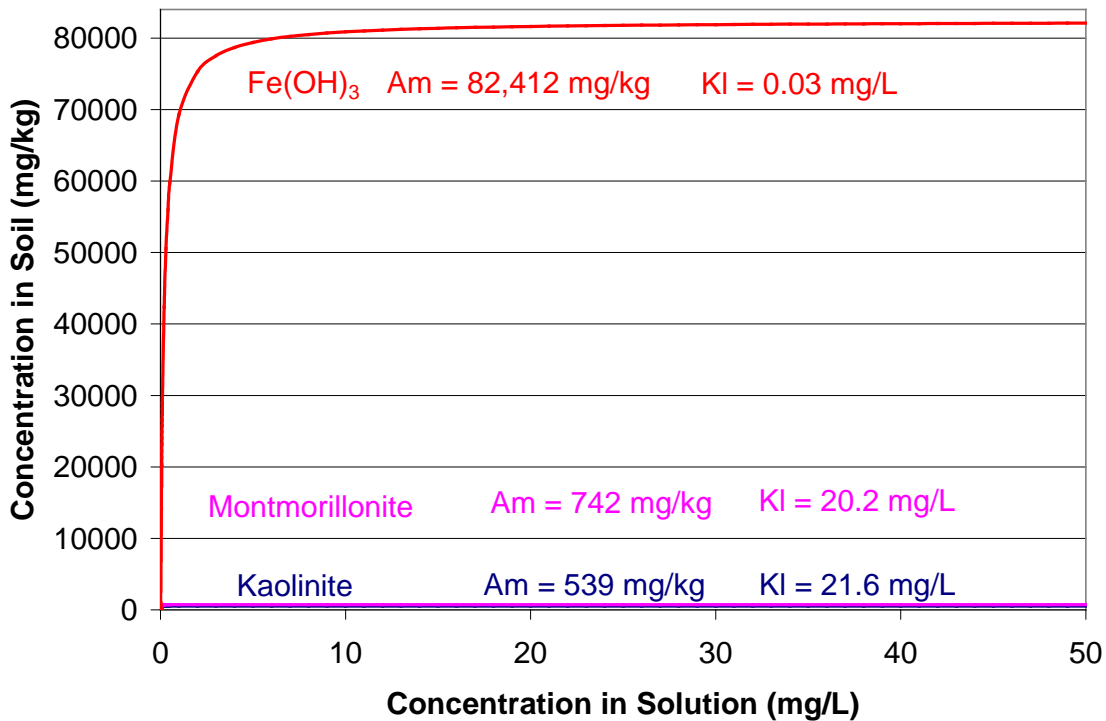
Figure 3 – Langmuir Isotherms illustrating arsenate adsorption capacities of Fe(OH)$_3$(s), kaolinite, and montmorillonite at a pH of 5 su. Langmuir adsorption constants (Kl and Am) are from Pierce and Moore (1982) for Fe(OH)$_3$(s) and Frost and Griffin (1977) for kaolinite and montmorillonite.

The adsorption of arsenate as illustrated in Figure 3 can be understood by imagining a "clean" soil or sediment which is subjected to waters with increasing arsenate concentrations (such as a with the expansion of an arsenate-bearing groundwater plume). As concentrations in the arsenate solution increase, increasingly greater amounts of arsenate can be "forced" onto the solid surface. This process is seen in Figure 3 as the steep part of the curve. As the arsenate concentrations on the soil continue to increase, a point is eventually reached where the solid surfaces are completely saturated with arsenate and there is no more capacity for additional arsenate adsorption. No matter how high the dissolved arsenate concentrations become, the solid arsenate concentration remains constant. The flat part of the curve describes the saturation point of the solid. The Langmuir Am constant is the adsorption capacity and determines the

level of the flat portion of the curve, while the Kl constant determines the rate at which Am is reached (the steepness of the initial segment of the curve).

Figure 3 shows that at pH 5, iron hydroxide has a much higher arsenate adsorption capacity than montmorillonite or kaolinite clays. Theoretically, a sample of ferric hydroxide could be analyzed, and the concentration of arsenic could be compared to Am. If the analytical result of the solid is significantly higher than Am, then arsenate is likely controlled by coprecipitation rather than adsorption. However, in practice, soils and sediments are rarely composed of a single phase, but are instead heterogeneous mixtures of different minerals with varying amounts of iron hydroxide present. However, the affinity of arsenate for iron minerals such as iron hydroxide can be used to evaluate the fate and transport of arsenate when exposed to soils of varying iron contents.

pH also has a significant effect on the adsorption capacity of arsenic, as shown in Table 2.

Table 2 - Adsorption Capacity of Arsenate and Arsenite vs. pH

| pH | Arsenate Adsorption Capacity (mg/kg) | | Arsenite Adsorption Capacity (mg/kg) |
	$Fe(OH)_3$ (s)[1]	$Al(OH)_3$ (s)[2]	$Fe(OH)_3$ (s)[1]
5	82,412	119,872	34,688
6	63,682	110,732	37,685
7	34,014	88,331	38,434
8	16,932	62,783	36,561
9	10,189	37,535	31,242

1. Pierce and Moore (1982)

2. Anderson et al. (1976)

The pH dependence is due to the speciation of arsenic and the surface charge of the solid at different pH values. Arsenate is a negatively charged ion (anion) at pH values greater than about 2 (Figure 1), while the aluminum and iron hydroxides tend to be positively charged. However, as the pH increases, the surfaces of the solids become less positive and the arsenate species become increasingly negative resulting in fewer adsorption sites. Arsenite, being a neutral species below pH 9 (Figure 2), is relatively insensitive to changes in pH.

5.0 Adsorption Kinetics

The kinetics of arsenic adsorption onto iron oxyhydroxides has been found to be generally very rapid. Luengo et al., (2007) found that arsenic adsorption onto granular ferric hydroxide (GFH) occurs in two stages, the first of which occurs in less than 5 minutes and the second over the course of several hours or more. The second, slower stage was thought to be controlled by diffusion of the water into the small pore spaces of the media.

6.0 Competing Chemical Species

The following paragraphs discuss various constituents that will compete with arsenic for the adsorption sites on an solid media.

Silica

Silica competes with arsenic for adsorption sites, and can affect both the effectiveness and the adsorption capacity of adsorption media such as E33. As the pH of the solution increases (above about 8.5 su), not only does the surface charge of the media become negative, which tends to repel negatively charged arsenic oxyanions, but the dissolved silica species go from neutral species to predominantly charged anions, which compete with arsenic for specific adsorption sites (see Figure 4).
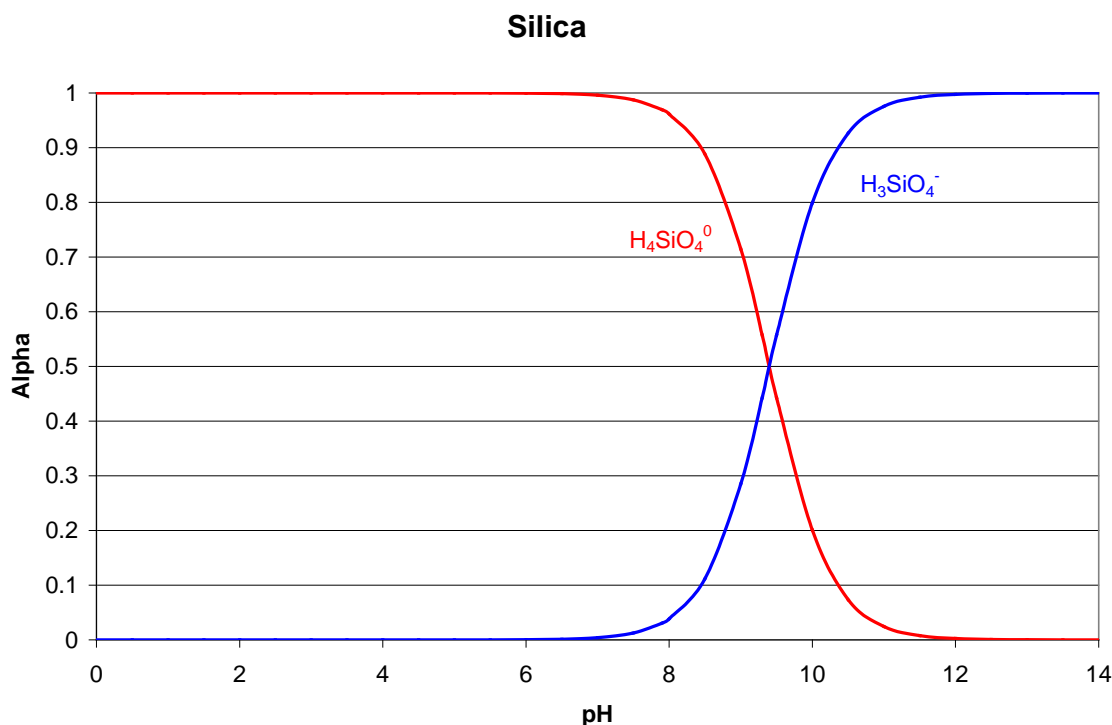
Silica

Figure 4 - Silica speciation as a function of pH (alpha is the fraction of the total dissolved silica consisting of the given species).

Gustafssona and Bhattacharyaa (2007) found that silica concentrations of 0.14 mg/L had only a minor effect on the adsorption of arsenic, while concentrations of 14 mg/L silica had a very significant effect. Based on their calibrated modeling results, adsorption of arsenate onto ferrihydrite in the presence of 0.14 mg/L silica (as Si) was predicted to have a partition coefficient (Kd) of 20,000 (mol/L adsorbed As / mol/L dissolved As). However, in the presence of only 14 mg/L silica, the Kd decreased by three orders of magnitude to just 20.

Highfield (2002) found that the arsenic adsorption capacity was significantly decreased by the presence of silica as well. A capacity of 1 mg As/g GFH (1000 mg/kg) was obtained for a pH 7 water spiked with 28 mg/L Si, compared to a baseline capacity of 15 mg As/g GFH (15,000 mg/kg). Möller and Sylvestera (2007) found that the presence of dissolved silica results in increased competition and a decease in the adsorption capacity of the media as the pH is increased (as predicted by Figure 4). In the presence of 31 mg/L silica, the capacity of the iron oxide-based media tested was decreased 71.8% when the pH was increased from 7 to 9 su.

Phosphate
Phosphate competes with arsenate for adsorption sites resulting in less arsenate adsorption and greater mobility. Gustafsson and Bhattacharya (2007) reviewed spectroscopic data (EXAFS/XANES) conducted by a number of investigators which showed that arsenate and arsenite both form strong inner sphere complexes with the surface of a metal oxide. An inner sphere complex is one in which the oxygen atoms of the arsenate or arsenite ion are shared with the oxygen atoms associated with the metal oxide surface (forming a covalent bond). Phosphate ion was found to be adsorbed in a similar fashion, which helps to explain why competition between arsenic and phosphorous is prevalent over the entire pH range. Modeling results showed that at pH = 8 su, and a phosphate concentration of 0.03 mg/L the As Kd was 15,800 (dimensionless), but when the phosphate was increased by two orders of magnitude (3 mg/L), the Kd decreased to 630. Stachowicz et al., (2007) found that competition between arsenate and phosphate was significant and of much greater magnitude than for other anions such as carbonate/bicarbonate.

Dissolved Organic Matter (DOM)
Bauer and Blodau (2006) found that up to 53.3% of the arsenic adsorbed onto iron oxide could be desorbed by a 25-50 mg/L solution of DOM derived from peat. The authors determined that the leaching effect was due mainly to competition between DOM and arsenic, as iron and arsenic reduction was minor under the conditions of the experiment. Gustafsson and Bhattacharya (2007) found that DOM is a particularly important competing ion when the surface of the iron oxide is coated with humic substances. The anionic nature of DOM and the affinity of the carboxylic and phenolic function group of the DOM for the oxide surface help to explain the adsorption of DOM onto iron oxyhydroxides.

Carbonate/Bicarbonate
In the absence of phosphate and at high CO_2 partial pressures, carbonate/bicarbonate competition with arsenic can be significant. Gustafsson and Bhattacharya (2007) found that at near-neutral pH, and CO_2 partial pressures ranging up to 1.8×10^{-2} atm (50 times the atmospheric value), competition between carbonate species and arsenic is very similar to the effect of 14 mg/L Si (a decrease in the Kd of three orders of magnitude).

Other Ions
Other ions such as chloride, sulfate, and nitrate have little or no effect on arsenic adsorption, while the effect of selenium, molybdenum, and vanadium is minor (Youngran et al., 2007).

Summary of Ions that Compete With Arsenic
A summary of the importance of each species as a competitor with arsenic for adsorption sites on iron oxyhydroxide media is presented in Table 3.

Table 3 – Summary of Ions Which Compete with Arsenic for Adsorption Sites on Oxide Surfaces

Competing Species	Importance
Phosphate (HPO_4^{-2}, $H_2PO_4^{-1}$), Silicate ($H_4SiO_4^0$, $H_3SiO_4^{-1}$), Carbonate (CO_3^{-2}, HCO_3^{-1})	Significant
Dissolved Organic Matter (DOM), Vanadate (VO_4^{-3}, HVO_4^{-2}, $H_2VO_4^{-1}$), Molybdenate (MoO_4^{-2}, $HMoO_4^{-1}$) and selenite (SeO_3^{-2}, and $HSeO_3^{-1}$)	Moderate
Sulfate (SO_4^{-2}), Chloride (Cl^{-1}), and Nitrate (NO_3^{-2}) Selenate (SeO_4^{-3}, $HSeO_4^{-2}$, $H_2SeO_4^{-1}$)	Minor

The qualification of each species as "significant", "moderate", or "minor" is obviously subjective and is influenced by the amount of the species present. For example, competition between arsenic and vanadium is moderate at best unless the water under consideration happens to have high concentrations of vanadium, in which case the importance could become significant.

7.0 References

Bauer, M., and C. Blodau. 2006. Mobilization of arsenic by dissolved organic matter from iron oxides, soils and sediments. *Science of the Total Environment*, v. 354 p. 179-190.

Gustafsson, J.P. and P. Bhattacharya. 2007. Geochemical modelling of arsenic adsorption to oxide surfaces. *Trace Metals and Other Contaminants in the Environment*, ch. 9 p. 159-206.

Highfield, D. 2002. *Arsenic Occurrence in Metro Phoenix Groundwater and Treatment by Granular Ferric Hydroxide*. MS. Thesis, Arizona State University, Tempe, AZ.

Luengo, C., Brigante, M. and M. Avena. 2007. Adsorption kinetics of phosphate and arsenate on goethite. A comparative study. *Journal of Colloid and Interface Science*, v. 311, p. 354-360.

Möller, T. and P. Sylvester. 2007. Effect of silica and pH on arsenic uptake by resin/iron oxide hybrid media. *Water Research*, v. ?? p. ??

Parkhurst, D.L. and Appelo, C.A.J. 1999. User's Guide to PHREEQC (Version 2)- A Computer Program for Speciation, Batch-Reaction, One-Dimensional Transport, and Inverse Geochemical Calculations. USGS Water-Resources Investigations Report 99-4259.

Stachowicz, M., T. Hiemstra, and W. H. van Riemsdijk. 2007. Multi-competitive interaction of As(III) and As(V) oxyanions with Ca2+, Mg2+, PO3−4, and CO2−3 ions on goethite. *Journal of Colloid and Interface Science*, v. ?? p. ??

Youngran, J, M. FAN, J. Van Leeuwena and J. F. 2007. Belczykc Effect of competing solutes on arsenic(V) adsorption using iron and aluminum oxides. *Journal of Environmental Sciences*, v. 19 no. 8 p. 910-919.

Anderson, M.A., J.F. Ferguson and J. Gavis. 1976. Arsenate adsorption on amorphous aluminum hydroxides. *J. Colloid & Interface Sci.* v. 54 p. 391-399.

Duel, L.E. and A. R. Swoboda. 1972. Arsenic solubility in a reduced environment. Soil Sci. Soc. Am. Proc. 36:276-278.

Electric Power Research Institute (EPRI). 1984. *Chemical Attenuation Rates, Coefficients, and Constants in Leachate Migration. Volume 1: A Critical Review.* EPRI EA-3356 Volume 1 Project 2198-1 February 1984.

Frost, R.R. and R.A. Griffin. 1977. Effect of pH on adsorption of arsenic and selenium from landfill leachate by clay minerals. *Soil Sci. Soc. Am. J.* v. 41 p. 53-57.

Hem, J.D. 1971. Study and Interpretation of the Chemical Characteristics of Natural Water. Second Edition. USGS Water Supply Paper 1473.

Hounslow, A.W. 1980. Ground Water Geochemistry: Arsenic in Landfills. *Ground Water* v. 18 n. 4 p. 331-333.

Pierce, M.L. and C.B. Moore. 1982. Adsorption of arsenite and arsenate on amorphous iron hydroxide. Water Res. 16:1247-1253.

Powell, R.M., Puls, R.W., Hightower, S.K., and D.A. Sabatini. 1995. Coupled iron corrosion and chromate reduction: mechanisms for subsurface remediation. Environ. Sci. Technol. 29:1913-1922.

Shnyukov, E.F. 1963. Arsenic in the Cimmerian iron ores of the Azov-Black Sea region. Geochemistry (Geokhimiya), 87-93.

Stow, S.H. 1969. The occurrence of arsenic and the color-causing components in Florida land-pebble phosphate rock. Economic Geology. V. 64, p. 667-671.

Stumm, W. and J.J. Morgan. 1981. Aquatic Chemistry: An Introduction Emphasizing Chemical Equilibria in Natural Waters. 2nd ed. John Wiley and Sons, NY.

Whiting, K.S. 1992. The Thermodynamics and Geochemistry of Arsenic, with Application to Subsurface Waters at the Sharon Steel Superfund Site at Midvale, Utah. MS Thesis T-4128 Colorado School of Mines, Golden Colorado.

Woolsen, E.A., J.H. Axley, and P.C. Kearney. 1971. The chemistry and phytotoxicity of arsenic in soils: I Contaminated field soils. Soil Sci. Soc. Am. Proc. 35:938-943.

Attachment F

							Species			
pH =	7	su								
[Ca] =	700	mg/L								
Eh =	400	mv								
Conductivity=	1950	umho/cm		3.32E-02	ionic strength					
				Gamma		Activity	Concentration	As Atoms	As Conc.	
log K			Charge (z)	(Davies)		(molar)	(molar)		(molar)	M%
-18.1	log[AsO4-3]=		-3	0.19	-6.41	3.86E-07	1.99E-06	1	1.987E-06	0.0%
11.50	log[HAsO4-2]=		-2	0.48	-1.91	0.012211	2.55E-02	1	0.0255074	66.86%
6.93	log[H2AsO4-]=		-1	0.82	-1.98	0.010393	1.26E-02	1	0.0126386	33.13%
2.21	log[H3AsO40]=		0	0.98	-6.77	1.69E-07	1.71E-07	1	1.711E-07	0.00%
19.44	log[H3AsO$_3^0$]=		0	0.98	-14.85	1.41E-15	1.44E-15	1	1.437E-15	0.00%
-9.23	log[H$_2$AsO$_3$-]=		-1	0.82	-17.08	8.37E-18	1.02E-17	1	1.018E-17	0.00%
-21.33	log[HAsO$_3^{2-}$]=		-2	0.48	-22.18	6.62E-23	1.38E-22	1	1.383E-22	0.00%
-34.74	log[AsO$_3^{3-}$]=		-3	0.19	-28.59	2.55E-29	1.31E-28	1	1.313E-28	0.00%
-12.70	log[Ca+2]=		2	0.48	-2.06	0.008733				
	log[CaSO4]=					0.008733				
									0.0381481	
Results										
Solubility =	**2858.133**	**mg/L as As**								

Technical Memorandum
Relative Bioavailability (RBA)
Risk Reduction Standards (RRSs)
Fire Station 19, HSI #10844
Duluth, Gwinnett County, Georgia
March 17, 2015

A Voluntary Investigation and Remediation Plan (VIRP) has been approved for the Fire Station 19 site. The VIRP recommended a bioavailability evaluation of the arsenic in soil. Soil In vitro bioavailability (IVBA) testing was completed to determine the arsenic bioavailability. Electron microprobe (EMP) analyses were also recommended in the VIRP to support the bioavailability evaluation and to evaluate potential arsenic at Fire Station 19. The sampling and bioavailability/ EMP analyses were completed from October 21st to November 24th of 2014. The Georgia Environmental Protection Division (EPD) approved the VIRP on January 15, 2015. This technical memorandum presents the IVBA results and proposed soil Risk Reduction Standards (RRSs).

1.0 Introduction

Twenty soil samples were collected from Fire Station 19 on October 21, 2014 (**Figure 1**). The samples were delivered to CDM Smith's Denver laboratory for preparation and then delivered to the University of Colorado Geological Sciences Laboratory for analyses. All samples were analyzed for total arsenic and IVBA testing. The EMP analyses are reported in a separate technical memorandum. Discussions are provided below related to arsenic bioavailability, IVBA methodology, calculations of the results, and the proposed soil arsenic RRSs for Fire Station 19.

2.0 Arsenic Bioavailability

Arsenic in soil can be naturally occurring with background concentrations in the United States typically ranging from 1 to 25 mg/kg (Smith et al. 2013). Higher soil arsenic concentrations can occur from mining, smelting, leather tanning, wood preservation, or pesticides. CDM Smith concluded from the EMP testing that the arsenic at Fire Station 19 is likely a result of historic agricultural land use. A soluble arsenic form such as calcium arsenate was likely applied to crops. The soluble arsenic was then attenuated in soil, by precipitation with iron oxyhydroxides or adsorbed onto existing iron oxyhydroxide minerals, resulting in a less soluble form.

Incidental soil ingestion is the primary exposure route to arsenic in soil. Accurate human health risk assessment resulting from incidental arsenic ingestion requires knowledge of the arsenic bioavailability in the soil. Oral bioavailability is the amount of arsenic absorbed into the body following ingestion, also referred to as the oral absorption fraction.

Arsenic absorption depends mainly on the physical and chemical attributes. Some arsenic forms such as sodium arsenate are highly soluble in gastrointestinal fluid and are efficiently absorbed into the blood of most animal species (Juhasz et al. 2006, ATSDR 2007). Arsenic adsorbed to iron-bearing soil particles are not as readily dissolved and passed from the body. Because the form of arsenic in soil varies, the arsenic bioavailability also varies.

Gastrointestinal absorption of ingested arsenic may be described either in absolute or relative terms. Absolute bioavailability (ABA) is the ratio of the amount of arsenic absorbed to the amount ingested; this ratio is also referred to as the oral absorption fraction. Relative bioavailability (RBA) is the ratio of

the absolute oral bioavailability of arsenic in soil (ABA_{test}) to the absolute oral bioavailability of arsenic in a reference material ($ABA_{reference}$), as shown below:

$$RBA = ABA_{test}/ABA_{reference}$$

Oral toxicity values for arsenic, including the oral reference dose and cancer slope factors, are based on studies of human populations exposed to arsenic in drinking water (U.S. Environmental Protection Agency [EPA] 1998). Therefore, the most appropriate form of arsenic for use as a reference material is a readily soluble arsenic compound, such as sodium arsenate. The National Environmental Policy Institute (NEPI) document, *Assessing the Bioavailability of Metals in Soil for Use in Human Health Risk Assessment* (NEPI 2000), provides additional information on the bioavailability of metals in soil.

3.0 IVBA Methodology

Although RBA can be measured *in vivo* using animals (e.g., swine, monkeys), such studies are generally slow and costly. An alternative strategy is to perform *in vitro* measurements of arsenic solubility in the laboratory. The IVBA laboratory method for arsenic (Drexler 2012) was derived from the IVBA laboratory method developed for lead (EPA 9200.2-86; EPA 2012b).

In brief, a sample of soil is screened to a <250 µm size fraction and arsenic is extracted using a fluid that has properties that resemble gastrointestinal fluid (i.e., pH 1.5), residence time in the stomach, temperature, and soil to liquid ratio (i.e., relative amounts of soil and gastrointestinal fluid). The soil <250 µm size fraction was used because this soil particle size is representative of that which adheres to children's hands and may be ingested (EPA 2000). The amount of arsenic solubilized from the sample into the fluid is measured. The fraction of arsenic that is solubilized is referred to as the IVBA. The IVBA is then utilized to predict the RBA through an empiric correlation model.

CDM Smith was part of the team of scientists that validated the arsenic IVBA method and developed the RBA correlation model for arsenic. This correlation model is presented in Brattin et al. (2013) and is based on 20 test materials from mining, smelting, herbicide, pesticide, wood-treating, and chemical plant sites across the United States that have both RBA and IVBA data. For this correlation model, the arsenic RBA measurements are based on *in vivo* juvenile swine studies (Brattin and Casteel 2013) and the arsenic IVBA measurements are based on an extraction fluid with a pH of 1.5. As shown in Brattin et al. (2013), arsenic RBA can be estimated from measurements of arsenic IVBA as follows:

$$RBA = 19.7 + (0.62 \bullet IVBA) \qquad (R^2 = 0.723)$$

Where:

      RBA = Estimated relative bioavailability (expressed as a percentage)

      IVBA = Measured in vitro bioavailability (expressed as a percentage)

Notice in the above equation that the intercept is 19.7%, which means that the lowest RBA that can be predicted using this model is 19.7%. This means that even if the actual IVBA is 0%, this model will conservatively estimate the RBA at 19.7%.

IVBA testing was conducted on 20 soil samples from Fire Station 19 to determine the site-specific arsenic RBA. IVBA analyses were performed by Dr. John Drexler at the University of Colorado in Boulder, Colorado. **Table 1** presents the results of the IVBA testing. The arsenic concentration in the

extraction fluid was below the method detection limit of <0.2 µg/L for 14 of 20 samples. For the six samples with detected concentrations of arsenic, the estimated IVBA values ranged from 0.6% to 13%. For the non-detect samples, the IVBA is less than 0.1%.

Table 1 also presents the arsenic RBA values calculated from the IVBA using the equation presented above. The calculated RBA values for the detected samples ranged from 20.1% to 27.8%. For the non-detect samples, the arsenic RBA equals the 19.7% intercept.

4.0 RBA Calculations

EPA's Risk Assessment Guidance for Superfund (RAGS) Part A (EPA 1989), Framework for Metals Risk Assessment (EPA 2007a), and Guidance for Evaluating the Bioavailability of Metals in Soils for Use in Human Health Risk Assessment (EPA 2007b) discuss how RBA data are used to make adjustments to exposure estimates in site-specific risk assessments.

The arsenic bioavailability in soil varies from site to site and depends on the chemical form, as well as the physical and chemical characteristics arsenic-bearing soil particles. For this reason, EPA recommends the collecting site-specific RBA data where feasible for improving the site risk characterization (EPA 2007b). The RBA can be used to adjust the toxicity values when quantifying cancer risks and non-cancer hazards as follows:

$SF_{o\text{-adjusted}} = SF_o \cdot RBA$

$RfD_{o\text{-adjusted}} = RfD_o / RBA$

Where:

SF_o = Oral slope factor $(mg/kg/day)$-1

RfD_o = Oral reference dose (mg/kg/day)

RBA = Relative bioavailability (dimensionless)

These adjusted toxicity values are used to develop risk-based remediation goals for soil (EPA 2002). The site-specific RBA ranges from approximately 20-30%. To be conservative, a site-specific RBA of 30% was selected. The following RBA-adjusted toxicity values for arsenic were calculated based on the site-specific data.

Arsenic $SF_{o\text{-adjusted}} = 1.5 \ (mg/kg/day)^{-1} \cdot 0.3 = 0.45 \ (mg/kg/day)^{-1}$

Arsenic $RfD_{o\text{-adjusted}} = 3.0E\text{-}04 \ mg/kg/day / 0.3 = 1.0E\text{-}03 \ mg/kg/day$

5.0 Proposed RRSs

The following arsenic RSSs for soil were presented in the VIRP.

- Type 1 Residential: 20 mg/kg

- Type 3 Non-Residential: 20 mg/kg

- Type 4 Non-Residential: 38 mg/kg in surface soil

- Type 5 Construction Worker: 881 mg/kg in surface soil

CDM Smith has recalculated the Type 4 and the Type 5 construction worker scenario RRSs using the conservative 30% RBA. Additional RRSs included in Attachment A include a Type 2 soil RRS and a Type 5 RRS based on a trespasser exposure scenario that also use the 30% RBA. The RRS calculations, input parameters, and assumptions are provided in **Attachment A** and discussed below.

Type 2 Residential Exposure

The Type 2 RRS equations, inputs, and assumptions all conform to Appendix III of the Georgia Rules for Hazardous Site Response (Rules) and the default child exposure parameters provided on the EPD website. $SF_{o-adjusted}$ and $RfD_{o-adjusted}$ values were used for toxicity. Based on calculation of child and adult exposures for carcinogenic and noncarcinogenic effects, the carcinogenic effect for a child is the lowest arsenic concentration and it is 20.3 mg/kg. As stated in the VIRP, this is a non-residential property and an Environmental Covenant (EC) is proposed. However, the property is not fenced or controlled. The current property uses for the County's fueling purposes and operation as a fire station require relatively free and unencumbered access. As a result, a Type 4 non-residential RRS and a Type 5 trespasser RRS have been developed, as described below.

Type 4 Non-Residential Exposure

The Type 4 RRS equations, inputs, and assumptions all conform to Appendix III of the Rules. $SF_{o-adjusted}$ and $RfD_{o-adjusted}$ values were used for toxicity. Based on calculation adult exposures for carcinogenic and noncarcinogenic effects, the carcinogenic effect is the lowest arsenic concentration and it is 127 mg/kg.

Type 5 Trespasser Exposure

Assuming that a vagrant dwells on the property for an extended period of time is a commonly used trespasser scenario. However, this scenario has an extremely low probability because fire station personnel are at the property 24 hours per day and 7 days per week and the fire station personnel are responsible for determining the nature of anyone's business entering the property. CDM Smith learned this first hand during our initial site visits when we were questioned within about 10 minutes of arriving on the property.

A more realistic exposure scenario concerns the public crossing the property from residential areas to the west in order to access bus stops or commercial businesses to the east of the property. To be conservative, CDM Smith assumed that the trespasser included an adult and a child. While walking across the property from east to west can be easily completed in less than five minutes, CDM Smith conservatively assumed that the crossing duration would be one hour to account for loitering until a bus was scheduled to arrive or to entertain the child. CDM Smith also assumed that a return trip would also be required, resulting in the adult and child occupying the property for a daily duration of 2 hours.

The residential Type 2 equations, inputs, and assumptions were generally used for the adult and child trespasser scenario and the $SF_{o-adjusted}$ and $RfD_{o-adjusted}$ values were used for toxicity. However, modifications were made to account for occupying the property for 2 hours rather than 24 hours per day. This was accomplished by adjusting the default child and adult residential inhalation rates and

soil ingestion rates, which are based on a 24-hour exposure period per day, downward by a factor of 2/24. Based on calculation of child and adult exposures for carcinogenic and noncarcinogenic effects, the child carcinogenic effect is the lowest arsenic concentration for this scenario and it is 243 mg/kg.

Type 5 Construction Worker Exposure

The Type 5 construction worker scenario assumptions were presented in the VIRP and those assumptions were not changed in calculating the revised RRS using the $SF_{o\text{-adjusted}}$ and $RfD_{o\text{-adjusted}}$ values for toxicity. The revised RSS is for noncarcinogenic effects and it is 2,940 mg/kg.

Proposed Arsenic RRS

The lowest applicable RRSs have been selected for use at the property and their use is dependent on an EC being obtained that will restrict the property to non-residential use and disallow the use of groundwater from beneath the property. The Type 4 non-residential RRS of 127 mg/kg arsenic in soil will be applied for surface soil in open areas of the site that are not paved or covered by a building. Corrective action will be completed, as described in the VIRP, to the open areas that exceed 127 mg/kg arsenic in surface soil. Exposure to subsurface soil will be restricted to construction workers and the Type 5 construction worker RRS of 2,940 mg/kg arsenic in soil will apply. Because no soil areas exceed 2,940 mg/kg arsenic, corrective action is not required. However, any construction activities that occur on the property will properly manage soil as contaminated media.

6.0 References

ATSDR (Agency for Toxic Substances and Disease Registry). 2007. Toxicological Profile for Arsenic. U.S. Department of Health and Human Services, Public Health Service, Agency for Toxic Substances and Disease Registry. August 2007.

Brattin, W., and Casteel, S. 2013. Measurement of arsenic relative bioavailability in swine. J Toxicol Environ Health, Part A 76(7):449-457.
http://www.tandfonline.com/doi/abs/10.1080/15287394.2013.771562

Brattin, W., Drexler, J., Lowney, Y., Griffin, S., Diamond, G., Woodbury, L. 2013. An in vitro method for estimation of arsenic relative bioavailability in soil. J Toxicol Environ Health, Part A 76(7):458-478.
http://www.tandfonline.com/doi/abs/10.1080/15287394.2013.771765

CDM Smith. 2014. Corrective Action Plan. Fire Station #19, Gwinnett County, Georgia. Prepared for Gwinnett County. October.

Drexler, J. 2012. Standard Operating Procedure: In Vitro Bioacessibility (IVBA) Procedure for Arsenic. Revision 0 – 9/25/12. http://www2.epa.gov/sites/production/files/2014-05/documents/arsenicivba_sop25sep2012.pdf

EPA (U.S. Environmental Protection Agency). 1989. Risk Assessment Guidance for Superfund (RAGS), Volume I Human Health Evaluation Manual (Part A). Office of Emergency and Remedial Response, U.S. Environmental Protection Agency, Washington D.C. EPA/540/1-89/002.
http://www.epa.gov/oswer/riskassessment/ragsa/pdf/rags_a.pdf

EPA. 1991. Risk Assessment Guidance for Superfund (RAGS), Volume I Human Health Evaluation Manual (Part B, Development of Risk-based Preliminary Remediation Goals). Office of Emergency and Remedial Response, U.S. Environmental Protection Agency, Washington D.C. EPA/540/R-92/003. December. http://www.epa.gov/oswer/riskassessment/ragsb/

EPA. 1998. Integrated Risk Information System Summary: Arsenic, inorganic (CASRN 7440-38-2). Last updated: 4/10/1998. http://www.epa.gov/iris/subst/0278.htm

EPA. 2000. Short Sheet: TRW Recommendations for Sampling and Analysis of Soil at Lead (Pb) Sites. Office of Solid Waste and Emergency Response, U.S. Environmental Protection Agency, Washington, D.C. EPA-540-F-00-010. OSWER 9285.7-38. April. http://www.epa.gov/superfund/lead/products/sssiev.pdf

EPA. 2002. Supplemental Guidance for Developing Soil Screening Levels for Superfund Sites. Office of Emergency and Remedial Response U.S. Environmental Protection Agency, Washington, D.C. OSWER 9355.4-24. December. http://www.epa.gov/superfund/health/conmedia/soil/pdfs/ssg_main.pdf

EPA. 2007a. Framework for Metals Risk Assessment. Office of the Science Advisor, Risk Assessment Forum, U.S. Environmental Protection Agency, Washington, D.C. EPA 120/R-07/001. March. http://www.epa.gov/raf/metalsframework/pdfs/metals-risk-assessment-final.pdf

EPA. 2007b. Guidance for Evaluating the Oral Bioavailability of Metals in Soils for Use in Human Health Risk Assessment. Office of Solid Waste and Emergency Response, U.S. Environmental Protection Agency. OSWER 9285.7-80. May. http://epa.gov/superfund/bioavailability/bio_guidance.pdf

EPA. 2009. Risk Assessment Guidance for Superfund (RAGS), Volume I Human Health Evaluation Manual (Part F, Supplemental Guidance for Inhalation Risk Assessment). Office of Emergency and Remedial Response, U.S. Environmental Protection Agency, Washington D.C. EPA/540/R-070/002. OSWER 9285.7-82. January. http://www.epa.gov/oswer/riskassessment/ragsf/index.htm

EPA. 2012a. Recommendations for Default Value for Relative Bioavailability of Arsenic in Soil. Office of Solid Waste and Emergency Response, U.S. Environmental Protection Agency. OSWER 9200.1-113. December. http://www.epa.gov/superfund/bioavailability/pdfs/Arsenic%20Bioavailability%20POLICY%20Memorandum%2012-20-12.pdf

EPA. 2012b. Standard Operating Procedure for an In Vitro Bioaccessibility Assay for Lead in Soil. EPA 9200.2-86. April. http://epa.gov/superfund/bioavailability/pdfs/EPA_Pb_IVBA_SOP_040412_FINAL_SRC.pdf

EPA. 2014. Regional Screening Levels, User's Guide, Section 5.10 Arsenic. November. http://www.epa.gov/reg3hwmd/risk/human/rb-concentration_table/usersguide.htm

Juhasz, A.L., Smith, E., Weber, J., Rees, M., Rofe, A., Kuchel, T., Sansom, L., and Ravi Naidu, R. 2006. In Vivo Assessment of Arsenic Bioavailability in Rice and Its Significance for Human Health Risk Assessment. Environ. Health Perspect. 114(12):1826-1831.

NEPI (National Environmental Policy Institute). 2000. Assessing the Bioavailability of Metals in Soil for Use in Human Health Risk Assessment. Bioavailability Policy Project Phase II, Metals Task Force Report. http://geoweb.tamu.edu/Faculty/Herbert/geol641/docs/MetalsBioavailability.pdf

Smith, D.B., Cannon, W.F., Woodruff, L.G., Solano, Federico, Kilburn, J.E., and Fey, D.L. 2013. Geochemical and mineralogical data for soils of the conterminous United States. U.S. Geological Survey Data Series 801, 19 pp. http://pubs.usgs.gov/ds/801/

Figure 1
RBA Soil Sampling Locations
Fire Station No. 19 (HSI #10844)
Gwinnett County, Duluth, Georgia

Scale in Feet

0   80   160

● Soil Boring Location   - - - Property Lines

CDM Smith

Table 1: Soil Arsenic and RBA Data Summary

Fire Station 19, HSI #10844

Duluth, Gwinnett County, Georgia

Boring Location	Processed [1] Soil Arsenic mg/kg	Extraction Soil Mass g	Extract Arsenic µg/L	Fluid Volume L	Arsenic IVBA [2] %	Arsenic RBA %
SB-1	99	1.00152	<0.2	0.1	NA	NA
SB-3	554	1.005	102	0.1	1.8%	20.8%
SB-8	125	1.0004	<0.2	0.1	NA	NA
SB-9	99	1.0009	<0.2	0.1	NA	NA
SB-14	310	1.00801	<0.2	0.1	NA	NA
SB-15	34	1.00157	<0.2	0.1	NA	NA
SB-18	67	1.00116	<0.2	0.1	NA	NA
SB-19	89	1.00442	<0.2	0.1	NA	NA
SB-20	89	1.00838	<0.2	0.1	NA	NA
SB-21	144	1.00157	<0.2	0.1	NA	NA
SB-24	314	1.0044	39	0.1	1.2%	20.4%
SB-25	207	1.00789	14	0.1	0.7%	20.1%
SB-27	205	1.00253	12	0.1	0.6%	20.1%
SB-30	134	1.00456	<0.2	0.1	NA	NA
SB-34	103	1.00947	139	0.1	13%	27.8%
SB-35	104	1.01199	<0.2	0.1	NA	NA
SB-38	62	1.0053	<0.2	0.1	NA	NA
SB-39	127	1.00568	<0.2	0.1	NA	NA
SB-43	88	1.00497	<0.2	0.1	NA	NA
SB-52	195	1.00547	15	0.1	0.8%	20.2%

NA - Not Applicable: No calculation for arsenic below the detection limit in the extract.

Notes

1 - Soil was processed to contain particle sizes less than 250 µm.

2 - *In vitro* bioavailability (IVBA) = $\dfrac{\text{Extract Arsenic x Fluid Volume}}{\text{Processed Soil Arsenic x Extraction Soil Mass / 1,000}}$ X 100

If Extract Arsenic is less than 0.2 µg/L, then IVBA is less than 0.1%

3 - Relative Bioavailability (RBA) = 19.7 + (0.62 x IVBA): Brattin *et al.* 2013.

If arsenic is not detected in the extract, the RBA = 19.7%.

CDM Smith

Appendix A

**CDM
Smith**

RAGS Equation 6
Type 2 Site-Specific Residential Soil - Carcinogenic Effects

$$C_{car} \text{ mg/kg} = \frac{TR \times BW \times AT_{car} \times 365 \text{ days/year}}{EF \times ED \times [(SFo \times 10^{-6} \text{ kg/mg} \times IR_{soil}) + (SF_i \times IR_{air} \times \{1/VF + 1/PEF\})]}$$

Parameter	Definition (units)	Default Value	Source
$C_{car} =$	Concentration in soil (mg/kg)	Calculated	Not Applicable
$TR_{A/B}$	Carcinogen Class A/B target excess lifetime cancer risk (none)	1.E-05	HSRA Rules
TR_C	Carcinogen Class C target excess lifetime cancer risk (none)	1.E-04	HSRA Rules
SF_i	Inhalation cancer slope factor $(mg/kg\text{-}dy)^{-1}$ $= IUR \times 1{,}000 \times BW \text{ 70 kg} / IR_{air} \text{ 20 m}^3/dy$	Chemical-Specific	Not Applicable
IUR	Inhalation unit risk $(ug/m^3)^{-1}$	Chemical-Specific	Not Applicable
SF_o	Oral cancer slope factor $(mg/kg\text{-}dy)^{-1}$	Chemical-Specific	Not Applicable
$AT_{car\text{-}adult}$	Adult averaging time (yr)	70	HSRA Rules
$AT_{car\text{-}child}$	child averaging time (yr)	70	HSRA Rules

RAGS Equation 7
Type 2 Site-Specific Residential Soil - Noncarcinogenic Effects

$$C_{noncar} \text{ mg/kg} = \frac{THI \times BW \times AT_{noncar} \times 365 \text{ days/year}}{ED \times EF \times [\{(1/RfD_o) \times 10^{-6} \text{ kg/mg} \times IR_{soil}\} + \{(1/RfD_i) \times IR_{air} \times (1/VF + 1/PEF)\}]}$$

Parameter	Definition (units)	Default Value	Source
$C_{noncar} =$	Concentration in soil (mg/kg)	Calculated	Not Applicable
THI	Target hazard index (none)	1	HSRA Rules
RfD_o	Oral chronic reference dose (mg/kg-dy)	Chemical-Specific	Not Applicable
RfD_i	Inhalation chronic reference dose (mg/kg-dy) $= RfC_i \times IR_{air} \text{ 20 m}^3/dy / BW \text{ 70 kg}$	Chemical-Specific	Not Applicable
RfC_i	Inhalation reference concentration (mg/m^3)	Chemical-Specific	Not Applicable
$AT_{noncar\text{-}adult}$	Adult averaging time (yr)	30	HSRA Rules
$AT_{noncar\text{-}child}$	child averaging time (yr)	6	HSRA Rules

CDM Smith

Type 2 Soil RRS Equations
Fire Station 19 (HSI #10844)
Duluth, Gwinnett County, Georgia

Standard Assumptions

BW$_{adult}$	Adult body weight (kg)	70	HSRA Rules
BW$_{child}$	child body weight (kg)	15	HSRA Rules
EF	Exposure frequency (dy/yr)	350	Site Specific
ED$_{adult}$	Adult exposure Duration (yr)	30	HSRA Rules
ED$_{child}$	child exposure Duration (yr)	6	HSRA Rules
IR$_{air-adult}$	Adult inhalation rate (m^3/dy)	15	HSRA Rules
IR$_{air-child}$	child inhalation rate (m3/dy)	15	HSRA Rules
IR$_{soil-adult}$	Adult soil ingestion rate (mg/dy)	114	HSRA Rules
IR$_{soil-child}$	child soil ingestion rate (mg/dy)	200	HSRA Rules
PEF	Particulate emission factor (m^3/kg)	4.63E+09	HSRA Rules

Soil-to-Air Volatilization Factor (VF)

$$VF \ (m^3/kg) = \frac{(LS \times V \times DH) \times (\pi \times \alpha \times T)^{1/2}}{A \times 2 \times D_{ei} \times E \times K_{as} \times 10^{-3} \ kg/g}$$

Parameter	Definition (units)	Default Value	Source
LS	Length of side of contaminated area (m)	45	HSRA Rules
V	Wind speed in mixing zone (m/s)	2.25	HSRA Rules
A	Area of contamination (cm^2)	2.03E+07	HSRA Rules
DH	Diffusion height (m)	2	HSRA Rules
α	$(D_{ei} \times E)/[E + (\rho_s \times (1-E)/K_{as})]$ (cm^2/s)	Chemical-specific	HSRA Rules
T	Exposure Interval (s)	7.90E+08	HSRA Rules
ρ_s	Density of soil solids (g/cm^3)	2.65	HSRA Rules
D$_{ei}$	Effective diffusivity (cm^2/s)	$D_i \times E^{0.33}$	HSRA Rules
D$_i$	Molecular Diffusivity (cm^2/s)	Chemical-specific	Not Applicable
E	Total soil porosity	0.35	HSRA Rules
K$_{as}$	Soil-air partition coefficient (g soil/cm^3 air)	$(H/K_d) \times 41$	HSRA Rules
H	Henry's Law Constant (atm-m^3/mole)	Chemical-specific	Not Applicable
K$_d$	Soil-water partition coefficient (cm^3/g)	$K_{OC} \times OC$	HSRA Rules
K$_{OC}$	Organic carbon partition coefficient (cm^3/g)	Chemical-specific	Not Applicable
OC	Soil Organic Carbon Content (none)	2.0E-02	HSRA Rules

HSRA Rules: Georgia Hazardous Response Act Rules, 391-3-19, Appendix III, Media Target Concentrations and Standard Exposure Assumptions.

http://rules.sos.state.ga.us/docs/391/3/19/Appendix%20I-IV.pdf

RAGS: Risk Assessment Guidance for Superfund, Volume I - Human Health Evaluation Manual (Part B, Chapter 3, Development of Risk-Based Preliminary Remediation Goals), U.S. Environmental Protection Agency, December 1991.

http://www.epa.gov/oswer/riskassessment/ragsb/pdf/chapt3.pdf

CDM Smith

Type 2 Soil RRS Equations
Fire Station 19 (HSI #10844)
Duluth, Gwinnett County, Georgia

| Substance | Carcinogen Class | RAGS Eq 6 - Carcinogenic Effects | | | | | | | RAGS Eq 7 - Noncarcinogenic Effects | | | | | | Type 2 Site-Specific Residential Soil RRS |
		TR	Sf_i $(mg/kg\text{-}dy)^{-1}$	IUR $(ug/m^3)^{-1}$	Sf_o $(mg/kg\text{-}dy)^{-1}$	$C_{car\text{-}adult}$ mg/kg	$C_{car\text{-}child}$ mg/kg	THI	RfD_o mg/kg-dy	RfC_i mg/kg-dy	RfD_i mg/kg-dy	$C_{noncar\text{-}adult}$ mg/kg	$C_{noncar\text{-}child}$ mg/kg	mg/kg
Arsenic	A	1.E-05	1.51E+01	4.30E-03	4.50E-01	**3.32E+01**	**2.03E+01**	1	1.00E-03	1.50E-05	4.29E-06	**6.40E+02**	**7.82E+01**	**2.03E+01**

Note: The above standard excludes leaching to groundwater.

CDM Smith

Type 2 Soil RRS Calculations
Fire Station 19 (HSI #10844)
Duluth, Gwinnett County, Georgia

RAGS Equation 6
Type 4 Site-Specific Non-Residential Soil - Carcinogenic Effects

$$C_{car} \text{ mg/kg} = \frac{TR \times BW \times AT_{car} \times 365 \text{ days/year}}{EF \times ED \times [(SFo \times 10^{-6} \text{ kg/mg} \times IR_{soil}) + (SF_i \times IR_{air} \times \{1/VF + 1/PEF\})]}$$

Parameter	Definition (units)	Default Value	Source
C_{car} =	Concentration in soil (mg/kg)	Calculated	Not Applicable
$TR_{A/B}$	Carcinogen Class A/B target excess lifetime cancer risk (none)	1.E-05	HSRA Rules
TR_C	Carcinogen Class C target excess lifetime cancer risk (none)	1.E-04	HSRA Rules
SF_i	Inhalation cancer slope factor $(mg/kg\text{-}dy)^{-1}$ $= IUR \times 1,000 \times BW\ 70\ kg\ /\ IR_{air}\ 20\ m^3/dy$	Chemical-Specific	Not Applicable
IUR	Inhalation unit risk $(ug/m^3)^{-1}$	Chemical-Specific	Not Applicable
SF_o	Oral cancer slope factor $(mg/kg\text{-}dy)^{-1}$	Chemical-Specific	Not Applicable
$AT_{car\text{-}adult}$	Adult averaging time (yr)	70	HSRA Rules
$AT_{car\text{-}child}$	child averaging time (yr)	NA	

RAGS Equation 7
Type 4 Site-Specific Non-Residential Soil - Noncarcinogenic Effects

$$C_{noncar} \text{ mg/kg} = \frac{THI \times BW \times AT_{noncar} \times 365 \text{ days/year}}{ED \times EF \times [\{(1/RfD_o) \times 10^{-6} \text{ kg/mg} \times IR_{soil}\} + \{(1/RfD_i) \times IR_{air} \times (1/VF + 1/PEF)\}]}$$

Parameter	Definition (units)	Default Value	Source
C_{noncar} =	Concentration in soil (mg/kg)	Calculated	Not Applicable
THI	Target hazard index (none)	1	HSRA Rules
RfD_o	Oral chronic reference dose (mg/kg-dy)	Chemical-Specific	Not Applicable
RfD_i	Inhalation chronic reference dose (mg/kg-dy) $= RfC_i \times IR_{air}\ 20\ m^3/dy\ /\ BW\ 70\ kg$	Chemical-Specific	Not Applicable
RfC_i	Inhalation reference concentration (mg/m^3)	Chemical-Specific	Not Applicable
$AT_{noncar\text{-}adult}$	Adult averaging time (yr)	25	HSRA Rules
$AT_{noncar\text{-}child}$	child averaging time (yr)	NA	

Standard Assumptions

BW$_{adult}$	Adult body weight (kg)	70	HSRA Rules
BW$_{child}$	child body weight (kg)	NA	
EF	Exposure frequency (dy/yr)	250	Site Speciifc
ED$_{adult}$	Adult exposure Duration (yr)	25	HSRA Rules
ED$_{child}$	child exposure Duration (yr)	NA	
IR$_{air-adult}$	Adult inhalation rate (m^3/dy)	20	HSRA Rules
IR$_{air-child}$	child inhalation rate (m3/dy)	NA	
IR$_{soil-adult}$	Adult soil ingestion rate (mg/dy)	50	HSRA Rules
IR$_{soil-child}$	child soil ingestion rate (mg/dy)	NA	
PEF	Particulate emission factor (m^3/kg)	4.63E+09	HSRA Rules

Soil-to-Air Volatilization Factor (VF)

$$VF \ (m^3/kg) = \frac{(LS \times V \times DH) \times (\pi \times \alpha \times T)^{1/2}}{A \times 2 \times D_{ei} \times E \times K_{as} \times 10^{-3} \ kg/g}$$

Parameter	Definition (units)	Default Value	Source
LS	Length of side of contaminated area (m)	45	HSRA Rules
V	Wind speed in mixing zone (m/s)	2.25	HSRA Rules
A	Area of contamination (cm^2)	2.03E+07	HSRA Rules
DH	Diffusion height (m)	2	HSRA Rules
α	$(D_{ei} \times E)/[E + (\rho_s \times (1-E)/K_{as})]$ (cm^2/s)	Chemical-specific	HSRA Rules
T	Exposure Interval (s)	7.90E+08	HSRA Rules
ρ_s	Density of soil solids (g/cm^3)	2.65	HSRA Rules
D$_{ei}$	Effective diffusivity (cm^2/s)	$D_i \times E^{0.33}$	HSRA Rules
D$_i$	Molecular Diffusivity (cm^2/s)	Chemical-specific	Not Applicable
E	Total soil porosity	0.35	HSRA Rules
K$_{as}$	Soil-air partition coefficient (g soil/cm^3 air)	$(H/K_d) \times 41$	HSRA Rules
H	Henry's Law Constant (atm-m^3/mole)	Chemical-specific	Not Applicable
K$_d$	Soil-water partition coefficient (cm^3/g)	$K_{OC} \times OC$	HSRA Rules
K$_{OC}$	Organic carbon partition coefficient (cm^3/g)	Chemical-specific	Not Applicable
OC	Soil Organic Carbon Content (none)	2.0E-02	HSRA Rules

HSRA Rules: Georgia Hazardous Response Act Rules, 391-3-19, Appendix III, Media Target Concentrations and Standard Exposure Assumptions.

http://rules.sos.state.ga.us/docs/391/3/19/Appendix%20I-IV.pdf

RAGS: Risk Assessment Guidance for Superfund, Volume I - Human Health Evaluation Manual (Part B, Chapter 3, Development of Risk-Based Preliminary Remediation Goals), U.S. Environmental Protection Agency, December 1991.

http://www.epa.gov/oswer/riskassessment/ragsb/pdf/chapt3.pdf

CDM Smith

Type 4 Soil RRS Equations
Fire Station 19 (HSI #10844)
Duluth, Gwinnett County, Georgia

Substance	Carcinogen Class	RAGS Eq 6 - Carcinogenic Effects					RAGS Eq 7 - Noncarcinogenic Effects					Type 4 Site-Specific Non-Residential Soil RRS mg/kg
		TR	Sf_i $(mg/kg\text{-}dy)^{-1}$	IUR $(ug/m^3)^{-1}$	Sf_o $(mg/kg\text{-}dy)^{-1}$	$C_{car\text{-}adult}$ mg/kg	THI	RfD_o mg/kg-dy	RfC_i mg/kg-dy	RfD_i mg/kg-dy	$C_{noncar\text{-}adult}$ mg/kg	
Arsenic	A	1.E-05	1.51E+01	4.30E-03	4.50E-01	**1.27E+02**	1	1.00E-03	1.50E-05	4.29E-06	**2.04E+03**	**1.27E+02**

Note: The above standard excludes leaching to groundwater.

CDM Smith

Type 4 Soil RRS Calculations
Fire Station 19 (HSI #10844)
Duluth, Gwinnett County, Georgia

RAGS Equation 6			
Type 5 Trespasser Soil - Carcinogenic Effects			

$$C_{car}\ mg/kg = \frac{TR \times BW \times AT_{car} \times 365\ days/year}{EF \times ED \times [(SFo \times 10^{-6}\ kg/mg \times IR_{soil}) + (SF_i \times IR_{air} \times \{1/VF + 1/PEF\})]}$$

Parameter	Definition (units)	Default Value	Source
$C_{car} =$	Concentration in soil (mg/kg)	Calculated	Not Applicable
$TR_{A/B}$	Carcinogen Class A/B target excess lifetime cancer risk (none)	1.E-05	HSRA Rules
TR_C	Carcinogen Class C target excess lifetime cancer risk (none)	1.E-04	HSRA Rules
SF_i	Inhalation cancer slope factor $(mg/kg\text{-}dy)^{-1}$ = IUR x 1,000 x BW 70 kg / IR_{air} 20 m^3/dy	Chemical-Specific	Not Applicable
IUR	Inhalation unit risk $(ug/m^3)^{-1}$	Chemical-Specific	Not Applicable
SF_o	Oral cancer slope factor $(mg/kg\text{-}dy)^{-1}$	Chemical-Specific	Not Applicable
$AT_{car\text{-}adult}$	Adult averaging time (yr)	70	HSRA Rules
$AT_{car\text{-}child}$	child averaging time (yr)	70	HSRA Rules

RAGS Equation 7			
Type 5 Trespasser Soil - Noncarcinogenic Effects			

$$C_{noncar}\ mg/kg = \frac{THI \times BW \times AT_{noncar} \times 365\ days/year}{ED \times EF \times [\{(1/RfD_o) \times 10^{-6}\ kg/mg \times IR_{soil}\} + \{(1/RfD_i) \times IR_{air} \times (1/VF + 1/PEF)\}]}$$

Parameter	Definition (units)	Default Value	Source
$C_{noncar} =$	Concentration in soil (mg/kg)	Calculated	Not Applicable
THI	Target hazard index (none)	1	HSRA Rules
RfD_o	Oral chronic reference dose (mg/kg-dy)	Chemical-Specific	Not Applicable
RfD_i	Inhalation chronic reference dose (mg/kg-dy) = RfC_i x IR_{air} 20 m^3/dy / BW 70 kg	Chemical-Specific	Not Applicable
RfC_i	Inhalation reference concentration (mg/m^3)	Chemical-Specific	Not Applicable
$AT_{noncar\text{-}adult}$	Adult averaging time (yr)	30	HSRA Rules
$AT_{noncar\text{-}child}$	child averaging time (yr)	6	HSRA Rules

Standard Assumptions

BW_{adult}	Adult body weight (kg)	70	HSRA Rules
BW_{child}	child body weight (kg)	15	HSRA Rules
EF	Exposure frequency (dy/yr)	350	Site Speciifc
ED_{adult}	Adult exposure Duration (yr)	30	HSRA Rules
ED_{child}	child exposure Duration (yr)	6	HSRA Rules
$IR_{air-adult}$	Adult inhalation rate (m^3/dy)	1.67	Site Speciifc
$IR_{air-child}$	child inhalation rate (m3/dy)	1.67	Site Speciifc
$IR_{soil-adult}$	Adult soil ingestion rate (mg/dy)	9.5	Site Speciifc
$IR_{soil-child}$	child soil ingestion rate (mg/dy)	16.7	Site Speciifc
PEF	Particulate emission factor (m^3/kg)	4.63E+09	HSRA Rules

Soil-to-Air Volatilization Factor (VF)

$$VF\ (m^3/kg) = \frac{(LS \times V \times DH) \times (\pi \times \alpha \times T)^{1/2}}{A \times 2 \times D_{ei} \times E \times K_{as} \times 10^{-3}\ kg/g}$$

Parameter	Definition (units)	Default Value	Source
LS	Length of side of contaminated area (m)	45	HSRA Rules
V	Wind speed in mixing zone (m/s)	2.25	HSRA Rules
A	Area of contamination (cm^2)	2.03E+07	HSRA Rules
DH	Diffusion height (m)	2	HSRA Rules
α	$(D_{ei} \times E)/[E + (\rho_s \times (1-E)/K_{as})]$ (cm^2/s)	Chemical-specific	HSRA Rules
T	Exposure Interval (s)	7.90E+08	HSRA Rules
ρ_s	Density of soil solids (g/cm^3)	2.65	HSRA Rules
D_{ei}	Effective diffusivity (cm^2/s)	$D_i \times E^{0.33}$	HSRA Rules
D_i	Molecular Diffusivity (cm^2/s)	Chemical-specific	Not Applicable
E	Total soil porosity	0.35	HSRA Rules
K_{as}	Soil-air partition coefficient (g soil/cm^3 air)	$(H/K_d) \times 41$	HSRA Rules
H	Henry's Law Constant (atm-m^3/mole)	Chemical-specific	Not Applicable
K_d	Soil-water partition coefficient (cm^3/g)	$K_{OC} \times OC$	HSRA Rules
K_{OC}	Organic carbon partition coefficient (cm^3/g)	Chemical-specific	Not Applicable
OC	Soil Organic Carbon Content (none)	2.0E-02	HSRA Rules

HSRA Rules: Georgia Hazardous Response Act Rules, 391-3-19, Appendix III, Media Target Concentrations and Standard Exposure Assumptions.

http://rules.sos.state.ga.us/docs/391/3/19/Appendix%20I-IV.pdf

RAGS: Risk Assessment Guidance for Superfund, Volume I - Human Health Evaluation Manual (Part B, Chapter 3, Development of Risk-Based Preliminary Remediation Goals), U.S. Environmental Protection Agency, December 1991.

http://www.epa.gov/oswer/riskassessment/ragsb/pdf/chapt3.pdf

| Substance | RAGS Eq 6 - Carcinogenic Effects | | | | | | | RAGS Eq 7 - Noncarcinogenic Effects | | | | | | Type 5 Trespasser Soil RRS |
	Carcinogen Class	TR	Sf_i (mg/kg-dy)$^{-1}$	IUR (ug/m^3)$^{-1}$	Sf_o (mg/kg-dy)$^{-1}$	$C_{car-adult}$ mg/kg	$C_{car-child}$ mg/kg	THI	RfD_o mg/kg-dy	RfC_i mg/kg-dy	RfD_i mg/kg-dy	$C_{noncar-adult}$ mg/kg	$C_{noncar-child}$ mg/kg	mg/kg
Arsenic	A	1.E-05	1.51E+01	4.30E-03	4.50E-01	**3.98E+02**	**2.43E+02**	1	1.00E-03	1.50E-05	4.29E-06	**7.68E+03**	**9.37E+02**	**2.43E+02**

Note: The above standard excludes leaching to groundwater and excludes vapor intrusion.

CDM Smith

Type 5 Trespasser Soil RRS Calculations
Fire Station 19 (HSI #10844)
Duluth, Gwinnett County, Georgia

RAGS Equation 6
Type 5 Construction Worker Soil - Carcinogenic Effects

$$C_{car}\ mg/kg = \frac{TR \times BW \times AT_{car} \times 365\ days/year}{EF \times ED \times [(SFo \times 10^{-6}\ kg/mg \times IR_{soil}) + (SF_i \times IR_{air} \times \{1/VF + 1/PEF\})]}$$

Parameter	Definition (units)	Default Value	Source
$C_{car} =$	Concentration in soil (mg/kg)	Calculated	Not Applicable
$TR_{A/B}$	Carcinogen Class A/B target excess lifetime cancer risk (none)	1.E-05	HSRA Rules
TR_C	Carcinogen Class C target excess lifetime cancer risk (none)	1.E-04	HSRA Rules
SF_i	Inhalation cancer slope factor $(mg/kg\text{-}dy)^{-1}$ $= IUR \times 1,000 \times BW\ 70\ kg / IR_{air}\ 20\ m^3/dy$	Chemical-Specific	Not Applicable
IUR	Inhalation unit risk $(ug/m^3)^{-1}$	Chemical-Specific	Not Applicable
SF_o	Oral cancer slope factor $(mg/kg\text{-}dy)^{-1}$	Chemical-Specific	Not Applicable
$AT_{car\text{-}adult}$	Adult averaging time (yr)	70	HSRA Rules
$AT_{car\text{-}child}$	child averaging time (yr)	NA	

RAGS Equation 7
Type 5 Construction Worker Soil - Noncarcinogenic Effects

$$C_{noncar}\ mg/kg = \frac{THI \times BW \times AT_{noncar} \times 365\ days/year}{ED \times EF \times [\{(1/RfD_o) \times 10^{-6}\ kg/mg \times IR_{soil}\} + \{(1/RfD_i) \times IR_{air} \times (1/VF + 1/PEF)\}]}$$

Parameter	Definition (units)	Default Value	Source
$C_{noncar} =$	Concentration in soil (mg/kg)	Calculated	Not Applicable
THI	Target hazard index (none)	1	HSRA Rules
RfD_o	Oral chronic reference dose (mg/kg-dy)	Chemical-Specific	Not Applicable
RfD_i	Inhalation chronic reference dose (mg/kg-dy) $= RfC_i \times IR_{air}\ 20\ m^3/dy / BW\ 70\ kg$	Chemical-Specific	Not Applicable
RfC_i	Inhalation reference concentration (mg/m^3)	Chemical-Specific	Not Applicable
$AT_{noncar\text{-}adult}$	Adult averaging time (yr)	1	HSRA Rules
$AT_{noncar\text{-}child}$	child averaging time (yr)	NA	

Standard Assumptions

BW_{adult}	Adult body weight (kg)	70	HSRA Rules
BW_{child}	child body weight (kg)	NA	
EF	Exposure frequency (dy/yr)	174	Site Speciifc
ED_{adult}	Adult exposure Duration (yr)	1	HSRA Rules
ED_{child}	child exposure Duration (yr)	NA	
$IR_{air-adult}$	Adult inhalation rate (m^3/dy)	20	HSRA Rules
$IR_{air-child}$	child inhalation rate (m3/dy)	NA	
$IR_{soil-adult}$	Adult soil ingestion rate (mg/dy)	50	HSRA Rules
$IR_{soil-child}$	child soil ingestion rate (mg/dy)	NA	
PEF	Particulate emission factor (m^3/kg)	4.63E+09	HSRA Rules

Soil-to-Air Volatilization Factor (VF)

$$VF\ (m^3/kg) = \frac{(LS \times V \times DH) \times (\pi \times \alpha \times T)^{1/2}}{A \times 2 \times D_{ei} \times E \times K_{as} \times 10^{-3}\ kg/g}$$

Parameter	Definition (units)	Default Value	Source
LS	Length of side of contaminated area (m)	45	HSRA Rules
V	Wind speed in mixing zone (m/s)	2.25	HSRA Rules
A	Area of contamination (cm^2)	2.03E+07	HSRA Rules
DH	Diffusion height (m)	2	HSRA Rules
α	$(D_{ei} \times E)/[E + (\rho_s \times (1-E)/K_{as})]$ (cm^2/s)	Chemical-specific	HSRA Rules
T	Exposure Interval (s)	7.90E+08	HSRA Rules
ρ_s	Density of soil solids (g/cm^3)	2.65	HSRA Rules
D_{ei}	Effective diffusivity (cm^2/s)	$D_i \times E^{0.33}$	HSRA Rules
D_i	Molecular Diffusivity (cm^2/s)	Chemical-specific	Not Applicable
E	Total soil porosity	0.35	HSRA Rules
K_{as}	Soil-air partition coefficient (g soil/cm^3 air)	$(H/K_d) \times 41$	HSRA Rules
H	Henry's Law Constant (atm-m^3/mole)	Chemical-specific	Not Applicable
K_d	Soil-water partition coefficient (cm^3/g)	$K_{OC} \times OC$	HSRA Rules
K_{OC}	Organic carbon partition coefficient (cm^3/g)	Chemical-specific	Not Applicable
OC	Soil Organic Carbon Content (none)	2.0E-02	HSRA Rules

HSRA Rules: Georgia Hazardous Response Act Rules, 391-3-19, Appendix III, Media Target Concentrations and Standard Exposure Assumptions.

http://rules.sos.state.ga.us/docs/391/3/19/Appendix%20I-IV.pdf

RAGS: Risk Assessment Guidance for Superfund, Volume I - Human Health Evaluation Manual (Part B, Chapter 3, Development of Risk-Based Preliminary Remediation Goals), U.S. Environmental Protection Agency, December 1991.

http://www.epa.gov/oswer/riskassessment/ragsb/pdf/chapt3.pdf

CDM Smith

| Substance | RAGS Eq 6 - Carcinogenic Effects | | | | | | RAGS Eq 7 - Noncarcinogenic Effects | | | | | Type 5 Construction Worker Soil RRS |
	Carcinogen Class	TR	Sf_i $(mg/kg\text{-}dy)^{-1}$	IUR $(ug/m^3)^{-1}$	Sf_o $(mg/kg\text{-}dy)^{-1}$	$C_{car\text{-}adult}$ mg/kg	THI	RfD_o mg/kg-dy	RfC_i mg/kg-dy	RfD_i mg/kg-dy	$C_{noncar\text{-}adult}$ mg/kg	mg/kg
Arsenic	A	1.E-05	1.51E+01	4.30E-03	4.50E-01	**4.57E+03**	1	1.00E-03	1.50E-05	4.29E-06	**2.94E+03**	**2.94E+03**

Note: The above standard excludes leaching to groundwater and excludes vapor intrusion.

CDM Smith